ASSESSMENT OF INTERPLATE AND INTRAPLATE EARTHQUAKES

A Thesis

by

SRIGIRI SHANKAR BELLAM

Submitted to the Office of Graduate Studies of
Texas A&M University
in partial fulfillment of the requirements for the degree of

MASTER OF SCIENCE

August 2012

Major Subject: Construction Management

Assessment of Interplate and Intraplate Earthquakes

ASSESSMENT OF INTERPLATE AND INTRAPLATE EARTHQUAKES

A Thesis

by

SRIGIRI SHANKAR BELLAM

Submitted to the Office of Graduate Studies of
Texas A&M University
in partial fulfillment of the requirements for the degree of

MASTER OF SCIENCE

Approved by:

Chair of Committee,	John M. Nichols
Committee Members,	Anne B. Nichols
	Douglas F. Wunneburger
	Leslie H. Feigenbaum
Head of Department,	Joseph P. Horlen

August 2012

Major Subject: Construction Management

ABSTRACT

Assessment of Interplate and Intraplate Earthquakes.

(August 2012)

Srigiri Shankar Bellam, B. Tech, National Institute of Technology, India

Chair of Advisory Committee: Dr. John M. Nichols

The earth was shown in the last century to have a surface layer composed of large plates. Plate tectonics is the study of the movement and stresses in the individual plates that make up the complete surface of the world's sphere. Two types of earthquakes are observed in the surface plates, interplate and intraplate earthquakes, which are classified, based on the location of the origin of an earthquake either between two plates or within the plate respectively. Limited work has been completed on the definition of the boundary region between the plates from which interplate earthquakes originate, other than the recent work on the Mid Atlantic Ridge, defined at two degrees and the subsequent work to look at the applicability of this degree based definition. Others suggested an alternative view of a constant width for the interplate region in recent work at Texas A&M University.

The objective of the paper is to determine whether the assumption of a linear width of the region along the tectonic plate boundaries to classify earthquakes as interplate and intraplate earthquakes using accepted statistical criteria provides a better fit to the data than the constant degree definition.

There are three types of interplate boundaries defined by the relative movement of the two plates to each other, which further complicates this study. The study used a nonrandom analysis of regions of the different types of boundary to compare the rate and decay of the intraplate earthquakes from a notional centerline for the known boundaries. The study used GIS software and EXCEL for the statistical analysis component of the research work.

The results show that a constant width definition provides a number of advantages in determining the relative definition of interplate and intraplate earthquakes when compared to the constant degree definition developed for work on the Mid Atlantic Ridge. Further research is suggested on a randomly selected set of study sites to improve the reliability and quality of the statistical work for each type of the boundary of the tectonic plates.

ACKNOWLEDGEMENTS

I would like to thank my committee chair, Dr. John Nichols, and my committee members, Dr. Douglas Wunneburger, Dr. Anne B. Nichols and Prof. Leslie H. Feigenbaum for their guidance and support throughout the course of this research.

I would also like to thank Ms. Miriam Olivares from the Maps and GIS Collections and Services at the Texas A&M University library for her guidance and support. Thanks also go to my friends and colleagues and the department faculty and staff for making my time at Texas A&M University a great experience. I also want to extend my gratitude to the United States Geological Survey's Earthquake Hazard Program, which was the primary source of the data required for the research.

Finally, I thank my family and friends for their love and encouragement.

NOMENCLATURE

CEUS	Central and Eastern United States, which represents an area of significant economic risk in earthquake events
NOAA	National Oceanic and Atmospheric Administration, the group that maintains the fatality database for earthquakes
USGS	United States Geological Survey, the group who maintains the key elements of the earthquake data repository for the USA
Intraplate	Within a stable continental mass as defined by Johnson and Kantor (A.C. Johnston & Kanter, 1990), which often have earthquakes with larger tolls for the same magnitude
Interplate	Between two stable landmasses as defined to be within two degrees of the boundary (Jogunoori, 2011; Wysession, Wilson, Bartkó, & Sakata, 1995)
Meizoseismal	Occurring with the area of highest movements (Kotò, 1893; Little, Fowler, Coulson, Onions, & Friedrichsen, 1973), which was first defined after a nineteenth century Japanese earthquake
Modified Mercalli Scale	A scale from I to XII indicating damage in an earthquake (Richter, 1958), which provides a good indicator as to damage potential (Nichols, 2005)

M_w	Intensity Measure for earthquakes
$EQ_{\deg}$	The distance in kilometers of a single degree at the equator
Ξ	Multiplier to indicate the number of $EQ_{\deg}$ at each boundary to determine the interplate boundary width

TABLE OF CONTENTS

Page

LIST OF FIGURES

LIST OF TABLES

Page

CHAPTER I

INTRODUCTION

Background to the Study

This research is the third in a series of TAMU studies that have worked on the differences between intraplate and interplate earthquakes. Earthquakes that occur on well-defined tectonic plate boundaries are called interplate earthquakes and those that occur within a tectonic plate are called intraplate earthquakes. The intra-plate boundaries have been defined according to a suggested two degrees outside the plate boundary for intra plate events by Wysession et al. (1995). Wysession's group was studying the mid-Atlantic Ridge and looking at the definition of interplate and intraplate.

Subsequently at this university, Jogunoori (2011) looked at the statistical distribution of the two earthquake types based on the adoption of the two degree definition. This research work represents a continuation of the first study, by considering a fundamental change in the definition of the interplate to intraplate boundary.

This paper presents a statistical investigation of the historically recorded earthquakes data set. Data from the United States Geological Survey global earthquake database was used to establish distribution histograms for the occurrences of the earthquakes along the tectonic plate boundaries. The independent variable was distance from the plate boundary and the dependent variable is the number of earthquakes with distance. The research is trying to determine if a fixed width definition is a better fit.

This thesis follows the style of Group Dynamics: Theory, Research, and Practice.

The earthquakes under consideration are studied broadly occurring at the three types of tectonic plate boundaries, namely, convergent, divergent and transform boundaries.

Problem Statement

The purpose of this thesis is to investigate the distribution pattern of the fatal interplate earthquake events above 5.0 M_w about the tectonic plate boundaries.

Hypothesis

The research hypothesis is:

A fixed width criterion for classifying an earthquake as interplate or intraplate earthquake provides a better statistical fit to the data, than a fixed angular amount.

Limitations

The limitations of this research are:

1. The study team does not randomly select locations for the analysis; this limits the statistical validity, but is required in the first stage to provide reasonable data for determining if a complete study of all the data is warranted.
2. The USGS data set from 1973 to the present is assumed as representative of world seismicity.

Significance of the Study

The study would enable the distinction of interplate earthquakes from intraplate earthquakes. The probability of occurrence of intraplate earthquake has been observed to be lower when compared to interplate earthquake (Johnson & Kanter, 1990). So, the proper distinction of interplate earthquakes from intraplate earthquakes could be used to improve the accuracy of the fatality models developed in the last decade.

CHAPTER II

LITERATURE REVIEW

Introduction

This literature review outlines the recent developments in the theory of plate tectonics and earthquakes related to the areas of interplate and intraplate earthquakes. The main research has been since the early 1960s with the development of plate tectonic theory and an improved understanding as to the mechanisms of earthquake generation. The literature review has sections on:

- Definitions
- Historical Data on Earthquakes
- Intraplate and Interplate Event Differences

Definitions

These definitions are taken from the definitions provided by Majmudar (2010) and Jogunoori (2011) who have completed previous research related to this area of study. The definitions are:

1. Earthquake: An earthquake is the result of a sudden release of energy in the Earth's crust caused by the movement of the plates or some mechanism within the plates. This movement produces seismic waves that can cause damage to man-made structures and death as observed recently in Japan

2. Fault: A planar fracture or discontinuity across which there has been significant displacement
3. Hypocenter: The point where the fault begins to rupture
4. Epicenter: The point directly above hypocenter on the earth's surface
5. Types of Earthquakes: Interplate and Intraplate
6. Interplate: Earthquake occurring at the tectonic plate boundaries
7. Intraplate: Earthquake occurring interior of the plate boundaries

Historical Data on Earthquakes

Earthquakes were called *seismos tes ges* in Greek, literally shaking of the Earth. The great Lisbon earthquake of 1 November 1755, which caused widespread destruction in that city and produced a large tsunami, may be considered as the starting point of modern seismology in Europe, although significant work in terms of data collection on earthquakes had occurred in China over the last few millennia. The famous balls in the mouth of the dragons' device provided a method for determining an approximate direction and to some extent magnitude (Jogunoori, 2011), which has been supplanted by modern seismic devices detailed in numerous texts over the last century (Gubbins, 1992; Richter, 1958).

Various ideas have been proposed since the time of the Greek philosophers to explain the causes of earthquakes, but it was during the latter part of the nineteenth century that systematic field studies were conducted on the earthquakes and an attempt to relate them to tectonic processes were made by numerous interested parties, Clarke

(1869), Cotton (1921), Hogben (1893), Kotò (1893), and Musson (1993) who have looked at the damage wrought by earthquakes and the impact.

Gubbins (1992) outlined the development of the theory of plate tectonics in the early 1960's. This work revolutionized the study of earthquakes as it built on the seminal work on data collection undertaken to that time and since by major governmental groups (Gutenberg & Richter, 1954, 1956). The plate areas with their boundaries are shown on Figure 1.

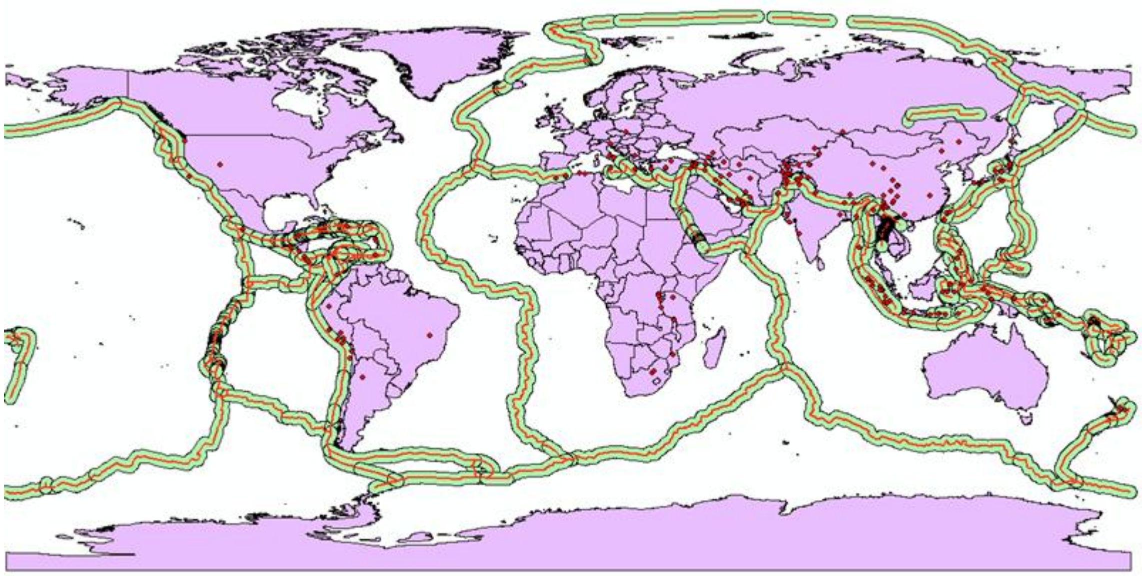

Figure 1 Plate Boundaries, after Jogunoori (2011)

The basic theory is that a geologic mechanism is driving the plates slowly across the face of the world resulting in a long-term energy accumulation of tectonic stress. An earthquake hence is the seismic-geological process of an abrupt release of this energy forming seismic waves that can cause damage to man-made structures and movement of entire landmasses, as in Japan in 2011 (Zhao & Xu, 2012). The devastation seen in Japan in 2011 is shown in Figure 2, which demonstrates the picture of devastation in the urban areas by comparing the Google satellite shots of Minamisanriku, Japan before-and-after the 2011 Tohoku earthquake and tsunami.

Figure 2 Before-and-after satellite imagery of Minamisanriku at the 2011 Tohoku Japan earthquake and tsunami. Retrieved from http://photos.mongabay.com/11/japan/Minamisanriku-2002.jpg and http://photos.mongabay.com/11/japan/Minamisanriku-after.jpg

The result of seismic waves created by a sudden release of energy in the earth's crust is termed as an earthquake. The recent Japanese event caused Honshu, Japan's largest island to move 2.4 meters east and shifted the Earth on its axis by estimates of between 10 cm and 25 cm. The measurement of these events is of significant concern to humanity in terms of safe urbanization.

Magnitude three on Richter scale or lower earthquakes are almost imperceptible but earthquakes of magnitude five and higher are potent and cause severe damage to life and property (Page, 1991, 1992) as shown in the damage in the Flour Mill in Newcastle, more than twenty kilometers from the epicenter and close by an area of fatalities caused by falling masonry. The largest earthquakes in the history have been of magnitude over nine. An earthquake essentially results in some or at times most of the known side effects being shaking or rupturing of the earth's crust, landslides and avalanches, fires, soil liquefaction, tsunami, floods and human impacts. The Newcastle 1989 earthquake had the highest level of recorded fatalities for the size of the event, until the tragic 2002 Italian event involving a school collapse (BBC, 2002). Figure 3 show a flourmill damaged in the 1989 earthquake in the suburb of Hamilton. The mill is about 600 meters from the heavily damaged Tudor Street, which resulted in fatalities.

Figure 3 Flour Mill damaged in 1989 Earthquake, courtesy Nichols (1999)

The event is essentially a relative displacement of the two sides of a tectonic plate boundary and the release of the accumulated elastic and plastic strain, produced by the tectonic processes movement of the plates or internal processes. The exception is the production of intraplate events, which are located on fault zones within the boundary. The fault that caused the 1989 event has also caused events in 1842, 1868, 1929 and 1992. The 1989 event caused a significant revision to the Australian standard for earthquake design loads (Standards Australia, 2001)

The difficulty in part is the analysis of the data to determine the impact on real structures from a theoretical event, which is the basis for design of most structures of importance to humanity (Atkinson & McCartney, 2005; Bommer et al., 2005; Boore, 2005; Boore, Azari Sisi, & Akkar, 2012; Di Alessandro, Bonilla, Boore, Rovelli, & Scotti, 2012; Liu & Tsai, 2005; Mai, Spudich, & Boatwright, 2005).

Three abbreviations proposed for the plate boundary movements to simplify the presentation of the results are:

1. TCP: Transform Plate Boundary, where two boundaries slide relative to each other
2. DPB: Divergent Plate Boundary, where two plate boundaries are pulled apart and there is an upwelling of magma onto the surface as occurs in the Mid Atlantic
3. CPB: Convergent Plate Boundary, where one plate dives beneath the other plate

Figure 4 shows the three types of plate interaction that causes earthquakes.

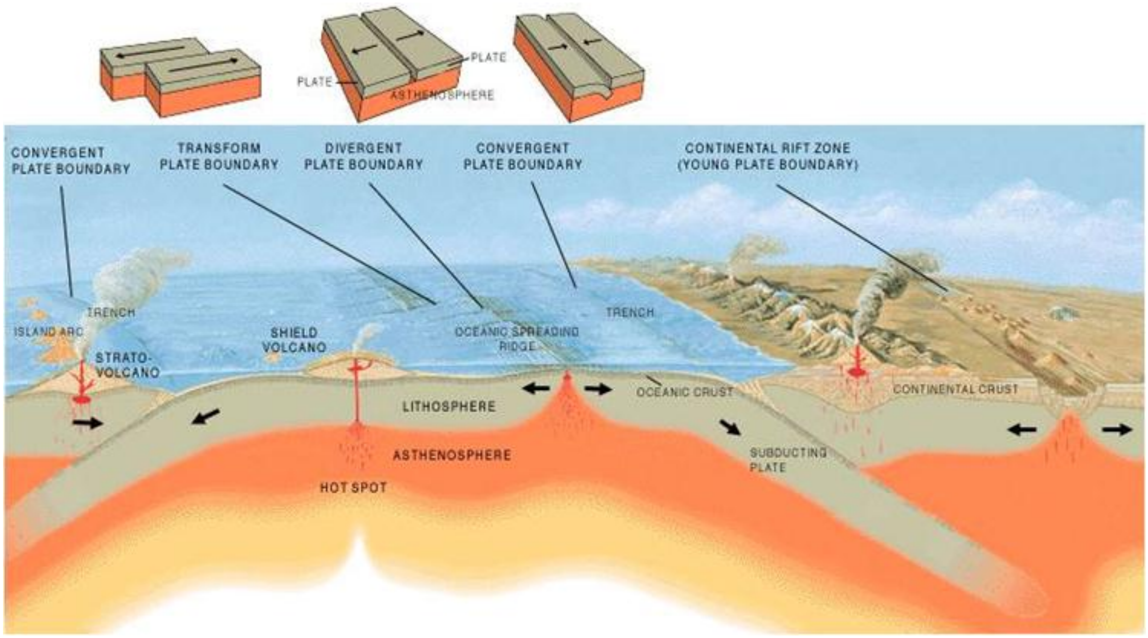

Figure 4 Picture depicting the different types of plate interactions at the convergent, divergent and transform plate boundaries (Cross section by José F. Vigil from *This Dynamic Planet* map produced by the U.S. Geological Survey, the Smithsonian Institution, and the U.S. Naval Research Laboratory)

Four types of edge surface exist because of these boundary movements, abbreviated as follows:

1. TCPE: Transform Plate Boundary Edge
2. DPBE: Divergent Plate Boundary Edge
3. CPBL: Convergent Plate Boundary Lower Edge, which is disappearing beneath the other plate

4. CPBU: Convergent Plate Boundary Upper Edge, which is sliding over the other plate

Recent work on plate tectonics points to the current range of research on this topic, (Altis, 2001; Kitamura & Kimura; Ricou, 2004; Zlotnik, Díez, Fernández, & Vergés, 2007), which is of interest in terms of the design and safety of nuclear power plants (Newmark & Hall, 1978, 1981, 1982). A method was developed in the early part of the twentieth century to describe the size of an earthquake is in terms of its intensity on the basis of observations on the Earth's surface of damage to buildings and other structures and ground effects such as fractures, cracks and landslides. Intensity is an indirect measure of the size of an earthquake. The first scale of the magnitude of an earthquake measured the energy released at the focus of the earthquake, currently defined using a series of equations as follows:

$$M_0 = \mu AD \tag{1}$$

Where M_0 is, the seismic moment measured in dyne centimeters, μ is the shear modulus of the rock in dyne/cm^2, A is the area of the rupture in cm^2 and D is the average displacement in cm. The use of the dyne-centimeter can be traced to the original development, and the non-standard SI is used here, as traditionally it is used for this work. The moment magnitude, M_w, is now used in place of the original earthquake magnitude scales, refer to early work by Gutenberg and Richter (Gutenberg & Richter, 1954, 1956; Richter, 1958). The moment magnitude defined in equation (2) is:

$$M_w = \frac{2}{3}(\log_{10} M_0 - 6.07) \tag{2}$$

The equation is designed to be consistent with the earlier scales and produces a dimensionless number. Bath (1981) provides a form of the moment magnitude equation for a specific site measurement system as follows:

$$M_w = \log_{10}(\frac{a}{T}) + f(\Delta, h) + C \tag{3}$$

where a is the ground amplitude, T is the corresponding period, Δ is the epicentral distance, h is the focal depth, f is function of these two variables (Borowski & Borwein, 1989) and C is a site constant. This type of equation is required to allow for a rapid and automated estimate to be provided for all the earthquakes that are recorded and analyzed by seismologists (Kim, Richards, Adushkin, & Ovtchinnilov, 2001).

Tectonic Plates

Bird (2003), shown on Figure 5, provides a guide as to the form of the tectonic plates and edges on the plates.

Bird's seminal work, (Bird, Kreemer, & Holt, 2010; Bird & Liu, 2007) on the plate model development for estimating future events provides a strong foundation for developing better seismic hazard maps for the USA and the world (Frankel et al., 2000). Gaba (2006) has redrawn the data shown on the map by Bird (2003) to highlight the boundary locations and the size of the current velocity field in terms of principal direction of movement, refer to Figure 6.

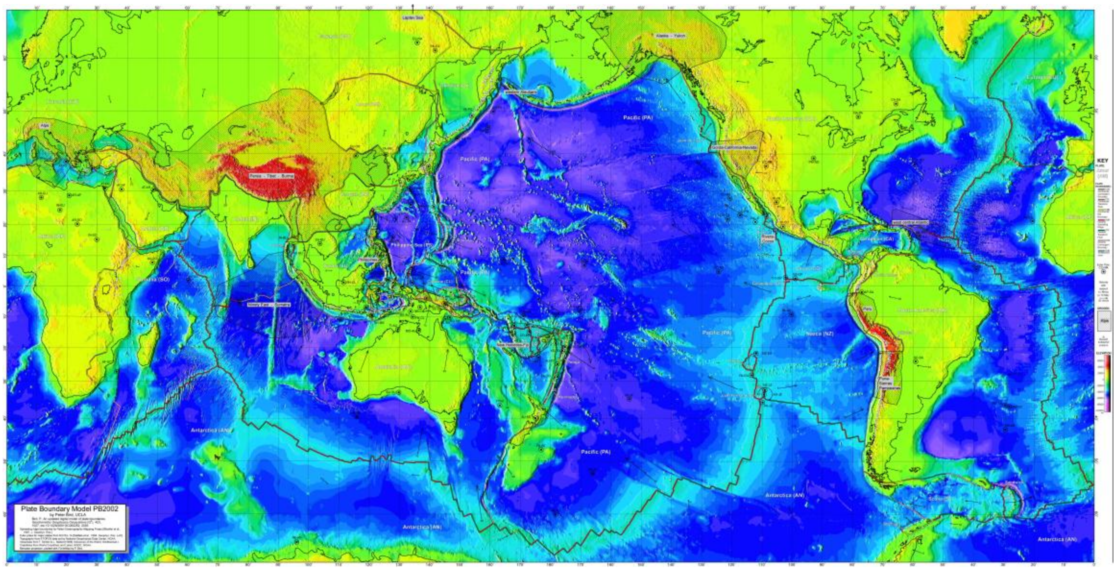

Figure 5 Tectonic Plates, after Bird (2003)

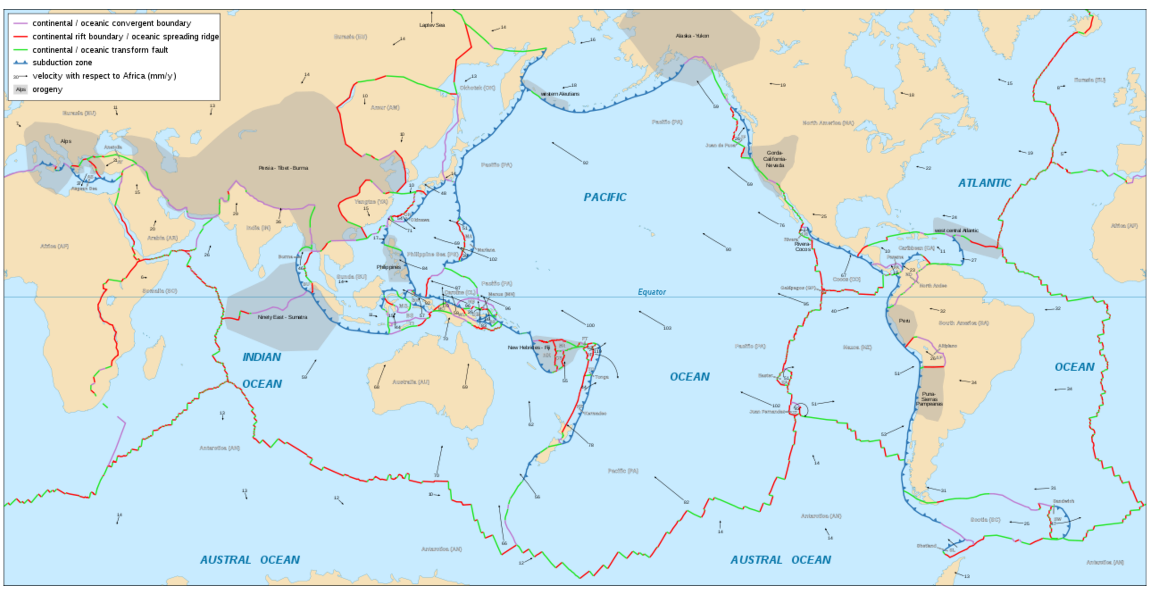

Figure 6 Detailed world map in English showing the tectonic plates with their movement vectors (Adapted from the Wikimedia Commons file by Eric Gaba. Accessed from http://en.wikipedia.org/wiki/File:Tectonic_plates_boundaries_detailed-en.svg)

U.S. Geological Survey (2011b) published a map of the tectonic plates to illustrate a color coded version of the other earlier figures, as shown on Figure 7. Earthquakes are classified broadly based on either occurring at the tectonic plate boundaries, called the interplate earthquakes and those occurring within the interior of the plate boundaries are termed as the intraplate earthquakes (Bath, 1981; A.C. Johnston & Kanter, 1990; A. C. Johnston & Nava, 1994; A.C. Johnston & Schweig, 1996).

Interplate earthquakes, according to the accepted theory, are strictly controlled by the motion of plates, and their epicenters are distributed in zones obliquely into the upper mantle layer, which is closely related to the large scale rising of the mantle. The intraplate earthquakes on the other hand are closely related to the rising of asthenosphere (Weiran et al., 2009).

According to the seismotectonic framework, a great thrust earthquake occurs when the ridge push and slab pull forces exceed the strength of the locked interface thrust zone (Andrade & Rajendran, 2011).

In looking further at the 2012 Indian Ocean Sequence, the authors noted that "*Faulting mechanism prior to 2004 suggests predominantly thrust faulting on the plate interface. Note that the earthquakes on the subducting plate (yellow beach balls) show distinctly different style of faulting (Rajendran, Andrade, & Rajendran, 2011). These distinctive styles have implications on plate deformation models (Paul, Rajendran, Lowry, Andrade, & Rajendran, 2012).*"

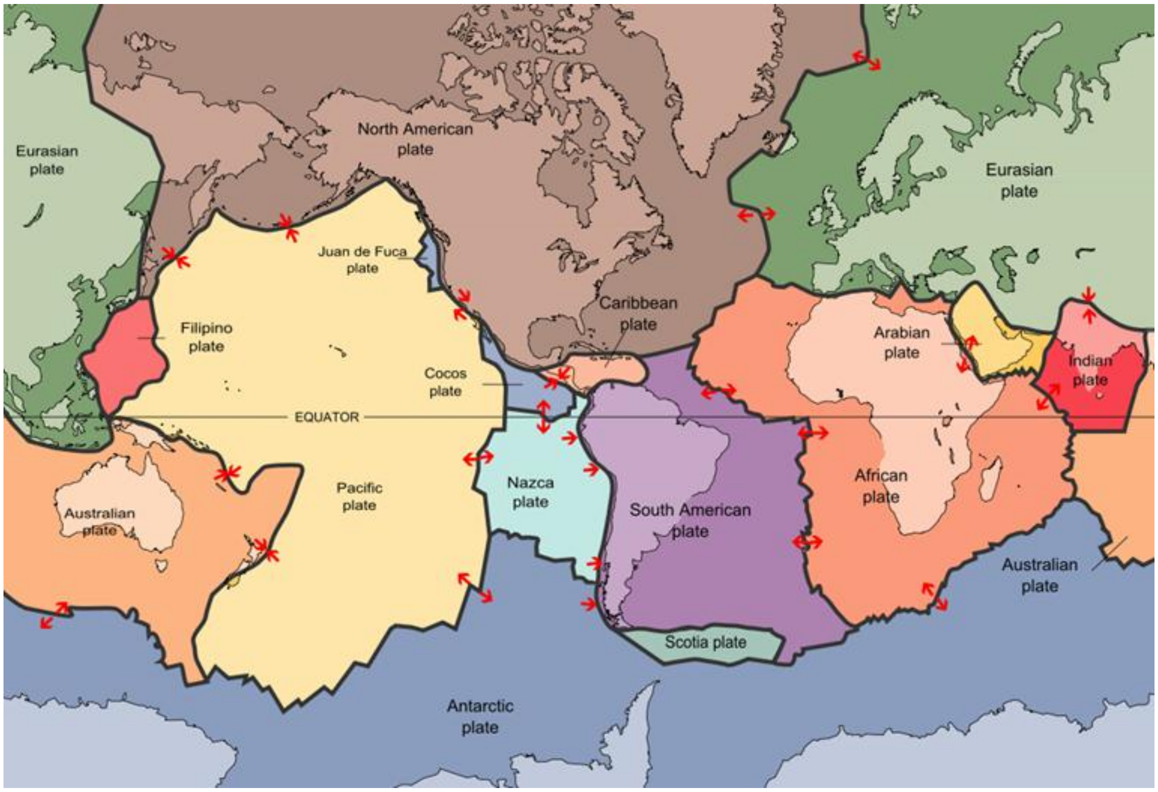

Figure 7 U.S.G.S. Map of the Tectonic Plates after U.S. Geological Survey (2011b)

Brune's Model

There are thousands of earthquakes annually. A small group are of significant research interest for a variety of reasons. Table 1 lists one such group from Nichols (2003), which show the types of earthquakes used in the seismic literature.

As Nichols (2003) noted "*Newmark and Hall (1978) establish the criteria for the design of nuclear power plants. This criteria still forms an integral part of the legal framework in the United States for the design of nuclear facilities. The earthquake spectrum developed for the nuclear power plant design was based on an extensive analysis of the seismicity of interplate regions and a rigorous mathematical review of the* *wave and pulse constraints on the limits of the design spectrum."* In reality a limited range of earthquakes are studied at a detailed level, because of the number each day. The earthquakes that are studied usually are significant because of location, damage or deaths.

Table 1
Significant Earthquakes

Earthquake	Date	Magnitude	Location Type	Comments
Imperial Valley	May 18, 1940	6.4	California / Interplate	Brune (1970) used earthquake as sample. El Centro originally digitized record
Kern County	July 21, 1952	7.6	Taft / Interplate	Brune (1970) used earthquake as sample
Nahanni	December 23, 1985	6.8	Station 1 Iverson Creek / Intraplate	Nichols used as a significant earthquake.
Saguenary (1) St 8.	November 25, 1988	5.9	La Malbaie, CA / Intraplate	Nichols used as a significant earthquake.
Marked Tree	Synthetic	7.25	Arkansas - NMSZ / Intraplate	Lamont Doherty synthetic earthquake.
Newcastle	December 28, 1989	5.4	Newcastle, AU / Intraplate	13 deaths
Irpinia, Calatrini	November 23, 1980	6.9	Italy / Interplate identified with 2000 year repeat	Benedetti used for the ISMES Tests.
Eureka	December 21, 1954	6.6	Station 22, East of Arcata / Interplate	Nichols used as a significant earthquake
Miramichi	Jan 9, 1982	5.7	Loggie Lodge/ Intraplate	
Bros	May 27, 1995	< 4	Tennessee/ Intraplate	CERI DATA. Minor Earthquake / Intraplate
Parkfield	June 27, 1966	5.6	Parkfield California/	Brune (1970) used earthquake as sample.

Brune (1970) developed a model for estimating the spectra of seismic shear waves from earthquakes, which forms a critical part of current design methods. The frequency function is:

$$\Omega(\omega) = \frac{\sigma\beta}{\mu} \frac{1}{\omega(\omega^2 + \tau^{-2})^{0.5}} \tag{4}$$

where ω is frequency (Hz), σ is effective stress (Pa), β is shear wave velocity (m/s), μ represents the rigidity, and τ (sec) represents the dimensional order of the fault divided by β. Brune accepted an upper limit for the initial velocities in earthquakes at one metre per second for the nominated earthquakes, and gave peak acceleration at 2g. Brune observed the frequencies of interest for seismic studies were from 0 to 10 Hertz.

Brune's model provides for a linear relationship between the effective stress and the spectrum amplitude for a constant frequency, and thus the critical value in the model is the time of rupture, τ. Brune allowed the Parkfield earthquake to have a rupture time of half of one second for a two kilometer long fault. The 1915 Abruzzo earthquake has an estimated fault length of twenty five kilometers (Nichols, 2005). Nichols provides an estimate for the time of rupture as six seconds. Brune's model has been recreated, by Nichols, using the site-specific values provided in Brune's paper, but with a rupture time that varies from 0.01 to ∞, as shown in Figure 8.

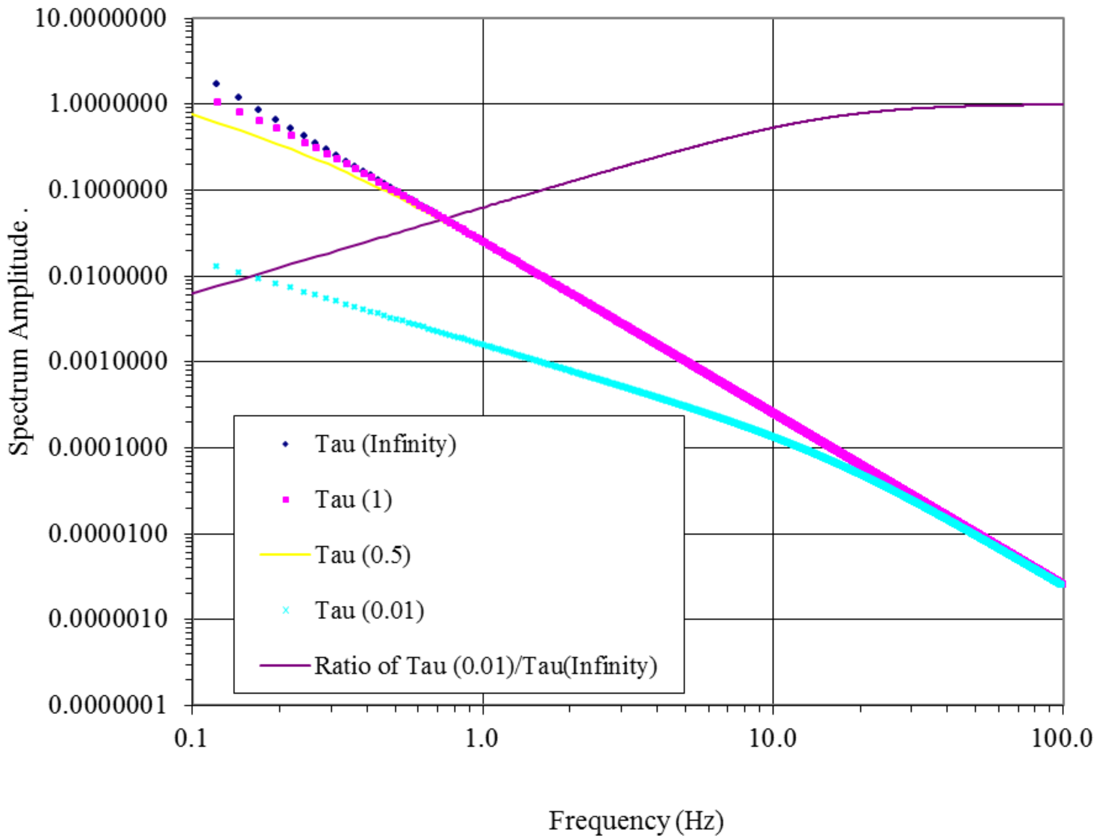

Figure 8 Brune's Model as shown after Nichols (2005)

The result of concern is the design values for earthquake, such as acceleration, velocity and displacement. Nichols (2005) development of the tri-part chart for a number of the significant earthquakes of the twentieth century and a number of the twentieth century standards is shown in Figure 9.

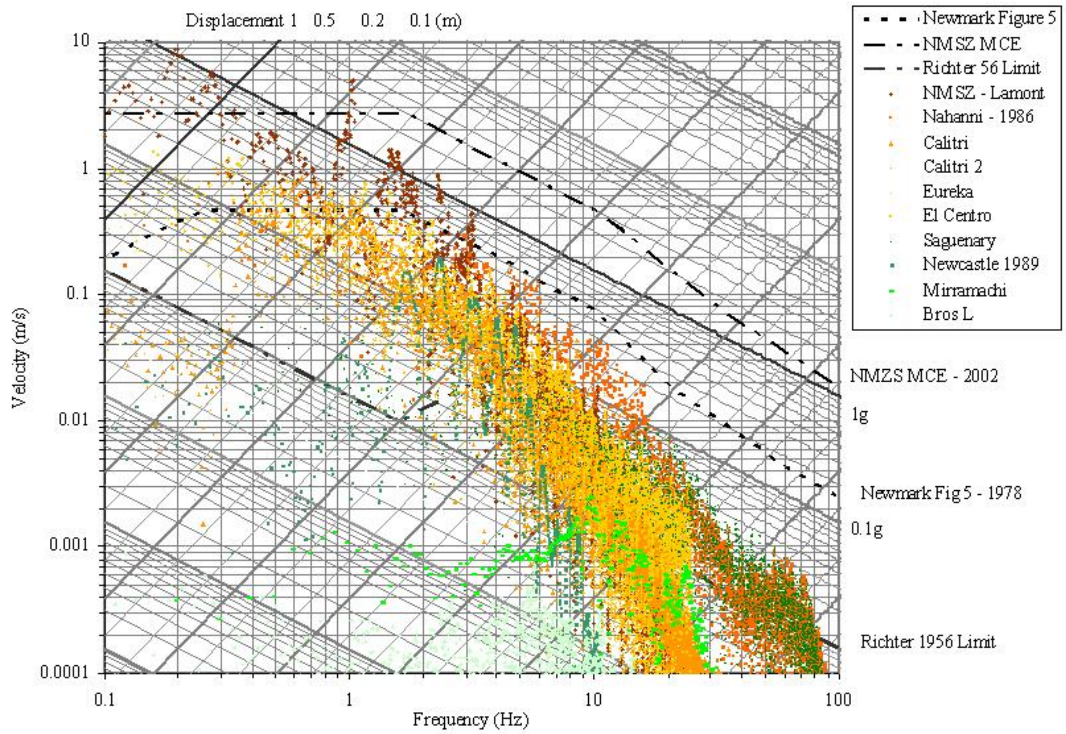

Figure 9 Tri-part Earthquake chart after Nichols (2005)

Nichols noted that "*The increase in length of the rupture plane for an increasing size of earthquake has two impacts, the first is the potential increase in the energy release, and the second is the increased duration of the rupture time. Brune's model provides an opportunity to consider the 'theoretical' difference in the amplitude spectrum for an event on a short rupture plane and an event on a long rupture plane. The results for generally competent bedrock have been shown in Figure 8. The significant effect is the increase in the energy of the earthquake that occurs in the low frequency spectrum compared to the higher frequency spectrum. The curvature introduced to the short rupture-plane frequency spectrum means that for a 0.01 second* *event the ratio of the energy at 1 Hertz is less than 8 per cent of the infinite value, whereas at 10 Hertz the difference is only 60 per cent."*

In summary, larger earthquakes carry a preponderance of the energy at lower frequencies, so that the thought those smaller events are larger events scaled down is not correct.

Intraplate and Interplate Event Differences

The difference between the impact of an interplate and intraplate event of the same magnitude can be considerable. Intermediate depth, intraplate events present larger corner frequencies and seismic energy for a given seismic moment, compared to interplate earthquakes. As shown in Figure 10.

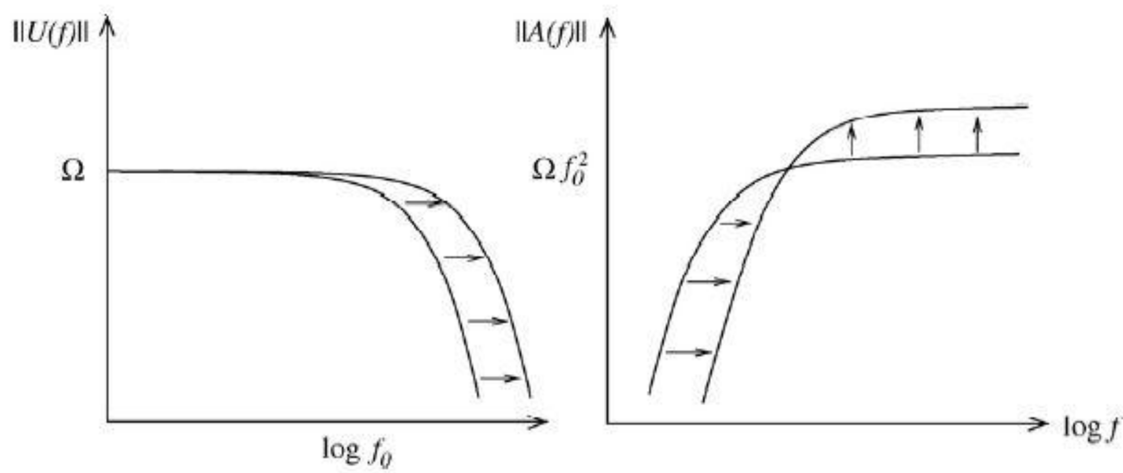

Figure 10 Brune's Model showing an increase of the corner frequency (f0), in displacement and acceleration spectrums after Leyton, Ruiz, Campos, and Kausel (2009)

Previous studies (mostly using global, teleseismic data) have shown certain differences between interplate and intraplate earthquakes, specially taking into account the seismic source, as shown on Figure 11 which show the relation of seismic moment, M_0 with corner frequency, f_0, (Garcia, Singh, Herraiz, Pacheco, & Ordaz, 2004).

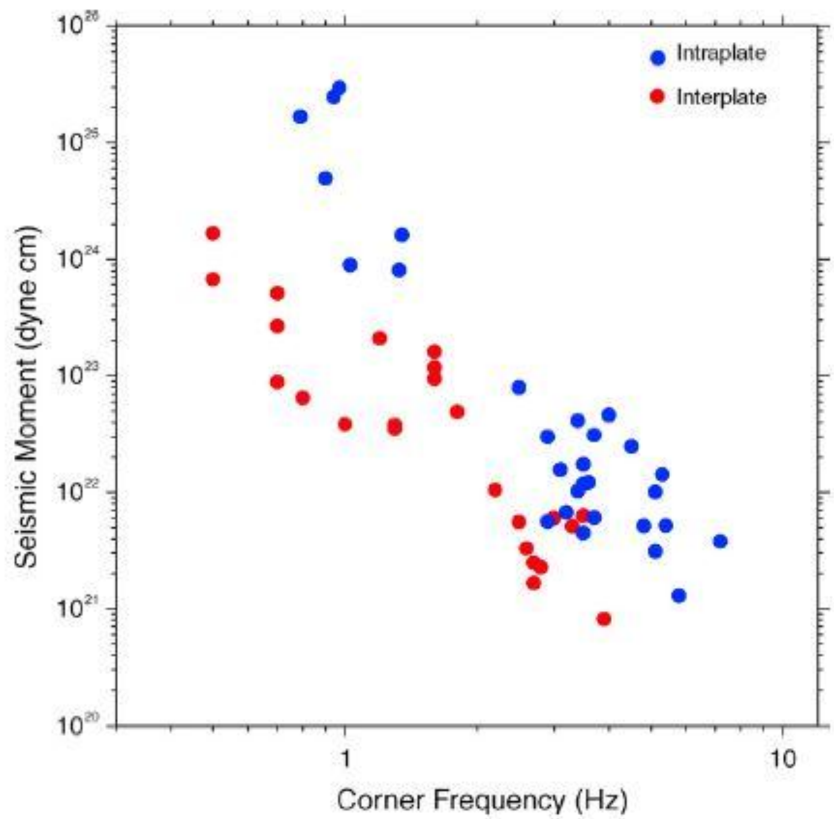

Figure 11 Relation of seismic moment, M_0 with corner frequency, f_0. Interplate earthquakes shown in red, whilst in blue are the intermediate depth, and intraplate ones after Leyton, Ruiz, Campos, and Kausel (2009)

Figure 12 show the seismic energy plotted as a function of the seismic moment. Interplate earthquakes are shown in red, whilst in blue are the intermediate depth and intraplate ones. The figure also show data from Choy and Boatwright (1995) for interplate events and from the USGS (2008)

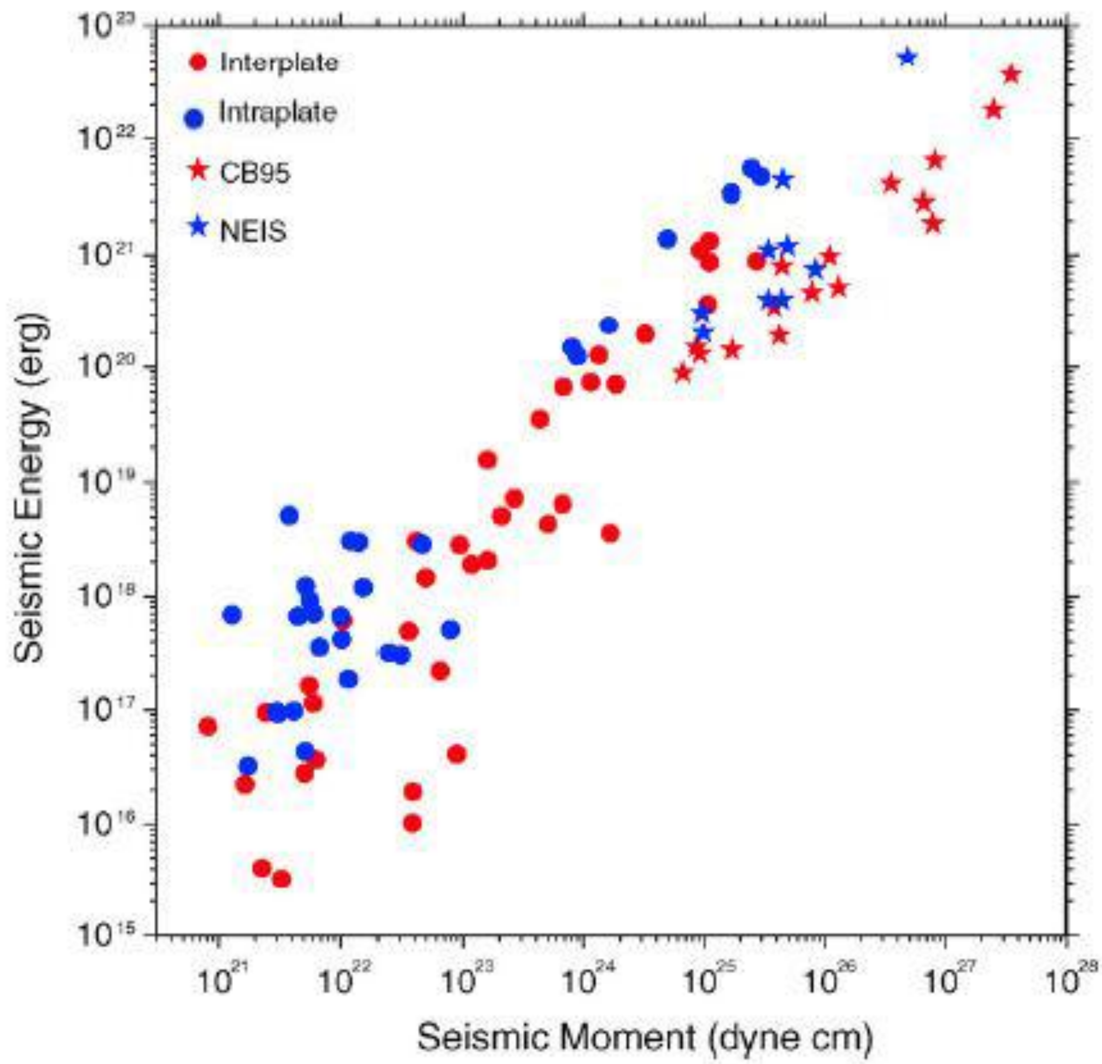

Figure 12 Seismic Moment plotted against Seismic Energy after Leyton, Ruiz, Campos, and Kausel (2009)

Intraplate earthquakes reach intensities of almost two points in MMI larger than interplate events in the epicentral region, despite the fact that the peak ground accelerations are very similar (Astroza, Sandoval, & Kausel, 2005; Kanamori & Anderson, 1975; Kausel & Campos, 1992; Saragoni, Astroza, & Ruiz, 2004; Scholz, Aviles, & Wesnousky, 1986). The occurrence of interplate earthquakes at the plate boundaries is more common relative to that of the occurrence of intraplate earthquakes within the more stable continental land mass (Jogunoori, 2011; Saragoni et al., 2004). This lower frequency of intraplate earthquakes can be attributed to the higher stress drops when compared to interplate earthquakes. The stress drops for the intraplate earthquakes are about six times higher than interplate earthquakes, assuming that the stress drop is proportional to the slip per unit area (Scholz et al., 1986), which indicates that the magnitude of intraplate earthquake is always going to be higher than interplate earthquake. The intraplate earthquakes have a higher averaged apparent stress drop ($\sigma_a \sim$ 9000000 pa) compared to interplate events ($\sigma_a \sim$ 3000000 pa). Once an intraplate earthquake releases the local stress, it takes long time for the stress to build up to its crustal strength, which explains the lower probability of occurrence of intraplate earthquakes when compared to interplate earthquake.

It has been demonstrated by Jogunoori (2011) that the interplate earthquakes occur 6.23 times as frequently as the intraplate, using the two degree definition of the boundary. On average, there are 22.4 interplate events per week or about 3 per day, whereas for the intraplate events there are 3.6 per week or about one, every two days. There have been about 11658 and 1869 interplate and intraplate earthquakes above 5.0

respectively in the last decade. It observed the data analysis for Jogunoori's study that about 86.18% of the earthquakes occur on the boundaries.

The research question of interest from this analysis is to determine the best statistically based definition of interplate earthquakes to distinguish them from intraplate earthquake events. The Haversine formula accounts for the variation in the linear width from the equator to the poles (Johnson, 2008; Robusto, 1957). Figure 13 show a triangle on a sphere, providing the basis for calculating the necessary formula.

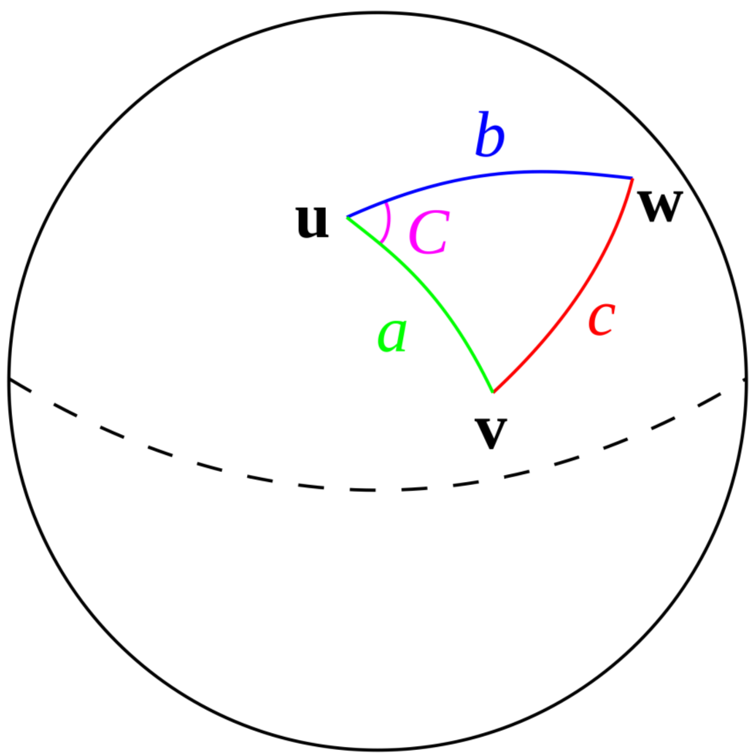

Figure 13 Globe with triangle and angles after Johnson (2008)

The required equations in spherical geometry are given below. If two points, p_1 and p_2, exist on a spherical surface, the Haversine of the central angle between the two points is given by equation (5):

$$\text{haversin}\left(\frac{d}{r}\right) = \text{haversin }(\phi_2 - \phi_1) + \cos(\phi_1)\cos(\phi_2)\text{haversin}(\psi_2 - \psi_1) \qquad (5)$$

where haversin is determined from the Haversine function, a versine function that is (Borowski & Borwein, 1989; Wikipedia contributors, 2012, June 4) given in equation (6)

$$\text{haversin}(\theta) = \sin(\frac{\theta}{2})^2 \qquad (6)$$

where d is the spherical distance or great circle distance between the two points, p_1 and p_2 then. r . is the radius of the sphere, which in terms of the earth for this work is assumed constant, $\frac{d}{r}$ is the central angle in radians, ϕ_1 and ϕ_2 are the latitude set and, ψ_1 and ψ_2 are the longitude set of p_1 and p_2 respectively. In terms of the variables shown on *Figure 13*, equation (5) can be expressed as:

$$\text{haversin }(c) = \text{haversin }(a - b) + \sin(a)\sin(b)\text{haversin(C)} \qquad (7)$$

Wysession et al. (1995) suggested a two degree angle as being adequate to define the edge of the interplate and intraplate regions. An alternative hypothesis is a fixed width as earthquake mechanics should not be related to a position on the earth as the fixed angle suggests.

Figure 14 show the variation in the width of a degree of longitude with changing latitude from the equation to the pole.

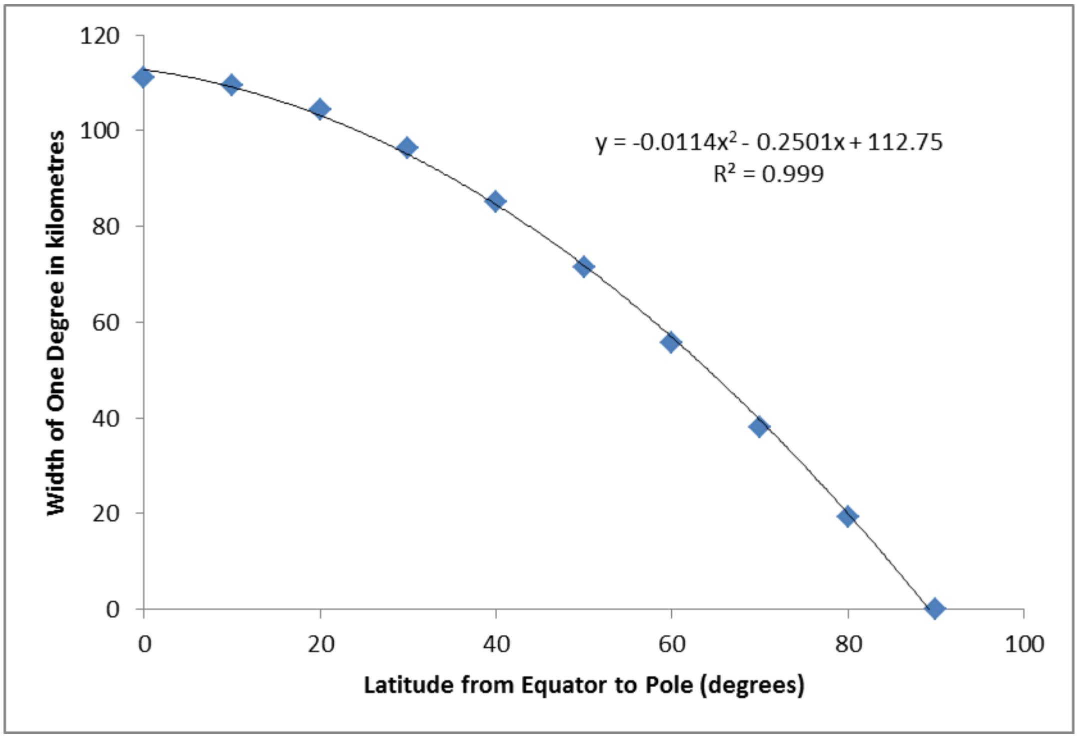

Figure 14 Width of a degree of longitude with latitude

In summary, the difference in the definition of the defined width of the interplate zone may have impact on the number of counted intraplate and interplate earthquakes. This study takes look at a fixed width.

CHAPTER III

METHODOLOGY

Introduction

The research stages are:

- Collect the data on earthquakes and tectonic plate boundaries
- Select the locations for the analysis of each boundary type
- Plot the tectonic plate boundaries in ArcGIS software
- Plot the earthquakes in ArcGIS with magnitude 5.0 and above
- Analyze the graphs plotted to determine the areal extent of the interplate areas based on the analysis assuming a linear width for the interplate earthquake region, so as to determine a statistically acceptable linear width

Data Collection

The data required for the analyses is obtained from the USGS/NEIC (PDE) 1973– 2012 earthquake database (U.S. Geological Survey, 2011a). The criteria used for the earthquake data is that the earthquakes need to have an intensity of 5.0 or greater for the analysis as no recorded fatal event has a lower threshold (BBC, 2002; Jogunoori, 2011; Nichols, 2005). The tectonic plate boundaries and the base map used for ArcGIS analysis are obtained from the USGS website and ESRI online database (reference). The earthquake points are imported onto ArcInfo (Geographical Information System) GIS system as graphical points as shown in Figure 15.

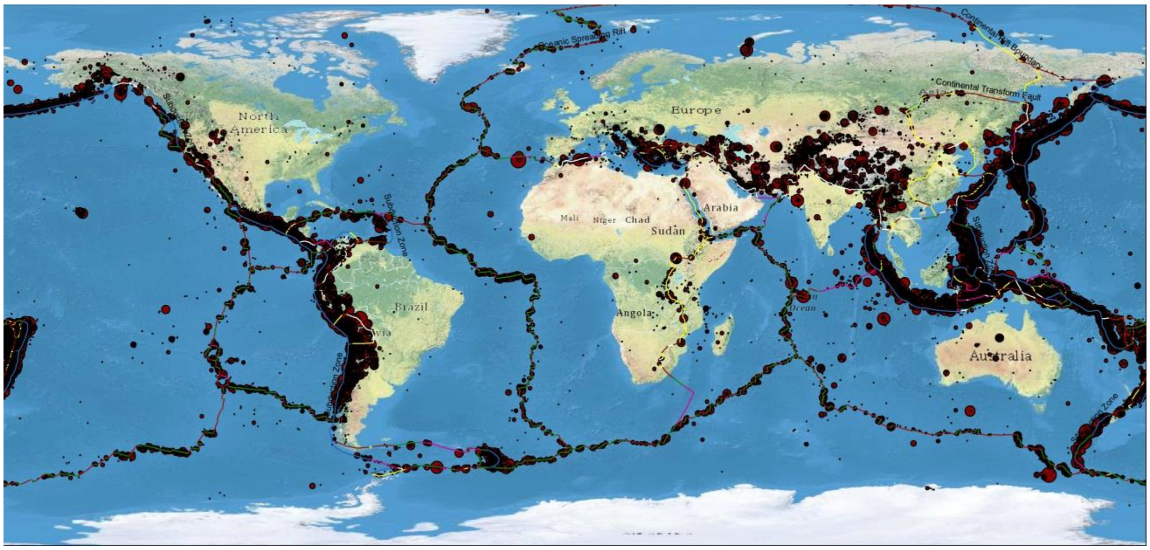

Figure 15 Plot of world earthquakes using ArcGIS

These points vary in size relative to its magnitude. Six segments spread over the geological locations are taken for each type of plate boundary, i.e., divergent, convergent, and transform boundary. The criteria utilized to choose the locations of these segments are:

1. Segments of arbitrary lengths for the tectonic plate boundary of certain type, among convergent, divergent and transform boundary are chosen for the analysis

2. The segments are chosen in such a way that the earthquake points being taken into consideration are spatially independent from other type of plate boundary at a time.

A buffer layer is created for each side of the plate boundary, namely left and right for the plate boundary as an aid for selection of the earthquake points. The selection by location tool is used to determine the number of earthquakes in each segment. The number of earthquakes is measured at distances of 20km, 40km, 60km, and so on up to 400km on either sides of the tectonic plate-boundary. The data, so obtained, is plotted as a graph with the distance of the earthquake points from the plate boundary against the percent of the number of the earthquakes observed in each 20km region.

Figure 16 illustrates the fifteen major plate boundaries color-coded outlined by the tectonic plate boundaries.

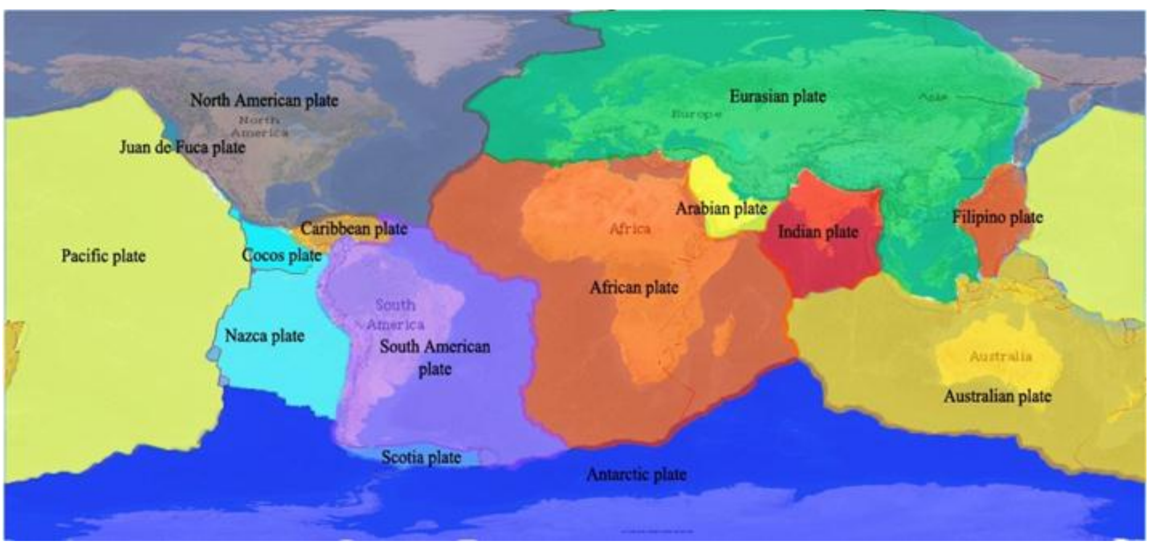

Figure 16 The fifteen major plate boundaries imported into the ArcGIS software

The following assumptions apply in the selection and analysis criteria for the research purpose:

- The interaction between the different types of tectonic plate boundaries namely convergent, divergent and transform is avoided using a spatial difference in the boundary overlap of the buffer regions created with a width of 400km on both the sides of the tectonic plate boundary
- The location of the earthquake data segments on the globe is projected using WGS-1984 projection
- The data segments taken into consideration for the research purpose are spread on the world map with locations selected that are not at problematic boundaries, such as northern Japan where multiple plate problems exist and are beyond the scope of this work.

Stages

Stage 1: Site Selection

Stage 1 is the location of the sites on the tectonic boundaries for the analysis of the earthquake location relative to the plate boundary.

Stage 2: USGS Data Collection

Stage 2 is the collection of the earthquake data from the USGS Sources.

Stage 3: Boundary Earthquake Data Sets

Stage 3 is the creation of the data sets for each length of boundary shown in Table 2, Table 3 and Table 4 in the results section of the thesis.

Stage 4: Analysis of the Results

Stage 4 provides a summary of the key results for the data and analysis shown in the several appendices.

Stage 5: Hypothesis Results

Stage 5 provides a review of the hypothesis and a suggestion for future work.

CHAPTER IV

RESULTS

Introduction

The analysis of the results has been completed in three stages.

Stage 1: Selection of Study Sites

Two methods are available for the selection of study sites:

1. Method 1 is an arbitrary selection of study sites by the researcher
2. Method 2 is a random selection of study sites using accepted statistical theory

This study is part of a group of studies into the definition of the boundary width between interplate and intraplate earthquakes. This study used Method 1 for the selection of the sites, the statistical issues associated with that decision are well understood by the researcher, but the point of the study is to determine if a change in the definition is warranted at this stage. If a change in the definition is warranted then a set of separate studies of each of the three different types of plate boundaries is warranted using Method-2.

The length of the equator calculated to be 40,075 km is utilized for the purpose of calculation of the linear width of the interplate earthquake region. The two degree angle at the equator is equivalent to 222.4 kilometers using the Haversine formula (Moritz, 1980; Robusto, 1957).

Six sites were selected that were free from interference in terms of impacts from different boundary types. The table provides the starting point and the ending point for the length of the boundary used in the analysis. The sites selected for the study are shown in Figure 17.

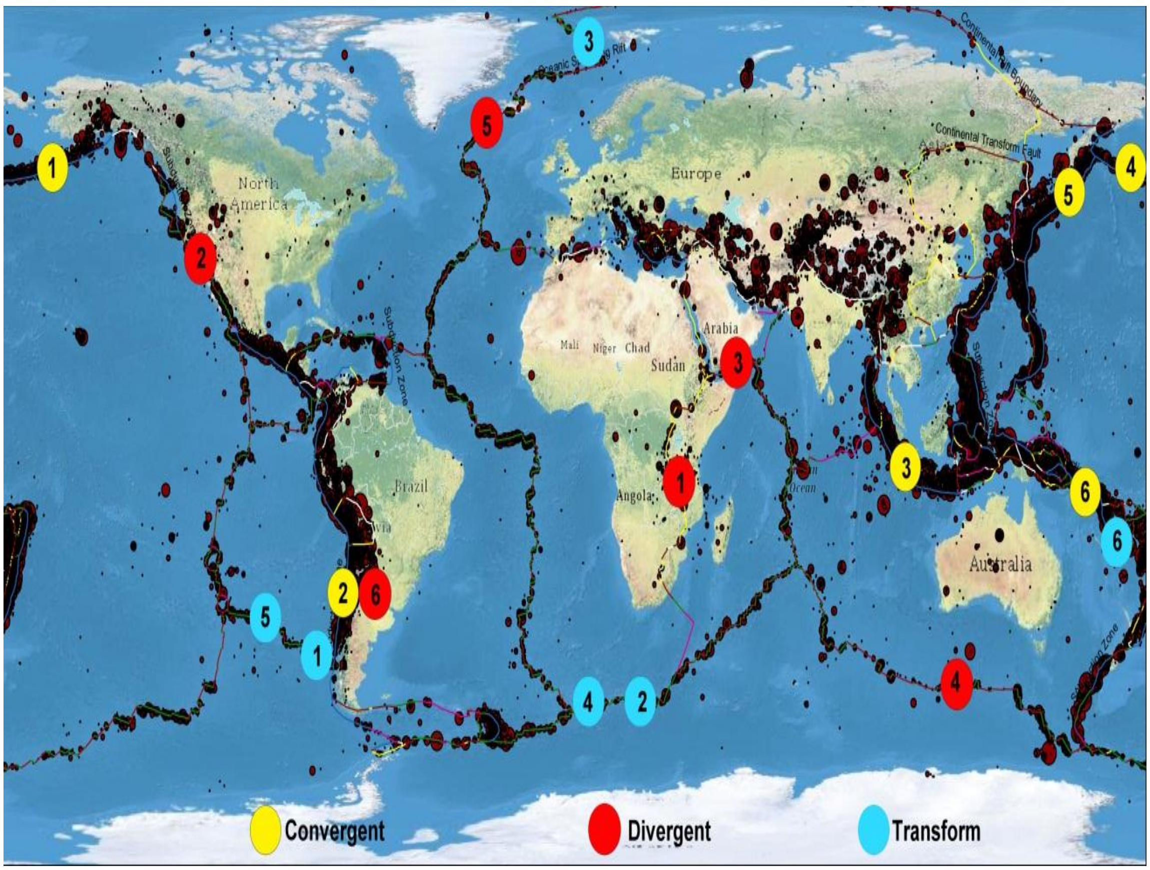

Figure 17 Selected sites for the study

Details of the selected convergent sites are presented in Table 2.

Table 2
Selected Sites – Convergent

Segment	Latitude and Longitude of plate end	Latitude and Longitude of plate end	Length (km)	Comments
C1	59.23N 145.82W	50.37N 180.12W	2375	This study is selected near the Gulf of Alaska at the intersection of the Pacific plate and the North American plate
C2	45.68S 76.07W	21.87S 71.33W	2682	This study is selected near Chile at the intersection of the Nazca plate and the South American plate
C3	11.5S 120.88E	1.37N 96.22E	3078	This study is selected near Indonesia at the intersection of the Australian plate and the Eurasian plate
C4	55.09N 164.06E	34.31N 141.71E	2882	This study is selected near the Bering sea at the intersection of the Pacific plate and the North American plate
C5	55.208N 163.97E	50.51N 179.92E	1188	This study is selected near Japan at the intersection of the Pacific plate and the North American plate
C6	8.24S 156.33E	22.93S 173.12E	2425	This study is selected near Papua New Guinea at the intersection of the Pacific plate and the Australian plate

Details of the selected divergent sites are presented in Table 3.

Table 3
Selected Sites - Divergent

Segment	Latitude and Longitude of plate end	Latitude and Longitude of plate end	Length (km)	Comments
D1	4.10N 30.48E	21.36S 33.01E	2844	This study is selected near the Democratic Republic of the Congo and Tanzania
D2	40.29N 124.41W	35N 119.35W	737.6	This study is selected near California at the intersection of the Pacific plate and the North American plate
D3	11.98N 43.72E	14.65N 56.17E	1379	This study is selected near the Gulf of Aden near Yemen at the intersection of the Arabian plate and the African plate
D4	47.26S 100.11E	49.74S 125.77E	1901	This study is selected in the Indian ocean at the intersection of the Australian plate and the Antarctic plate
D5	71.37N 3.71W	78.09N 7.72E	815.3	This study is selected near Iceland at the intersection of the Eurasian plate and the North American plate
D6	78.20N 125.63E	66.94N 141.22E	1345	This study is selected near Argentina at the intersection of the Nazca plate and the South American plate

Details of the selected transform sites are presented in Table 4.

Table 4
Selected Sites – Transform

Segment	Latitude and Longitude of plate end	Latitude and Longitude of plate end	Length (km)	Comments
T1	35.05S 108.84W	36.26S 97.43W	1039	This study is selected in the South Pacific ocean at the intersection of the Nazca plate and the Antarctic plate
T2	41.45S 90.06W	41.20S 83.83W	520.9	This study is selected in the Southern Ocean at the intersection of the African plate and the Antarctic plate
T3	80.36N 2.32W	78.26N 7.07E	302.7	This study is selected in the Greenland Sea at the intersection of the Eurasian and the North American plates
T4	53.25S 136.25W	55.50S 127.32W	5358	This study is selected in the Southern Ocean at the intersection of the African plate and the Antarctic plate
T5	54.99S 16.61W	56.04S 121.87W	629.6	This study is selected in the South Pacific ocean at the intersection of the Nazca plate and the Antarctic plate
T6	47.22S 31.88E	52.89S 21.07E	994.7	This study is selected near Papua New Guinea at the intersection of the Pacific plate and the Australian plate

Stage 2: USGS Earthquake Data

Earthquake data was obtained from the USGS database for recorded earthquakes from 1973 to the present. The data obtained was location in latitude and longitude, and magnitude. The data was entered into the ArcGIS Software (provide reference).

Stage 3: Boundary Earthquake Data Sets

There are three different types of plate boundary. The complete data set for each boundary type is summarized in a separate appendix for each boundary type as listed in Table 5.

Table 5
List of Data Sets in the Appendices

Appendix	Boundary Type
A	Convergent Plate Boundary
B	Divergent Plate Boundary
C	Transform Plate Boundary

Each data set has earthquake numbers grouped into twenty-kilometer lengths.

Stage 4: Analysis of the Results

The analysis steps completed on the data sets in each appendix are:

1. the number of earthquakes in each side of the boundary is compared in each data set

2. plot of the earthquake per cents with distance from the nominal centerline of the boundary

The results for the number of earthquakes on each side of the boundary show a most distinct difference for the convergent boundary with the side diving beneath the other plate having significantly greater numbers of earthquakes, the result is significant at the five percent level on a one sided Student's t Test (Miller & Freund, 1976). Similar although less statistically significant results were found on the other boundary types. This result has implications for fatality estimates in future earthquakes.

Graphs have been plotted of the number of earthquakes, expressed as a percentage, in binned distances of twenty kilometers from the nominal boundary line to four hundred kilometers from the centerline on either side of the boundary. The clear result is that single width does not exist to define interplate and interplate events. The width is distinct between boundary sides, varying from about 100 kilometers or one degree at the equator, termed an EQ_{deg} .

Stage 5: Hypothesis Results

The research hypothesis is:

A fixed width criterion for classifying an earthquake as interplate or intraplate earthquake provides a better statistical fit to the data, than a fixed angular amount.

Wysession et al. (1995) suggested in work on the Mid Atlantic Ridge that the definition of the boundary from interplate to interplate was two degrees either side of the nominal tectonic boundary or as specifically noted:

The epicenters were selected if they were at least 2 ° (222km) from a seismically active plate boundary. This was to avoid the inclusion of any transform, trench, or ridge earthquakes from contaminating our data set.

Jogunoori (2011), as part of a larger study, completed a study of the numbers of earthquakes within the two degree boundary and outside the two degree boundary for the world seismicity from 1973 to 2011, using the USGS database. Jogunoori used the literal definition of the two degrees. One alternative view is to take a strictly fixed width for the definition of the boundary width in the case of this research being the distance for two degrees at the equator, defined here as $2EQ_{\deg}$, but this fails to provide a satisfactory result because of the observed differences between boundaries and often the opposite sides of boundaries.

The reasonable conclusion is that future work is required on each of the boundary types to define a width at all locations on the earth's surface.

CHAPTER V

CONCLUSIONS

There is a widely accepted view that two types of earthquakes occur in the earth's crustal region, intraplate and interplate. Intraplate earthquake events are within a tectonic plate, and occur away from the margins of the plate. Interplate earthquake events occur in the immediate region of the nominal boundary between two plates. There are significant differences in the impact on urban areas between interplate and intraplate earthquakes of a given magnitude. This brings up a need to be able to determine the appropriate categories of earthquakes that to be used for the fatality models.

Wysession et al. (1995) showed for a small region of the Mid Atlantic Ridge that there were significant issues in defining the boundary between intraplate and interplate earthquakes. This work demonstrated the issues of correctly locating earthquakes and then determining if the earthquakes are interplate or intraplate. Wysession suggested that to define the boundary between intraplate and interplate earthquake events, a two-degree definition was a sufficient condition. Wysession's work centered on the area immediate north of the equator, so the two-degree definition equated to about two hundred and twenty kilometers.

This third study focuses solely on the definition of the boundary between the interplate and intraplate region. The first study, by Jogunoori (2011), showed that the adoption of a strict two degree definition of the boundary was not acceptable, assuming that the definition had a variable width, which is zero at the north and south poles, and about two hundred and twenty kilometers at the equator. The second study by Majmudar (2010) tested the fatality models for specific areas in India and Pakistan during the 2001 Bhuj (India) intraplate earthquake. This third study looked at the definition as a boundary width defined as two degrees at the equator, which is about two hundred and twenty kilometers, defined for simplicity using the symbol, $2EQ_{\mathrm{deg}}$. This definition removes the ambiguity from the angular width of a two-degree definition and provides a method to remove the angular component and hence provide more accurate fatality models.

This research work considered the definition of 220 kilometers on the boundary between interplate and intraplate events, as defining the distance used in this research, as $2EQ_{\mathrm{deg}}$. The research analyzed the distribution of earthquakes with distance from the nominal centerline for the tectonic boundary. The objectives are to determine if a break exists between the tectonically active interplate region and the tectonically less active intraplate region and to determine if the boundary was $2EQ_{\mathrm{deg}}$.

Wysession's study looked at the area, west of the Canary Islands. This study looked at eighteen locations not selected in a random fashion. The lack of random selection is a valid point of criticism, because the purpose of the work is only to review the option of using a constant width to differentiate the interplate and intraplate earthquake events. So, it was intended to avoid the possible effects of, adjacent tectonic plate boundaries, statistically insignificant number of earthquake events at the study sites, and geometrically non-linear plate boundaries, for this study using a manual selection of the study sites. Each of the boundary types, convergent, divergent and transform had six study regions selected that were away from the overlapping regions from the different plate boundaries. The study sites so selected were further divided into two parts, namely Side A (West or South of the plate boundary) and Side B (East or North of the plate boundary).

This proposed definition, $2EQ_{\deg}$, may be appropriate for discussion purposes, does not provide an acceptable definition for all boundary types, although it is an acceptable fit for Side A of Convergent Boundaries, but one would more properly conclude a number closer to $2.6EQ_{\deg}$ as appropriate for Side B of the Convergent Boundary. The analysis of the data also show the distinct feature of an increase in the frequency of earthquakes at equal intervals away from the tectonic plate boundary as shown in the figure on page 151 in Appendix E, which could represent the "buckling" of the tectonic plate boundaries due to the seismic stresses developed in the tectonic plates.

The results point to the difficulty of determining the difference between some interplate and intraplate earthquakes. Further work is required on all boundary types to determine the width of the interplate earthquake regions about the tectonic plate boundaries. The study should look at an average boundary length of five hundred kilometers for each study region. The issue of the apparent "buckling' of the divergent plate boundary at about one hundred kilometers also requires further work. Potential further studies could include the use a randomly selected set of regions of each boundary type, a study of all boundaries to determine the width at each point, and a full analysis of all boundaries is required to determine the width of the region that would differentiate between the interplate and intraplate earthquakes.

REFERENCES

Altis, S. (2001). Tectonic stress state in NE Japan as part of the Okhotsk plate. *Tectonophysics, 339*(3–4), 311-329. doi: 10.1016/s0040-1951(01)00139-1

Andrade, V., & Rajendran, K. (2011). Intraplate Response to the Great 2004 Sumatra-Andaman Earthquake: A Study from the Andaman Segment. *Bulletin of the Seismological Society of America, 101*(2), 506-514. doi: doi:10.1785/0120100155

Astroza, M., Sandoval, M., & Kausel, E. (2005b). Estudio comparativo de los efectos de los sismos chilenos de subducción del tipo intraplaca de profundidad intermedia. *Proc. IX Jornadas De Sismología e Ingeniería Antisísmica,* Paper A01-05, Concepción, Chile

Atkinson, G. M., & McCartney, S. E. (2005). A Revised Magnitude-Recurrence Relation for Shallow Crustal Earthquakes in Southwestern British Columbia: Considering the Relationships between Moment Magnitude and Regional Magnitudes. *Bulletin of the Seismological Society of America, 95*(1), 334-340. doi: 10.1785/0120040095

Bath, M. (1981). Earthquake magnitude - recent research and current trends. *Earth-Science Reviews, 17*(4), 315-398.

BBC. (2002). No more survivors in Italian School Fridy, 1 November, 2002, 15:23 GMT. Retrieved 21 August 2003, from http://news.bbc.co.uk/2/hi/europe/2384593.stm

Bird, P. (Cartographer). (2003). An updated digital model of plate boundaries, *Geochemistry Geophysics Geosystems*, 4(3), 1027, doi:10.1029/2001GC000252.

Bird, P., Kreemer, C., & Holt, W. E. (2010). A Long-Term Forecast of Shallow Seismicity Based on the Global Strain Rate Map. *Seismological Research Letters, 81*(2), 184-185

Bird, P., & Liu, Z. (2007). Seismic Hazard Inferred from Tectonics: California. *Seismological Research Letters, 78*(1), 37-38

Bommer, J. J., Scherbaum, F., Bungum, H., Cotton, F., Sabetta, F., & Abrahamson, N. A. (2005). On the Use of Logic Trees for Ground-Motion Prediction Equations in Seismic-Hazard Analysis. *Bulletin of the Seismological Society of America, 95*(2), 377-389. doi: 10.1785/0120040073

Boore, D. M. (2005). On Pads and Filters: Processing Strong-Motion Data. *Bulletin of the Seismological Society of America, 95*(2), 745-750. doi: 10.1785/0120040160

Boore, D. M., Azari Sisi, A., & Akkar, S. (2012). Using Pad-Stripped Acausally Filtered Strong-Motion Data. *Bulletin of the Seismological Society of America, 102*(2), 751-760. doi: 10.1785/0120110222

Borowski, E. J., & Borwein, J. M. (1989). *Dictionary of Mathematics* (Second ed.). Glasgow: Collins.

Brune, J. N. (1970). Tectonic Stress and the Spectra of Seismic Shear Waves from Earthquakes. *Journal of Geophysical Research, 75*(26), 4997 - 5009.

Clarke, W. (1869). On the causes and phenomena of earthquakes, especially in relation to shocks felt in New South Wales and in other provinces of New South Wales. *Proceedings and Journal of the Royal Society of New South Wales, 2*, 51-86.

Cotton, L. A. (1921). The Kurrajong Earthquake of August 15, 1919. *Proceedings and Journal of the Royal Society of New South Wales, 55*, 83-104.

Di Alessandro, C., Bonilla, L. F., Boore, D. M., Rovelli, A., & Scotti, O. (2012). Predominant Period Site Classification for Response Spectra Prediction Equations in Italy. *Bulletin of the Seismological Society of America, 102*(2), 680-695. doi: 10.1785/0120110084

Frankel, A. D., Mueller, C. S., Barnard, T. P., Leyendecker, E. V., Wesson, R. L., Harmsen, S. C., Hopper, M. G. (2000). USGS National Seismic Hazard Maps. *Earthquake Spectra, 16*(1), 1 - 19.

Gaba, E. (Cartographer). (2006). Detailed world map in English showing the tectonic plates with their movement vectors. Retrieved from http://en.wikipedia.org/wiki/File:Tectonic_plates_boundaries_detailed-en.svg

Garcia, D., Singh, S. K., Herraiz, M., Pacheco, J. F., & Ordaz, M. (2004). Inslab earthquakes of central Mexico: Q, source spectra, and stress drop. *Bulletin of the Seismological Society of America, 94*(3), 789.

Gubbins, D. (1992). *Seismology, and Plate Tectonics* (Second ed.). Cambridge: Cambridge University Press.

Gutenberg, B., & Richter, C. F. (1954). *Seismicity of the Earth and Associated Phenomena*. Princeton New Jersey: Princeton University Press.

Gutenberg, B., & Richter, C. F. (1956). Earthquake Magnitude, Intensity, Energy and Acceleration. *Bulletin of the Seismological Society of America, 46*, 105-143.

Hogben, G. (1893). The Tasmanian Earthquake of the 27th January, 1892. *Transactions - Chemistry and Physics, Tasmanian Royal Society*(Art LXI), 594-601.

Jogunoori, P. (2011). *Analysis of Deaths caused by Interplate and Intraplate Earthquakes.* MSc. Masters, TAMU, College Station.

Johnson, S. G. (Cartographer). (2008). Illustration of a spherical triangle, originally for illustrating the law of haversines and now used in other spherical trigonometry articles as well. Retrieved from http://en.wikipedia.org/wiki/File:Law-of-haversines.svg

Johnston, A. C., & Kanter, L. R. (1990). Earthquakes in Stable Continental Crusts. *Scientific American, 262*(3), 42-49.

Johnston, A. C., & Nava, S. J. (1994). *Seismic Hazard Assessment in the Central United States.* Paper presented at the ATC-35 Seminar on New Developments in Earthquake Ground Motion Estimation and Implications for Engineering Design Practice, Los Angles.

Johnston, A. C., & Schweig, E. S. (1996). The enigma of the New Madrid earthquakes of 1811-1812. *Annual Review of Earth and Planetary Science, 24*, 339-384.

Kanamori, H., & Anderson, D. L. (1975). Theoretical basis of some empirical relations in seismology. *Bulletin of the Seismological Society of America, 65*(5), 1073

Kausel, E., & Campos, J. (1992). The Ms= 8 tensional earthquake of 9 December 1950 of northern Chile and its relation to the seismic potential of the region. *Physics of the Earth and Planetary Interiors, 72*(3-4), 220-235.

Kim, W.-Y., Richards, P. G., Adushkin, V., & Ovtchinnilov, V. (2001). Borovoye Digital Seismogram Archive for Underground Nuclear Tests 1966-1996 (pp. 41). Boston: Columbia University Lamont -Doherty Earth Observatory.

Kitamura, Y., & Kimura, G. Dynamic role of tectonic mélange during interseismic process of plate boundary mega earthquakes. *Tectonophysics*(0). doi: 10.1016/j.tecto.2011.07.008

Kotò, B. (1893). On the causes of the great earthquake in Central Japan, 1891. *Journal of the College of Science Imperial University, Japan, 5*(4), 296 - 353.

Leyton, F., Ruiz, J., Campos, J., & Kausel, E. (2009). Intraplate and interplate earthquakes in Chilean subduction zone: A theoretical and observational comparison. *Physics of the Earth and Planetary Interiors, 175*(1-2), 37-46. doi: doi:10.1016/j.pepi.2008.03.017

Little, W., Fowler, H. W., Coulson, J., Onions, C. T., & Friedrichsen, G. W. S. (1973). *The Shorter Oxford English Dictionary on Historical Principles*. Oxford: Clarendon Press.

Liu, K.-S., & Tsai, Y.-B. (2005). Attenuation Relationships of Peak Ground Acceleration and Velocity for Crustal Earthquakes in Taiwan. *Bulletin of the Seismological Society of America, 95*(3), 1045-1058. doi: 10.1785/0120040162

Mai, P. M., Spudich, P., & Boatwright, J. (2005). Hypocenter Locations in Finite-Source Rupture Models. *Bulletin of the Seismological Society of America, 95*(3), 965-980. doi: 10.1785/0120040111

Majmudar, K. (2010). A Study of the fatalities with distance from the epicenter. *Professional paper submitted to Texas A&M University*.

Miller, I., & Freund, J. E. (1976). *Probability and Statistics for Engineers* (2nd. ed.). Englewood Cliffs, N.J.: Prentice-Hall.

Moritz, H. (1980). Geodetic reference system 1980. *Journal of Geodesy, 54*(3), 395-405.

Musson, R. M. W. (1993). Comrie : a historical Scottish Earthquake Swarm and its place in the history of Seismology. *Terra Nova, 5*(5), 477-480.

Newmark, N. M., & Hall, W. J. (1978). *Development of Criteria for Seismic Review of Selected Nuclear Power Plants*. Washington : Nuclear Regulatory Commission, Office of Nuclear Reactor Regulation, Division of Operating Reactor: Springfield, Va.

Newmark, N. M., & Hall, W. J. (1981). *Earthquake Resistant Design Considerations and Seismic Design Spectra*. [Berkeley, Calif.]: Earthquake Engineering Research Institute.

Newmark, N. M., & Hall, W. J. (1982). *Earthquake Spectra and Design*. Berkeley, Calif.: Earthquake Engineering Research Institute.

Nichols, J. M. (1999). The assessment and repairs of certain structures after the Newcastle earthquake. *Masonry International, 13*(1), 11 - 22.

Nichols, J. M. (2003). *A Mathematical Review of the Non-Conservative Criteria Related to the Seismic Design Spectrum used in Intraplate Regions.* Paper presented at the XIV Mexican National Conference on Earthquake Engineering, Leon Mexico.

Nichols, J. M. (2005, May 2005). *Suggested Changes to the Non-Conservative Low Frequency Criteria for the Seismic Design Spectrum Used in Intraplate Regions.* Paper presented at the ERES 2005, Greece.

Nichols, J. M., & Beavers, J. E. (2008). World Earthquake Fatalities from the Past -- Implications for the Present and Future. *Natural Hazards Review, 9*(4), 179-189.

Page, A. W. (1991). The Newcastle Earthquake - Behaviour of masonry structures. *Masonry International, 5*(1), 11-18.

Page, A. W. (1992). The design, detailing and construction of masonry - the lessons from the Newcastle earthquake. *Australian Civil Engineering Transactions, 34*(4), 343-353.

Paul, J., Rajendran, C. P., Lowry, A. R., Andrade, V., & Rajendran, K. (2012). Andaman post-seismic deformation observations: still slipping after all these years? *Bulletin of the Seismological Society of America, 102*(1), 343-351. doi: doi: 10.1785/0120110074

Rajendran, K., Andrade, V., & Rajendran, C. P. (2011). The June 2010 Nicobar Earthquake: Fault Reactivation on the Subducting Oceanic Plate. *Bulletin of the Seismological Society of America, 101*(5), 2568–2577. doi: doi: 10.1785/0120110002

Richter, C. F. (1958). *Elementary Seismology*. San Francisco: Freeman.

Ricou, L.-E. (2004). Earth's tectonic history revisited in the light of episodic misfits between plate network and mantle convection. *Tectonophysics, 384*(1–4), 285-300. doi: 10.1016/j.tecto.2004.04.004

Robusto, C. (1957). The cosine-haversine formula. *The American Mathematical Monthly, 64*(1), 38-40.

Saragoni, G. R., Astroza, M., & Ruiz, S. (2004). *Comparative study of subduction earthquake ground motion of North, Central and South America*. Paper presented at the Paper presented at the 13th World Conference on Earthquake Engineering, Vancouver.

Scholz, C. H., Aviles, C., & Wesnousky, S. G. (1986). Scaling differences between large interplate and intraplate earthquakes. *Bulletin of the Seismological Society of America, 76*(1), 65-67

Standards Australia. (2001). Masonry Structures. Sydney: Standards Australia.

U.S. Geological Survey. (2011a). Latest Earthquakes Retrieved 21 March, 2011, from http://earthquake.usgs.gov/

U.S. Geological Survey (Cartographer). (2011b). The layer of the Earth we live on is broken into a dozen or so rigid slabs (called tectonic plates by geologists) that are moving relative to one another.

Weiran, Y., Zuoxun, Z., Dewei, L., Jishan, X., Jie, W., & Wenxing, L. (2009). Three-level Tectonic Model for Intraplate Earthquakes. *Earth Science Frontiers, 16*(1), 206-217. doi: doi:10.1016/S1872-5791(08)60073-1

Wikipedia contributors. (2012, June 4). Haversine formula, from http://en.wikipedia.org/w/index.php?title=Haversine_formula&oldid=495964121

Wysession, M. E., Wilson, J., Bartkó, L., & Sakata, R. (1995). Intraplate seismicity in the Atlantic Ocean Basin: A teleseismic catalog. *Bulletin of the Seismological Society of America, 85*(3), 755-774.

Zhao, J. X., & Xu, H. (2012). Magnitude-Scaling Rate in Ground-Motion Prediction Equations for Response Spectra from Large Subduction Interface Earthquakes in

Japan. *Bulletin of the Seismological Society of America, 102*(1), 222-235. doi: 10.1785/0120110154

Zlotnik, S., Díez, P., Fernández, M., & Vergés, J. (2007). Numerical modelling of tectonic plates subduction using X-FEM. *Computer Methods in Applied Mechanics and Engineering, 196*(41–44), 4283-4293. doi: 10.1016/j.cma.2007.04.006

APPENDIX A

CONVERGENT BOUNDARY DATA

Introduction

Six boundary segments were selected for the analysis of the distribution of earthquakes on the convergent boundary. The six groups were placed into four data sets as shown in Table 6.

Table 6
Convergent Boundary Data Sets One to Four

Set Number	Segments	Comments
1	C4 & C5	These two segments are chosen near Japan at the juncture between the Pacific plate with the Filipino plate (C4) and the North American plate (C5)
2	C1 & C6	Data points chosen to represent the juncture between the Pacific plate with the North American plate (C1) and the Nazca plate (C6)
3	C3	This segment represents the juncture between the Antarctic plate and the Australian plate
4	C2	This data segment represents the juncture between the Nazca plate and the South American plate

Convergent set number one contains 10341 earthquakes with a magnitude M_w of five or greater on Side B and 514 earthquakes on Side A. Table 7 show the number of earthquakes recorded in each of the segments.

Table 7
Earthquake Numbers Counted in Convergent Segments

Segments	Earthquake Numbers Side A	Earthquake Numbers Side B	Ratio
C1	54	1376	25
C2	54	1293	23
C3	94	2108	22.5
C4	28	364	13
C5	3	492	162
C6	281	4708	16.7

Figure 18 show a plot of the data for Side A and Side B earthquake numbers.

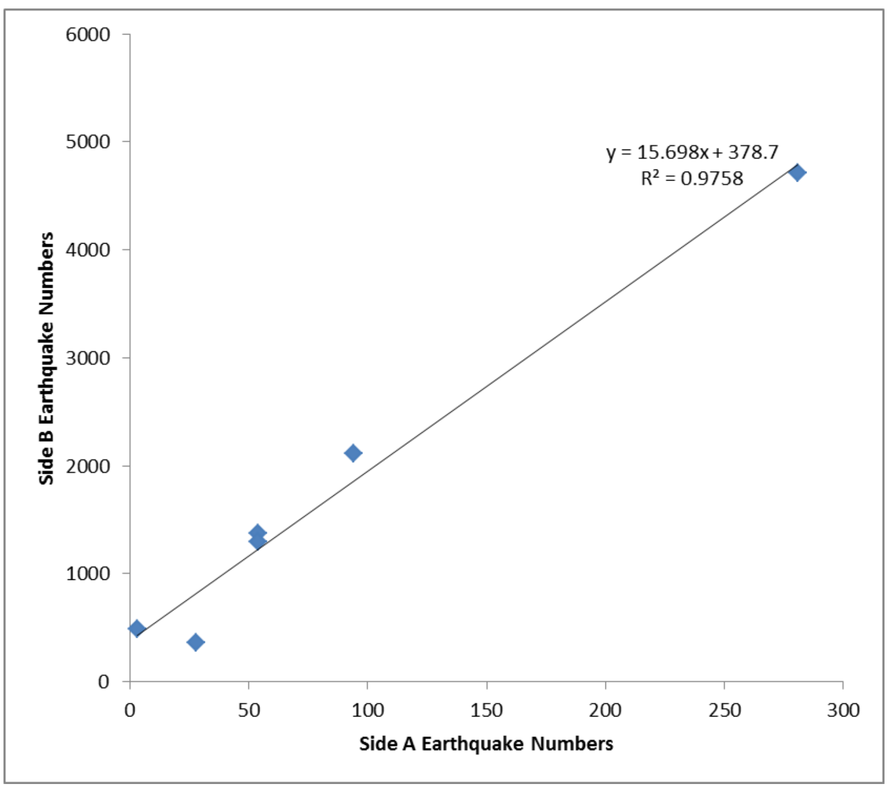

Figure 18 Convergent - number of earthquakes on each side of the boundary

As shown in Figure 18, the convergent boundary C5 is different to the remaining boundaries, with the number of earthquakes greater on Side B compared to Side A.

Convergent Boundary Set One

The data is shown in Table 8 and Table 9 for Side A and Side B respectively.

Table 8
Convergent Boundary Segment 1 Side A

Distance from boundary	No. of earthquakes	No. of earthquakes in the 20km segment	Per cent %	Difference %
20	5	5	9.26	
40	25	20	37.04	27.78
60	40	15	27.78	9.26
80	47	7	12.96	14.81
100	49	2	3.70	9.26
120	50	1	1.85	1.85
140	50	0	0.00	1.85
160	52	2	3.70	3.70
180	53	1	1.85	1.85
200	53	0	0.00	1.85
220	54	1	1.85	1.85
240	54	0	0.00	1.85
260	54	0	0.00	0.00
280	54	0	0.00	0.00
300	54	0	0.00	0.00
320	54	0	0.00	0.00
340	54	0	0.00	0.00
360	54	0	0.00	0.00
380	54	0	0.00	0.00
400	54	0	0.00	0.00

Figure 19 and Figure 20 show the results for Table 8 and Table 9 plotted with the distance from the nominal centerline of the boundary as the independent variable.

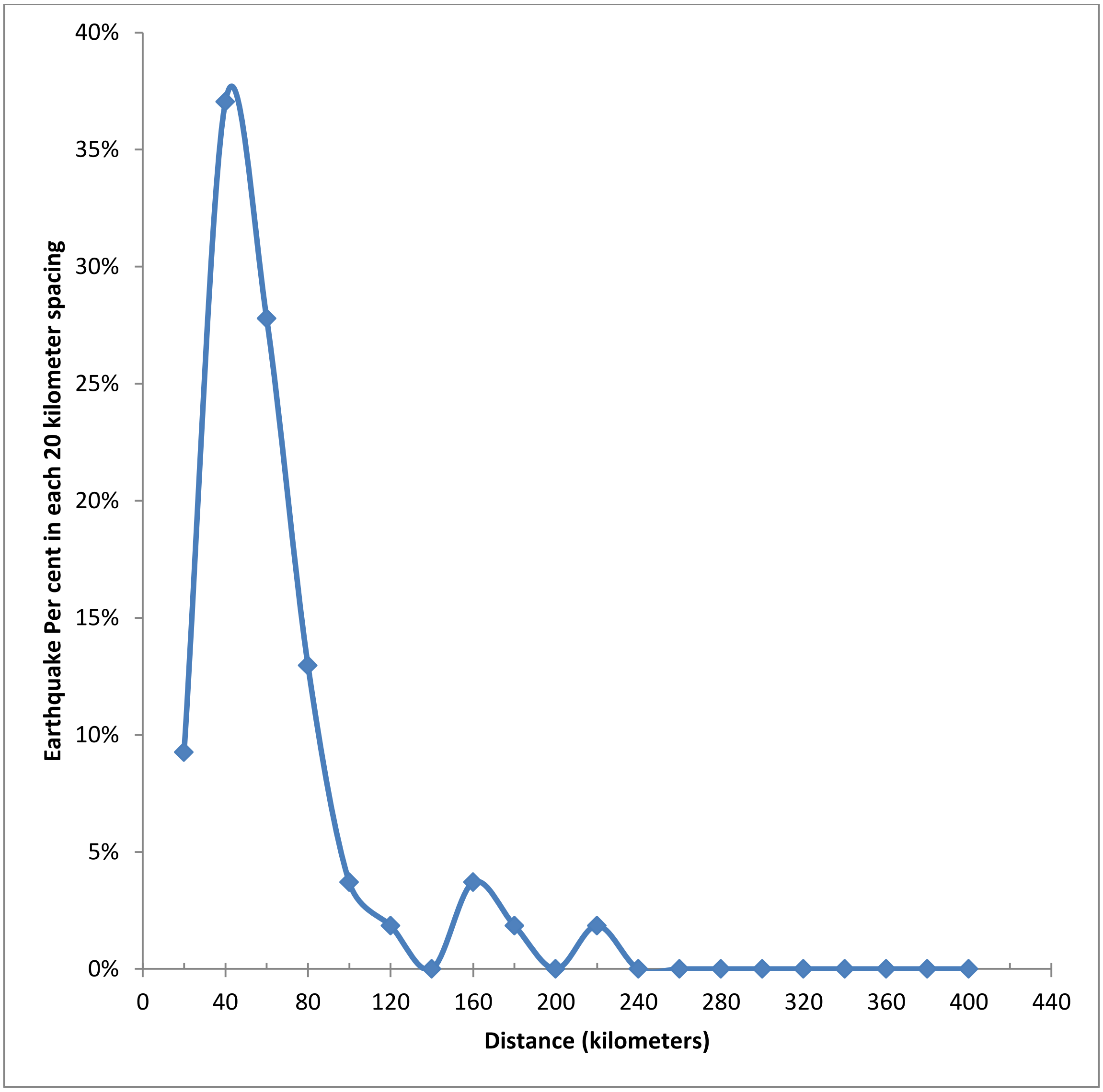

Figure 19 Convergent Boundary Segment 1 Side-A Results

Table 9
Convergent Boundary Segment 1 Side B

Distance from boundary	No. of earthquakes	No. of earthquakes in the 20km segment	Per cent %	Difference %
20	4	4	0.29	
40	37	33	2.40	2.11
60	236	199	14.46	12.06
80	558	322	23.40	8.94
100	808	250	18.17	5.23
120	1031	223	16.21	1.96
140	1127	96	6.98	9.23
160	1195	68	4.94	2.03
180	1237	42	3.05	1.89
200	1266	29	2.11	0.94
220	1293	27	1.96	0.15
240	1319	26	1.89	0.07
260	1333	14	1.02	0.87
280	1340	7	0.51	0.51
300	1347	7	0.51	0.00
320	1352	5	0.36	0.15
340	1358	6	0.44	0.07
360	1365	7	0.51	0.07
380	1367	2	0.15	0.36
400	1376	9	0.65	0.51

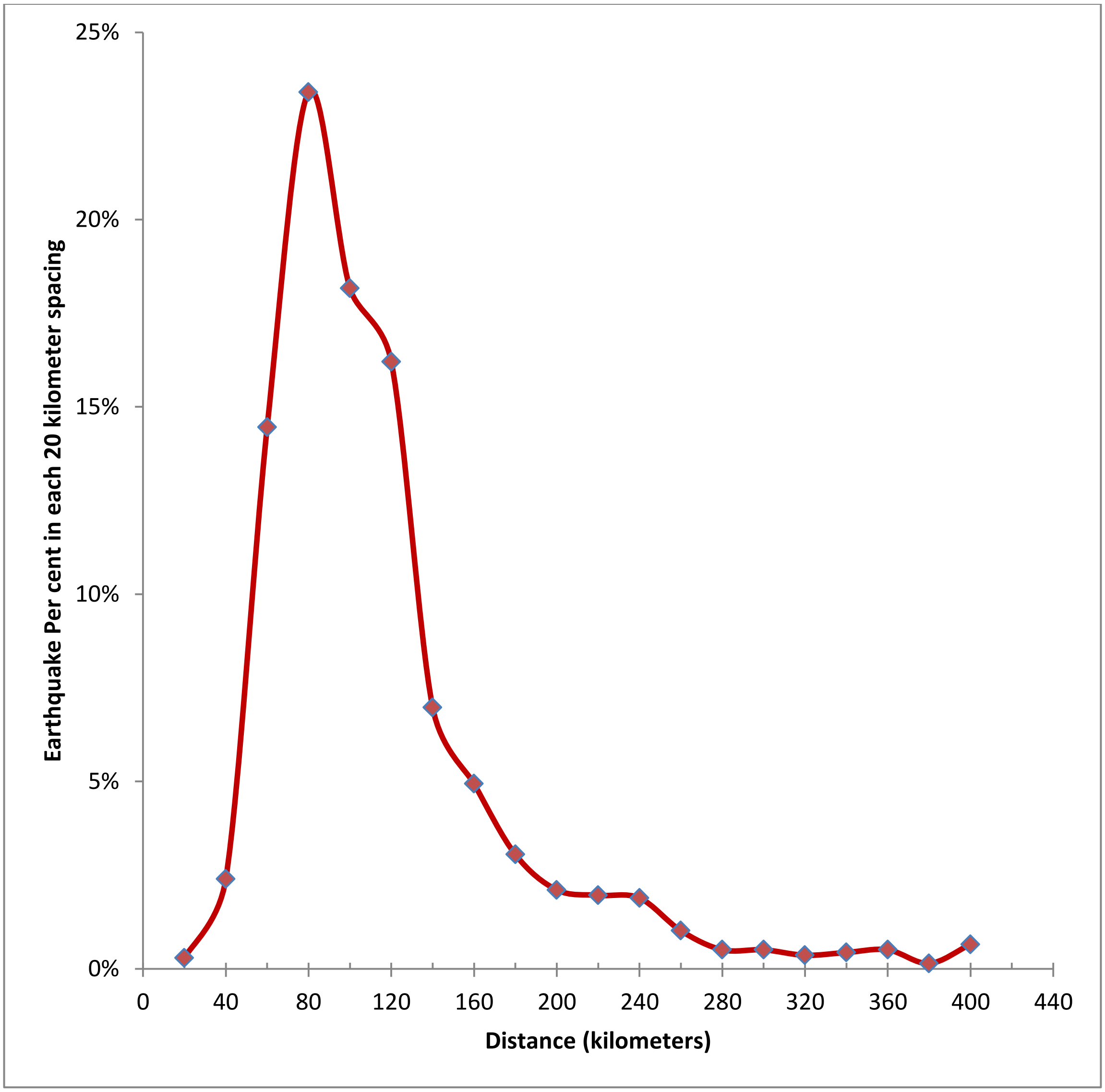

Figure 20 Convergent Boundary Segment 1 Side-B Results

Convergent Boundary Set Two

The data is shown in Table 10 and Table 11 for Side A and Side B respectively.

Table 10
Convergent Boundary Segment 2 Side A

Distance from boundary	No. of earthquakes	No. of earthquakes in the 20km segment	Per cent %	Difference %
20	21	21	38.89	
40	41	20	37.04	1.85
60	52	11	20.37	16.67
80	53	1	1.85	18.52
100	54	1	1.85	0.00
120	54	0	0.00	1.85
140	54	0	0.00	0.00
160	54	0	0.00	0.00
180	54	0	0.00	0.00
200	54	0	0.00	0.00
220	54	0	0.00	0.00
240	54	0	0.00	0.00
260	54	0	0.00	0.00
280	54	0	0.00	0.00
300	54	0	0.00	0.00
320	54	0	0.00	0.00
340	54	0	0.00	0.00
360	54	0	0.00	0.00
380	54	0	0.00	0.00
400	54	0	0.00	0.00

Figure 21 and Figure 22 show the results for Table 10 and Table 11 plotted with the distance from the nominal centerline of the boundary as the independent variable.

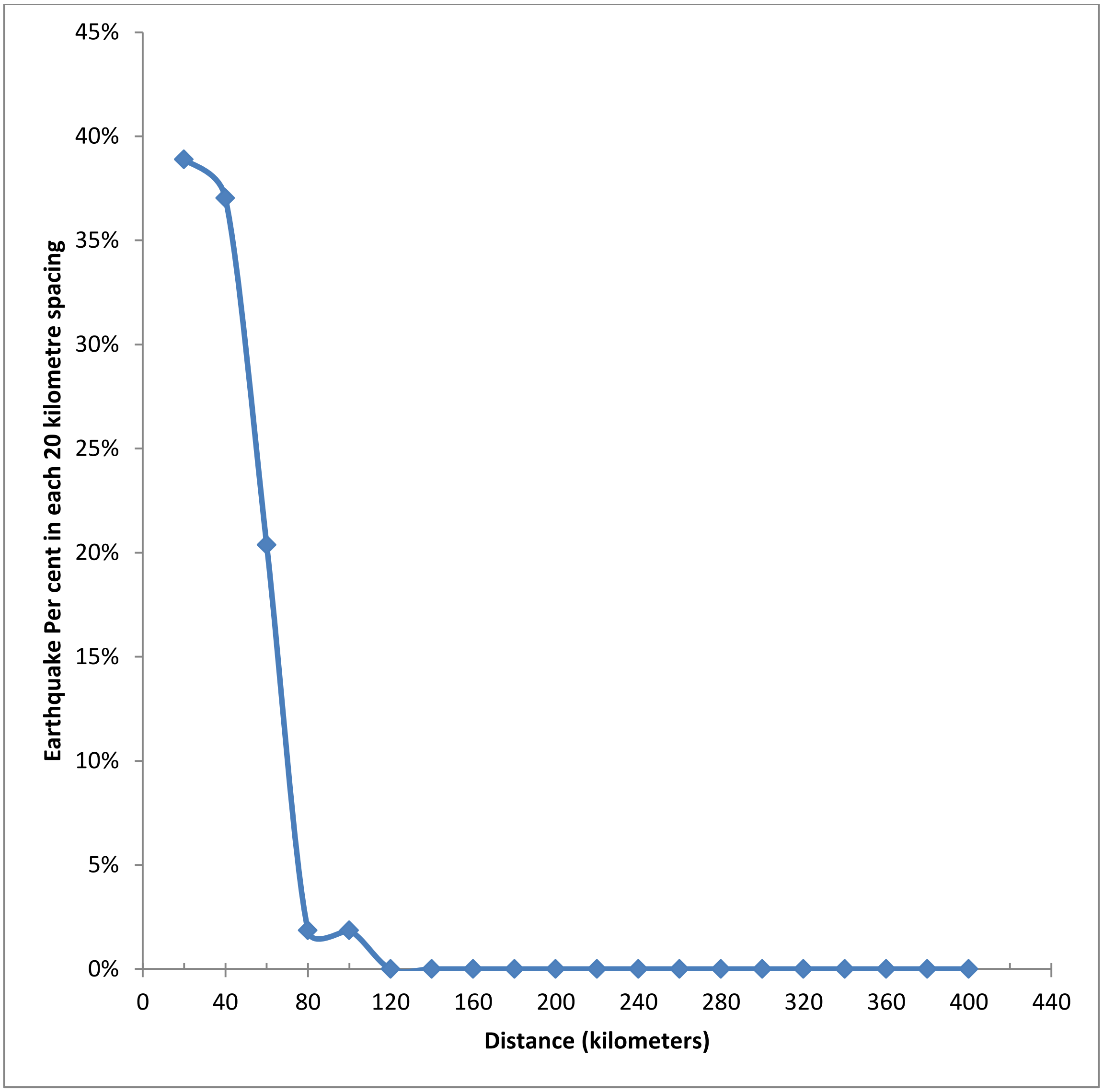

Figure 21 Convergent Boundary Segment 2 Side-A Results

Table 11
Convergent Boundary Segment 2 Side B

Distance from boundary	No. of earthquakes	No. of earthquakes in the 20km segment	Per cent %	Difference %
20	20	20	1.55	
40	50	30	2.32	0.77
60	89	39	3.02	0.70
80	221	132	10.21	7.19
100	433	212	16.40	6.19
120	661	228	17.63	1.24
140	874	213	16.47	1.16
160	1004	130	10.05	6.42
180	1067	63	4.87	5.18
200	1102	35	2.71	2.17
220	1123	21	1.62	1.08
240	1133	10	0.77	0.85
260	1146	13	1.01	0.23
280	1177	31	2.40	1.39
300	1196	19	1.47	0.93
320	1222	26	2.01	0.54
340	1239	17	1.31	0.70
360	1252	13	1.01	0.31
380	1269	17	1.31	0.31
400	1293	24	1.86	0.54

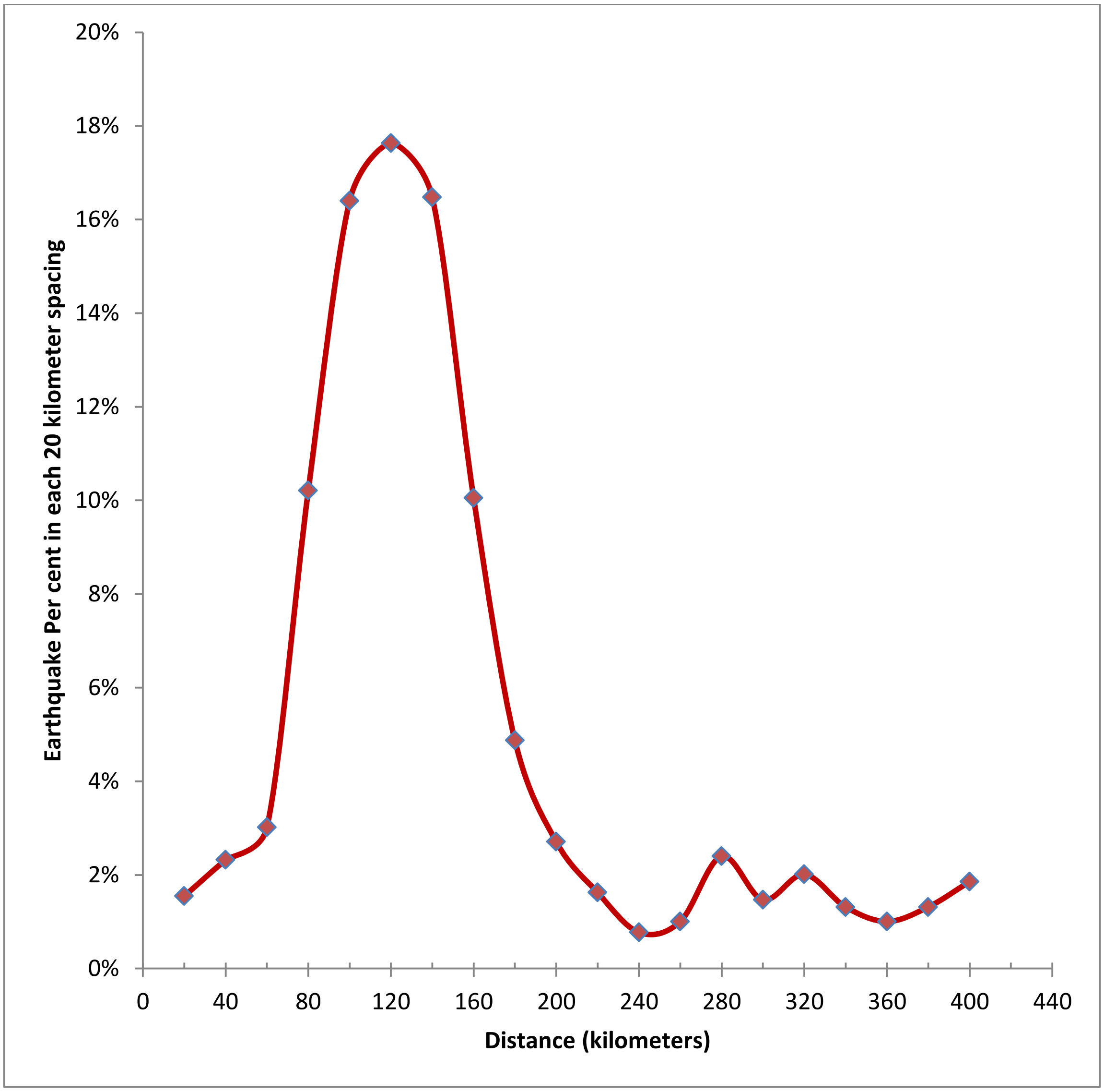

Figure 22 Convergent Boundary Segment 2 Side-B Results

Convergent Boundary Set Three

The data is shown in Table 12 and Table 13 for Side A and Side B respectively.

Table 12
Convergent Boundary Segment 3 Side A

Distance from boundary	No. of earthquakes	No. of earthquakes in the 20km segment	Per cent %	Difference %
20	27	27	28.72	
40	55	28	29.79	1.06
60	68	13	13.83	15.96
80	74	6	6.38	7.45
100	80	6	6.38	0.00
120	81	1	1.06	5.32
140	86	5	5.32	4.26
160	88	2	2.13	3.19
180	89	1	1.06	1.06
200	90	1	1.06	0.00
220	91	1	1.06	0.00
240	91	0	0.00	1.06
260	92	1	1.06	1.06
280	93	1	1.06	0.00
300	93	0	0.00	1.06
320	93	0	0.00	0.00
340	93	0	0.00	0.00
360	93	0	0.00	0.00
380	94	1	1.06	1.06
400	94	0	0.00	1.06

Figure 23 and Figure 24 show the results for Table 12 and Table13 plotted with the distance from the nominal centerline of the boundary as the independent variable.

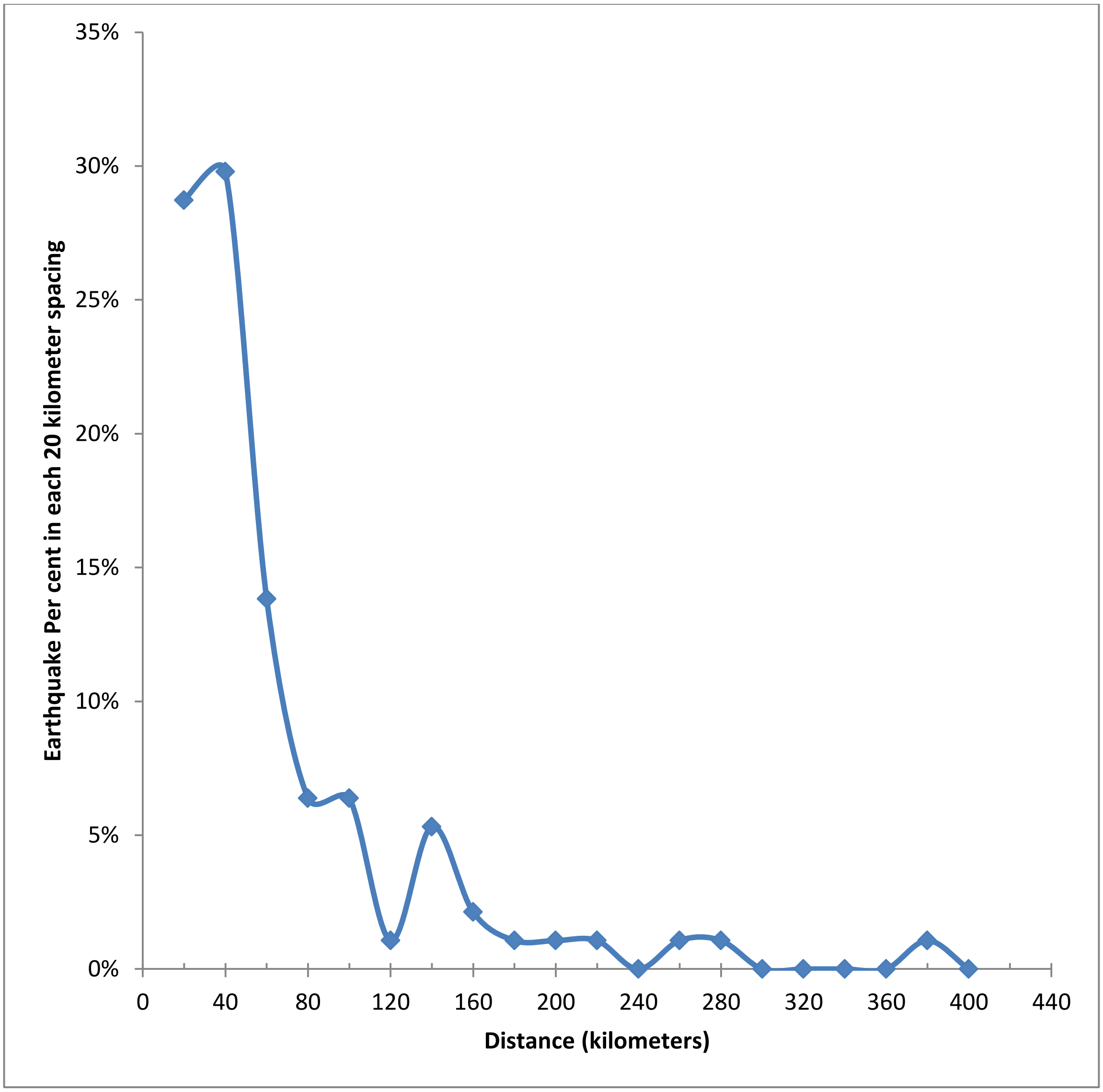

Figure 23 Convergent Boundary Segment 3 Side-A Results

Table 13
Convergent Boundary Segment 3 Side B

Distance from boundary	No. of earthquakes	No. of earthquakes in the 20km segment	Per cent %	Difference %
20	62	62	2.94	
40	133	71	3.37	0.43
60	259	126	5.98	2.61
80	398	139	6.59	0.62
100	541	143	6.78	0.19
120	743	202	9.58	2.80
140	895	152	7.21	2.37
160	1051	156	7.40	0.19
180	1206	155	7.35	0.05
200	1422	216	10.25	2.89
220	1587	165	7.83	2.42
240	1763	176	8.35	0.52
260	1896	133	6.31	2.04
280	1970	74	3.51	2.80
300	2011	41	1.94	1.57
320	2052	41	1.94	0.00
340	2081	29	1.38	0.57
360	2094	13	0.62	0.76
380	2101	7	0.33	0.28
400	2108	7	0.33	0.00

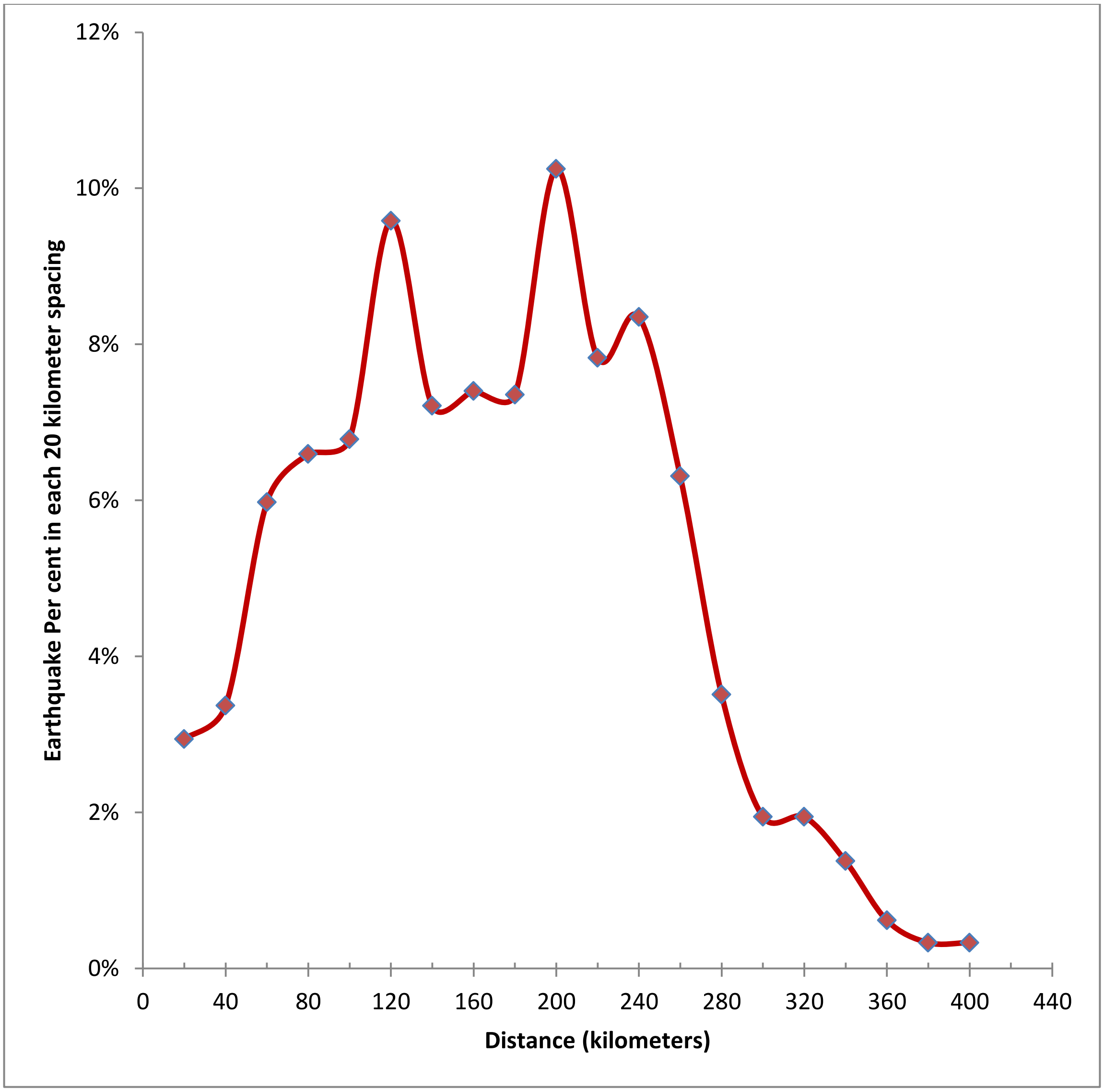

Figure 24 Convergent Boundary Segment 3 Side-B Results

Convergent Boundary Set Four

The data is shown in Table 14 and Table 15 for Side A and Side B respectively.

Table 14
Convergent Boundary Segment 4 Side A

Distance from boundary	No. of earthquakes	No. of earthquakes in the 20km segment	Per cent %	Difference %
20	7	7	25.00	
40	15	8	28.57	3.57
60	18	3	10.71	17.86
80	23	5	17.86	7.14
100	27	4	14.29	3.57
120	28	1	3.57	10.71
140	28	0	0.00	3.57
160	28	0	0.00	0.00
180	28	0	0.00	0.00
200	28	0	0.00	0.00
220	28	0	0.00	0.00
240	28	0	0.00	0.00
260	28	0	0.00	0.00
280	28	0	0.00	0.00
300	28	0	0.00	0.00
320	28	0	0.00	0.00
340	28	0	0.00	0.00
360	28	0	0.00	0.00
380	28	0	0.00	0.00
400	28	0	0.00	0.00

Figure 25 and Figure 26 show the results for Table 14 and Table 15 plotted with the distance from the nominal centerline of the boundary as the independent variable.

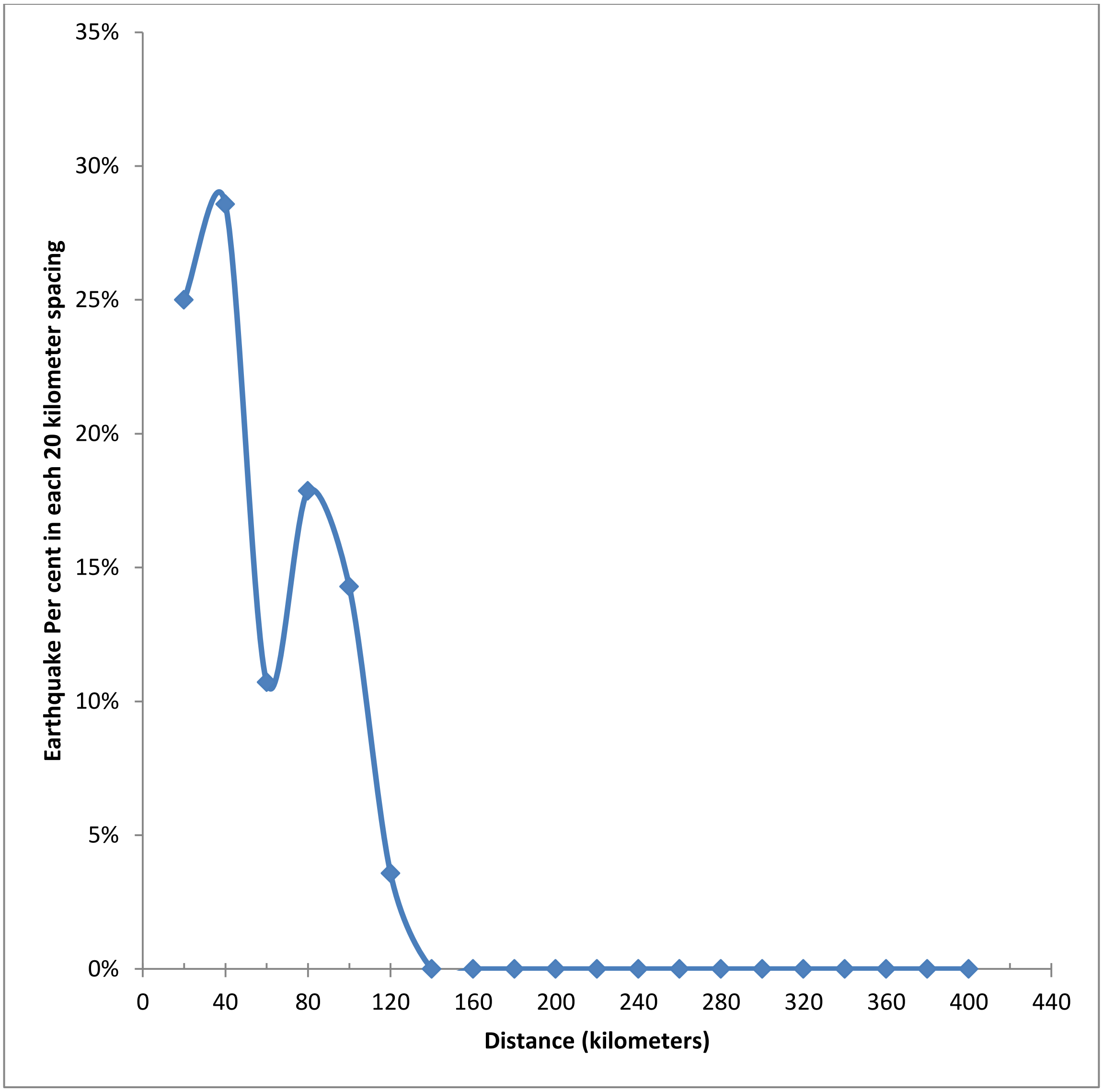

Figure 25 Convergent Boundary Segment 4 Side-A Results

Table 15
Convergent Boundary Segment 4 Side B

Distance from boundary	No. of earthquakes	No. of earthquakes in the 20km segment	Percentile	Difference
20	1	1	0.27	
40	15	14	3.85	3.57
60	81	66	18.13	14.29
80	207	126	34.62	16.48
100	275	68	18.68	15.93
120	309	34	9.34	9.34
140	330	21	5.77	3.57
160	346	16	4.40	1.37
180	357	11	3.02	1.37
200	362	5	1.37	1.65
220	364	2	0.55	0.82
240	364	0	0.00	0.55
260	364	0	0.00	0.00
280	364	0	0.00	0.00
300	364	0	0.00	0.00
320	364	0	0.00	0.00
340	364	0	0.00	0.00
360	364	0	0.00	0.00
380	364	0	0.00	0.00
400	364	0	0.00	0.00

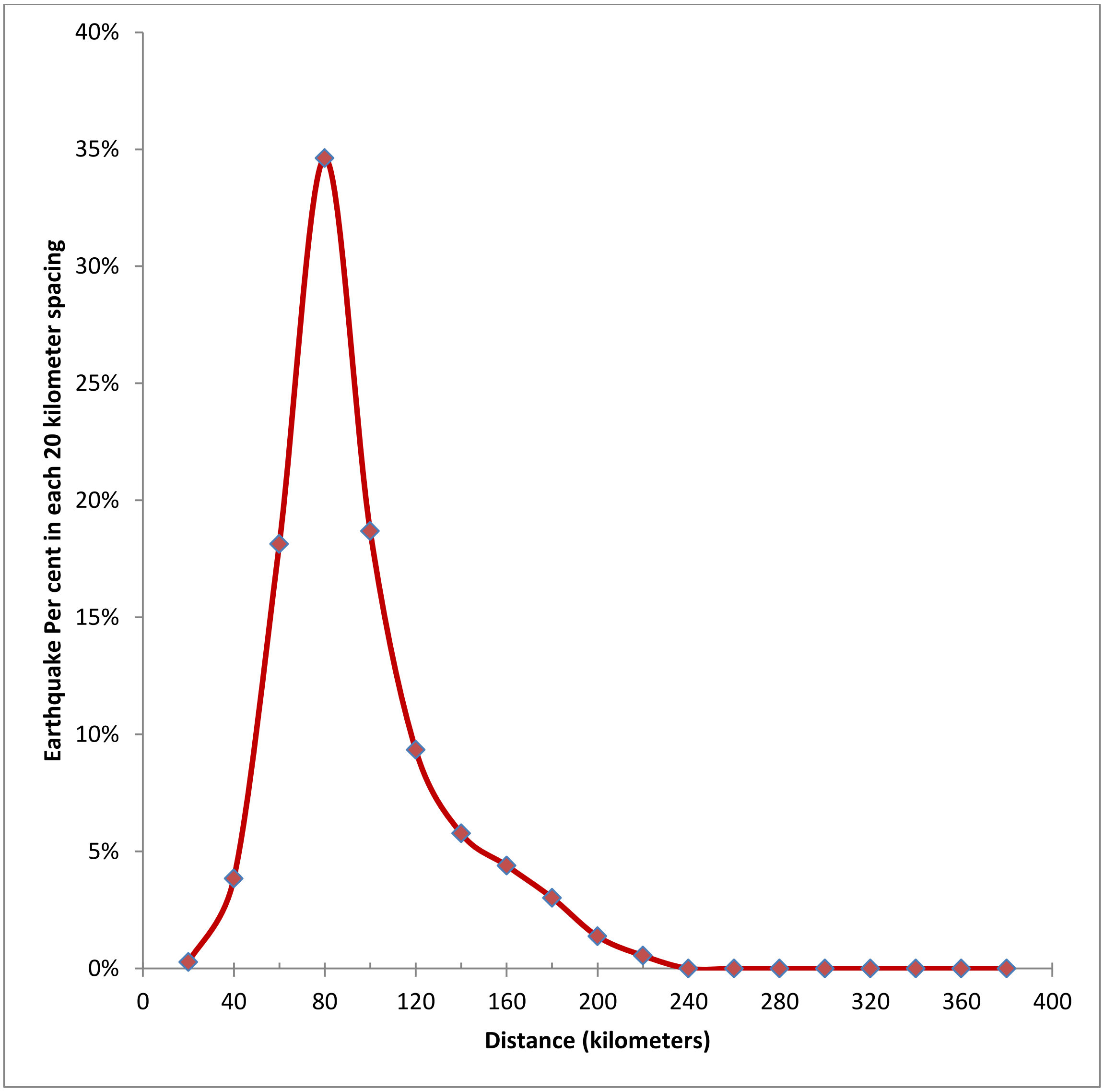

Figure 26 Convergent Boundary Segment 4 Side-B Results

Convergent Boundary Set Five

The data is shown in Table 16 and Table 17 for Side A and Side B respectively.

Table 16
Convergent Boundary Segment 5 Side A

Distance from boundary	No. of earthquakes	No. of earthquakes in the 20km segment	Per cent %	Difference %
20	1	1	33.33	
40	1	0	0.00	33.33
60	1	0	0.00	0.00
80	1	0	0.00	0.00
100	1	0	0.00	0.00
120	1	0	0.00	0.00
140	1	0	0.00	0.00
160	1	0	0.00	0.00
180	1	0	0.00	0.00
200	2	1	33.33	33.33
220	3	1	33.33	0.00
240	3	0	0.00	33.33
260	3	0	0.00	0.00
280	3	0	0.00	0.00
300	3	0	0.00	0.00
320	3	0	0.00	0.00
340	3	0	0.00	0.00
360	3	0	0.00	0.00
380	3	0	0.00	0.00
400	3	0	0.00	0.00

Figure 27 and Figure 28 show the results for Table 16 and Table 17 plotted with the distance from the nominal centerline of the boundary as the independent variable.

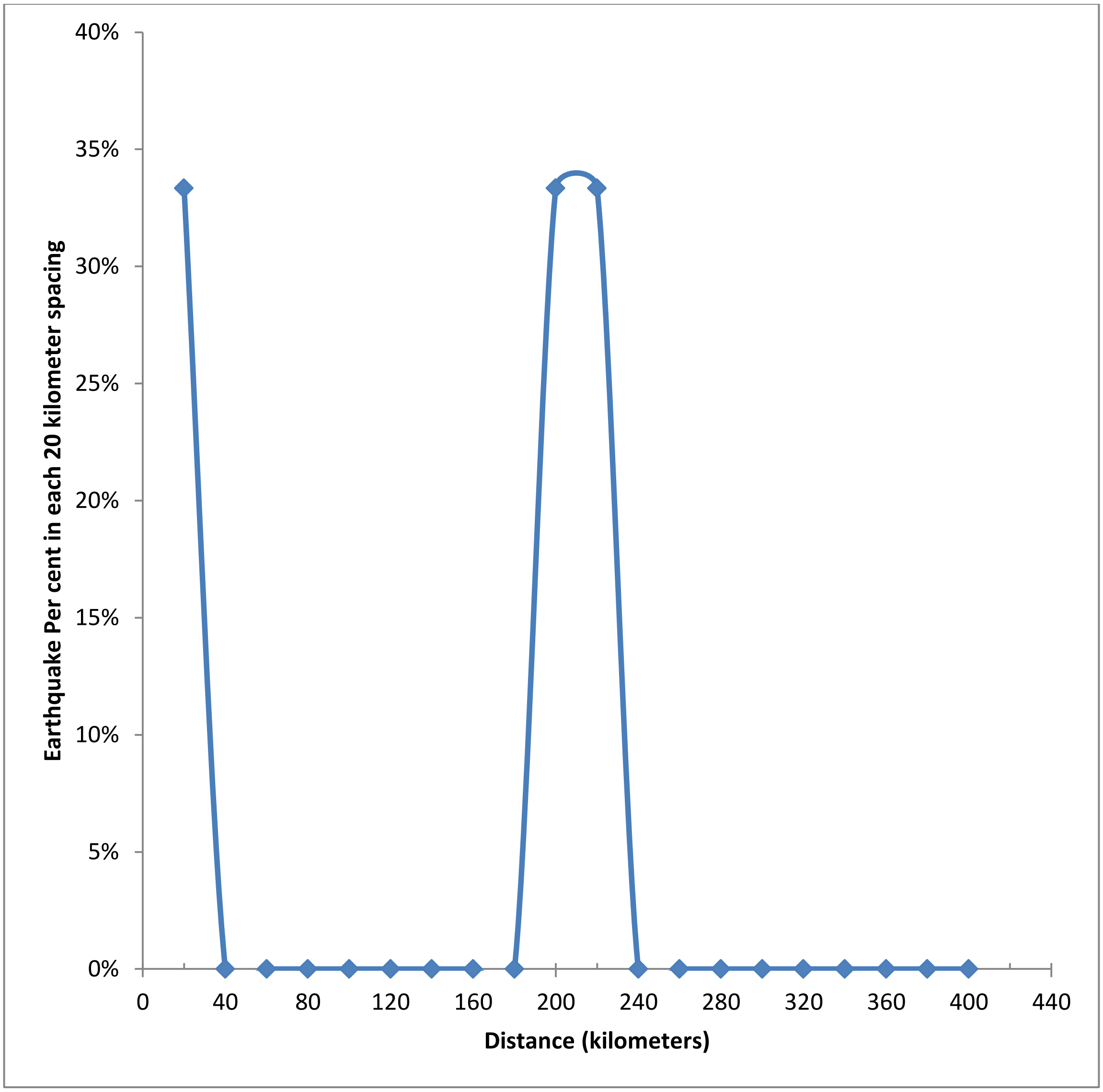

Figure 27 Convergent Boundary Segment 5 Side-A Results

Table 17
Convergent Boundary Segment 5 Side B

Distance from boundary	No. of earthquakes	No. of earthquakes in the 20km segment	Per cent %	Difference %
20	18	18	3.66	
40	99	81	16.46	12.80
60	222	123	25.00	8.54
80	374	152	30.89	5.89
100	446	72	14.63	16.26
120	469	23	4.67	9.96
140	475	6	1.22	3.46
160	479	4	0.81	0.41
180	481	2	0.41	0.41
200	489	8	1.63	1.22
220	491	2	0.41	1.22
240	491	0	0.00	0.41
260	492	1	0.20	0.20
280	492	0	0.00	0.20
300	492	0	0.00	0.00
320	492	0	0.00	0.00
340	492	0	0.00	0.00
360	492	0	0.00	0.00
380	492	0	0.00	0.00
400	492	0	0.00	0.00

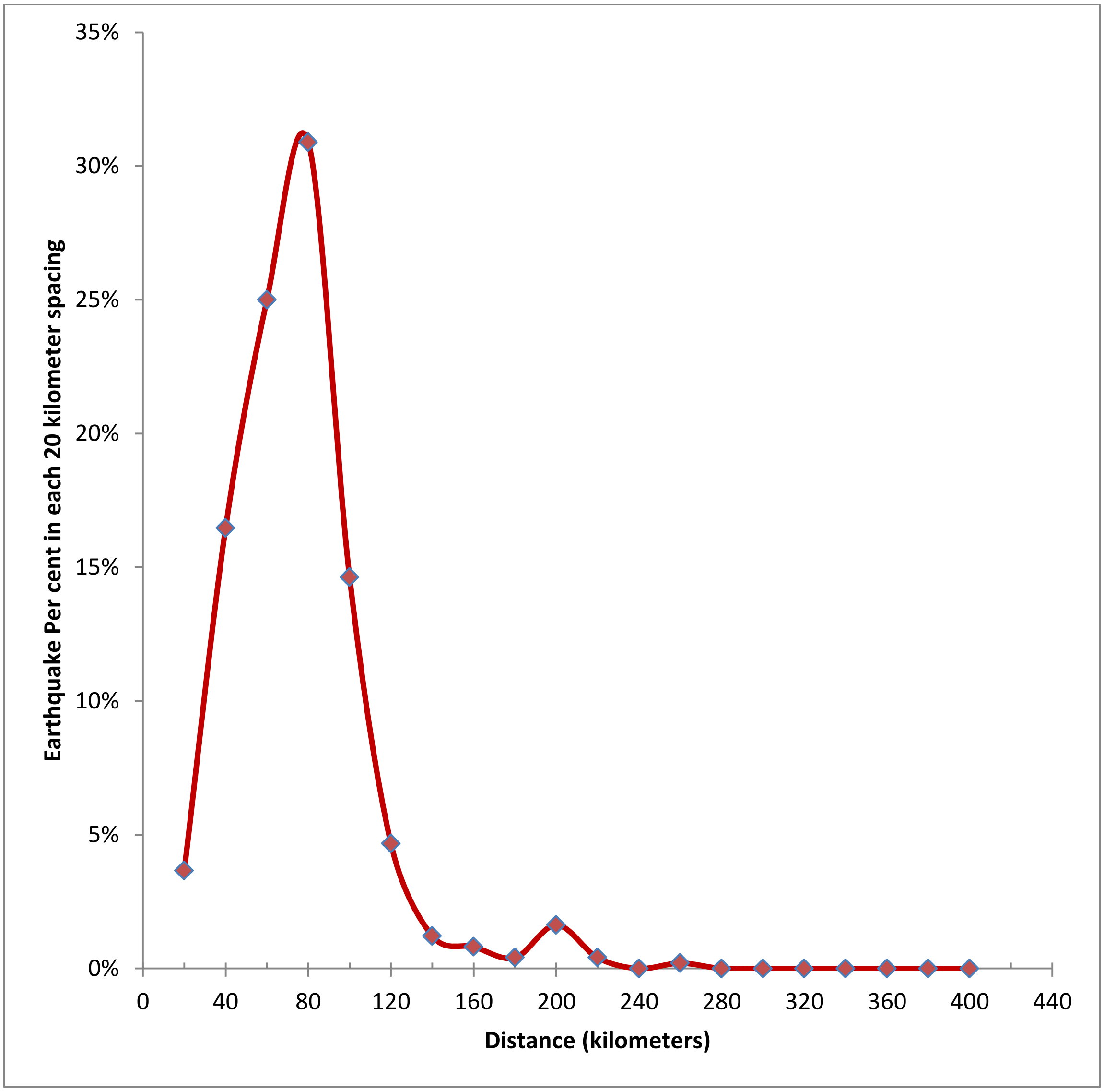

Figure 28 Convergent Boundary Segment 5 Side-B Results

Convergent Boundary Set Six

The data is shown in Table 18 and Table 19 for Side A and Side B respectively.

Table 18
Convergent Boundary Segment 6 Side A

Distance from boundary	No. of earthquakes	No. of earthquakes in the 20km segment	Per cent %	Difference %
20	54	54	19.22	
40	122	68	24.20	4.98
60	192	70	24.91	0.71
80	238	46	16.37	8.54
100	257	19	6.76	9.61
120	271	14	4.98	1.78
140	276	5	1.78	3.20
160	278	2	0.71	1.07
180	279	1	0.36	0.36
200	279	0	0.00	0.36
220	279	0	0.00	0.00
240	280	1	0.36	0.36
260	280	0	0.00	0.36
280	280	0	0.00	0.00
300	280	0	0.00	0.00
320	280	0	0.00	0.00
340	280	0	0.00	0.00
360	281	1	0.36	0.36
380	281	0	0.00	0.36
400	281	0	0.00	0.00

Figure 29 and Figure 30 show the results for Table 18 and Table 19 plotted with the distance from the nominal centerline of the boundary as the independent variable.

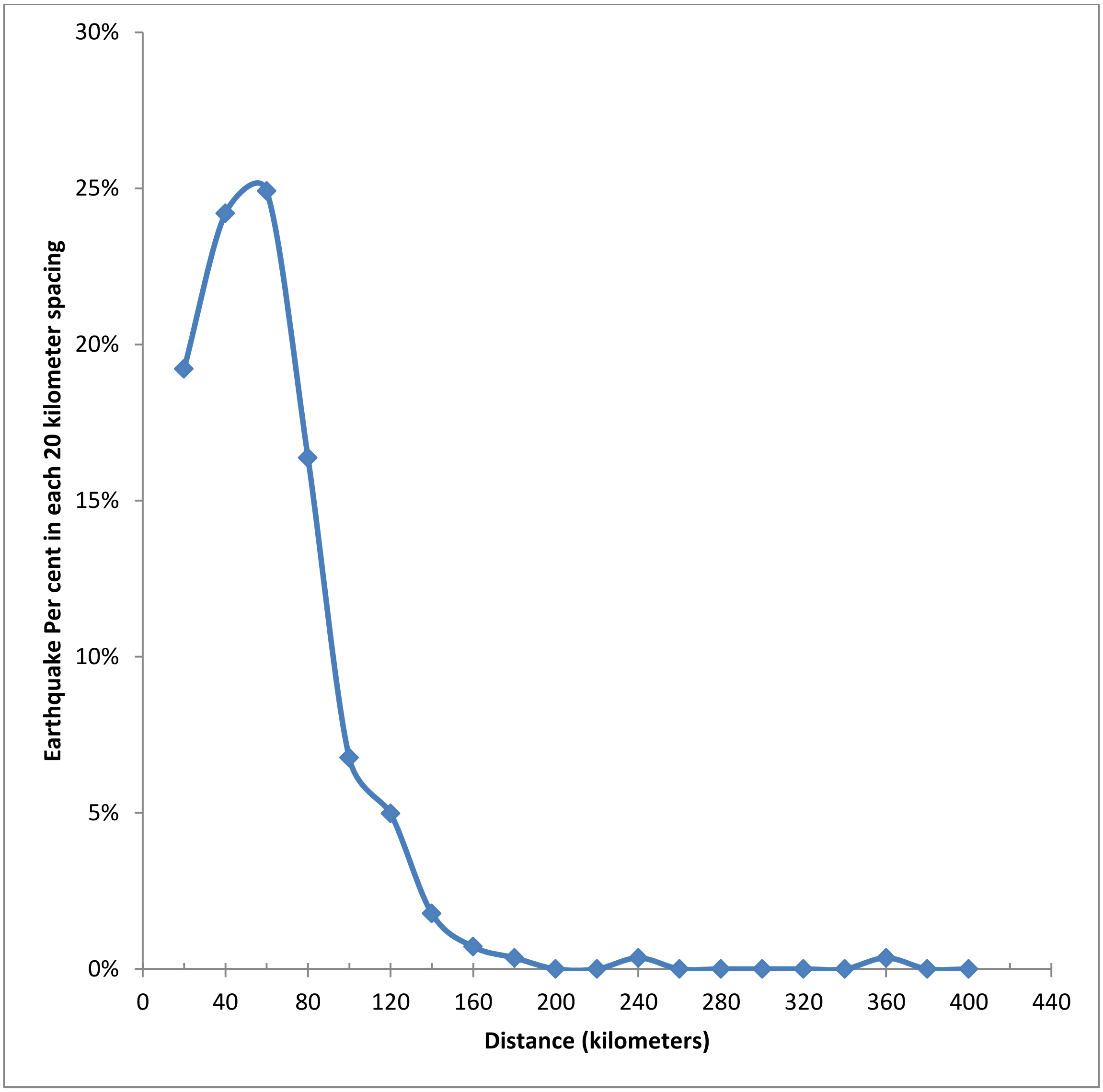

Figure 29 Convergent Boundary Segment 6 Side-A Results

Table 19
Convergent Boundary Segment 6 Side B

Distance from boundary	No. of earthquakes	No. of earthquakes in the 20km segment	Per cent %	Difference %
20	97	97	2.06	
40	340	243	5.16	3.10
60	851	511	10.85	5.69
80	1492	641	13.62	2.76
100	2128	636	13.51	0.11
120	2659	531	11.28	2.23
140	3121	462	9.81	1.47
160	3426	305	6.48	3.33
180	3693	267	5.67	0.81
200	3901	208	4.42	1.25
220	4110	209	4.44	0.02
240	4301	191	4.06	0.38
260	4448	147	3.12	0.93
280	4572	124	2.63	0.49
300	4650	78	1.66	0.98
320	4678	28	0.59	1.06
340	4690	12	0.25	0.34
360	4701	11	0.23	0.02
380	4705	4	0.08	0.15
400	4708	3	0.06	0.02

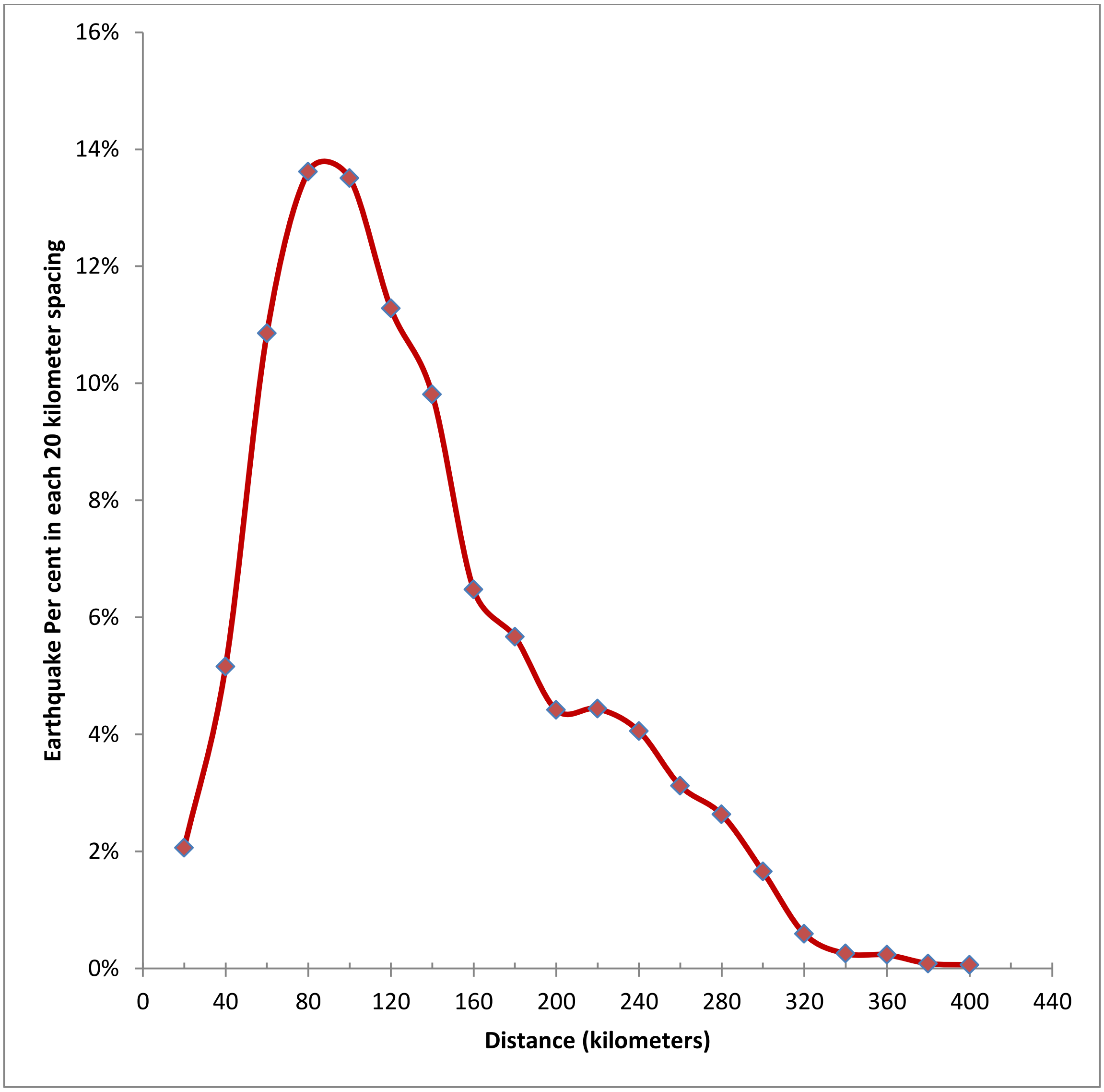

Figure 30 Convergent Boundary Segment 6 Side-B Results

APPENDIX B

DIVERGENT BOUNDARY DATA

Introduction

Six boundary segments were selected for the analysis of the distribution of earthquakes on the divergent boundary. The six groups were placed into four data sets as shown in Table 20.

Table 20
Divergent Boundary Data Sets One to Six

Set Number	Segment	Comments
1	D1	Represents the minor plate boundaries in the African plate
2	D2	Represents the juncture between the Pacific plate and the North American plate
3	D3	Represents the juncture between the Arabian plate and the African plate
4	D4	Represents the juncture between the Australian plate and the Antarctic plate
5	D5	Represents the juncture between the Eurasian plate and the North American plate
6	D6	Represents the juncture between the Eurasian plate and the North American plate

The difference between the convergent and the divergent sides is distinct in terms of the ratio of the numbers of earthquakes on the two sides. In terms of the divergent, there exists a High Side A and a Low Side B for the total recorded earthquakes.

Divergent boundary study consisted of contains 335 earthquakes with a magnitude M_w of five or greater on Side B and 143 earthquakes on Side A. The number of earthquakes recorded in each of the segments is summarized in Table 21.

Table 21
Earthquake Numbers Counted in Divergent Segments

Segments	Earthquake Numbers Side A	Earthquake Numbers Side B	Ratio
D1	87	47	0.54
D2	91	17	0.19
D3	73	51	0.70
D4	14	7	0.50
D5	56	17	0.30
D6	14	4	0.29

Figure 31 show a plot of the data for side A and Side B earthquake numbers.

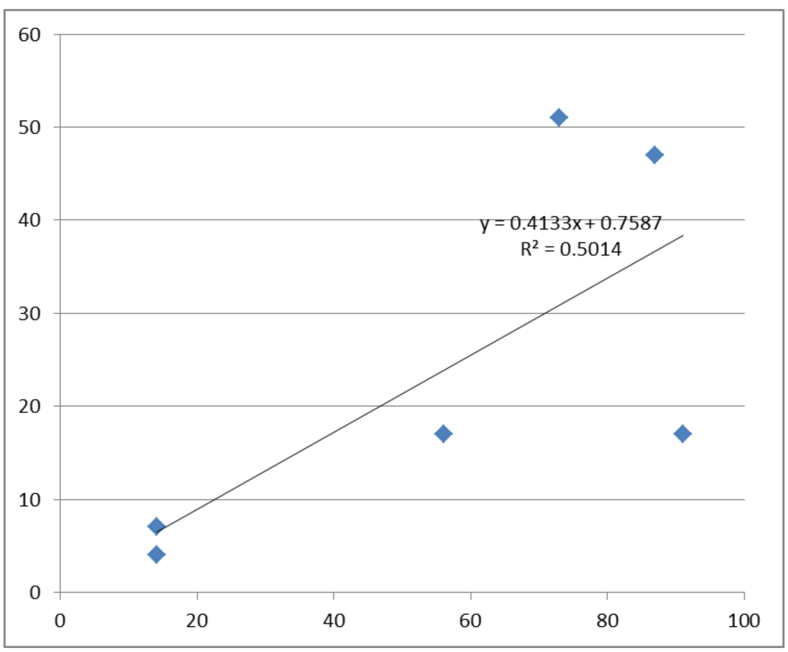

Figure 31 Divergent - Number of Earthquakes on Each Side of the Boundary

As shown in Figure 31 the divergent boundaries provide a statistically distinct set for a one-tailed analysis at the five per cent level using Student's t Test. As shown in Figure 31, the convergent boundary segments D4 and D6 are different to the remaining boundaries, with the number of earthquakes greater on Side A as compared to Side B.

Divergent Boundary Set One

The data is shown in Table 22 and Table 23 for Side A and Side B respectively.

Table 22
Divergent Boundary Segment 1 Side A

Distance from boundary	No. of earthquakes	No. of earthquakes in the 20km segment	Per cent %	Difference %
20	39	39	44.83	
40	54	15	17.24	27.59
60	57	3	3.45	13.79
80	61	4	4.60	1.15
100	68	7	8.05	3.45
120	69	1	1.15	6.90
140	70	1	1.15	0.00
160	72	2	2.30	1.15
180	74	2	2.30	0.00
200	75	1	1.15	1.15
220	75	0	0.00	1.15
240	80	5	5.75	5.75
260	81	1	1.15	4.60
280	81	0	0.00	1.15
300	81	0	0.00	0.00
320	83	2	2.30	2.30
340	87	4	4.60	2.30
360	87	0	0.00	4.60
380	87	0	0.00	0.00
400	87	0	0.00	0.00

Figure 32 and Figure 33 show the results for Table 22 and Table 23 plotted with the distance from the nominal centerline of the boundary as the independent variable.

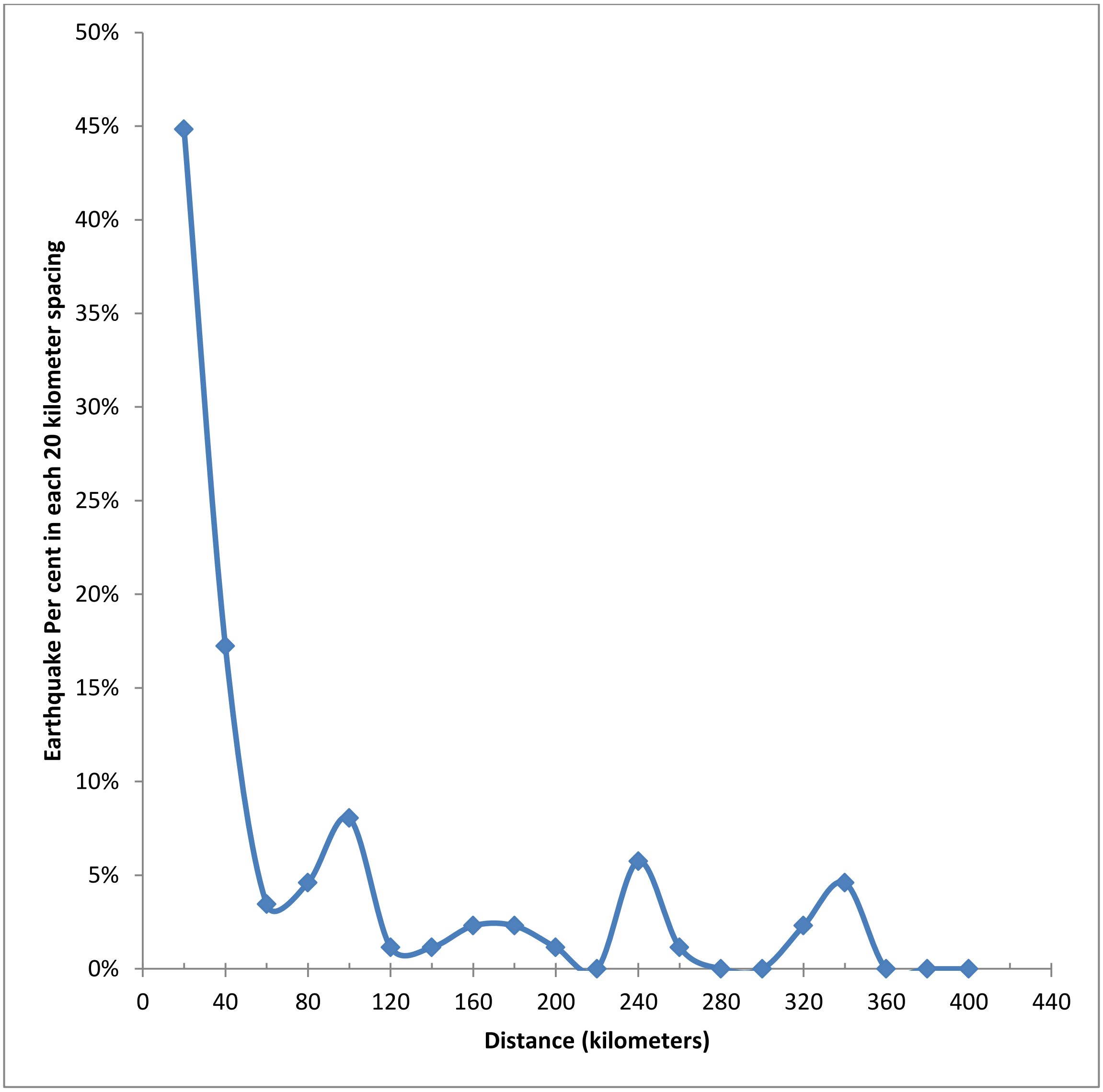

Figure 32 Divergent Boundary Segment 1 Side-A Results

Table 23
Divergent Boundary Segment 1 Side B

Distance from boundary	No. of earthquakes	No. of earthquakes in the 20km segment	Per cent %	Difference %
20	23	23	48.94	
40	32	9	19.15	29.79
60	41	9	19.15	0.00
80	45	4	8.51	10.64
100	45	0	0.00	8.51
120	46	1	2.13	2.13
140	46	0	0.00	2.13
160	46	0	0.00	0.00
180	46	0	0.00	0.00
200	46	0	0.00	0.00
220	46	0	0.00	0.00
240	46	0	0.00	0.00
260	46	0	0.00	0.00
280	46	0	0.00	0.00
300	46	0	0.00	0.00
320	46	0	0.00	0.00
340	47	1	2.13	2.13
360	47	0	0.00	2.13
380	47	0	0.00	0.00
400	47	0	0.00	0.00

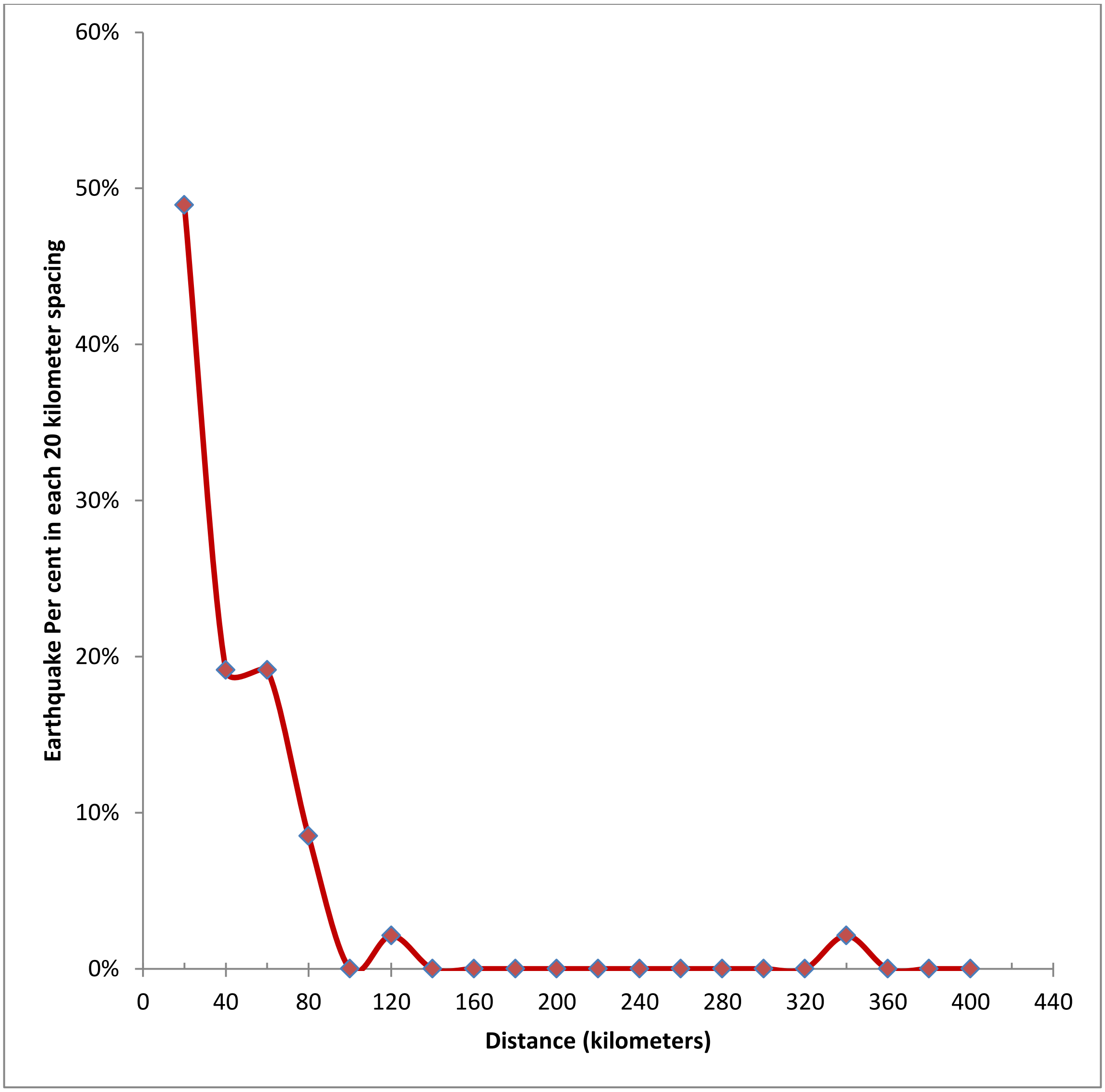

Figure 33 Divergent Boundary Segment 1 Side-B Results

Divergent Boundary Set Two

The data is shown in Table 24 and Table 25 for Side A and Side B respectively.

Table 24
Divergent Boundary Segment 2 Side A

Distance from boundary	No. of earthquakes	No. of earthquakes in the 20km segment	Per cent %	Difference %
20	12	12	70.59	
40	12	0	0.00	70.59
60	12	0	0.00	0.00
80	17	5	29.41	29.41
100	17	0	0.00	29.41
120	17	0	0.00	0.00
140	17	0	0.00	0.00
160	17	0	0.00	0.00
180	17	0	0.00	0.00
200	17	0	0.00	0.00
220	17	0	0.00	0.00
240	17	0	0.00	0.00
260	17	0	0.00	0.00
280	17	0	0.00	0.00
300	17	0	0.00	0.00
320	17	0	0.00	0.00
340	17	0	0.00	0.00
360	17	0	0.00	0.00
380	17	0	0.00	0.00
400	17	0	0.00	0.00

Figure 34 and Figure 35 show the results for Table 24 and Table 25 plotted with the distance from the nominal centerline of the boundary as the independent variable.

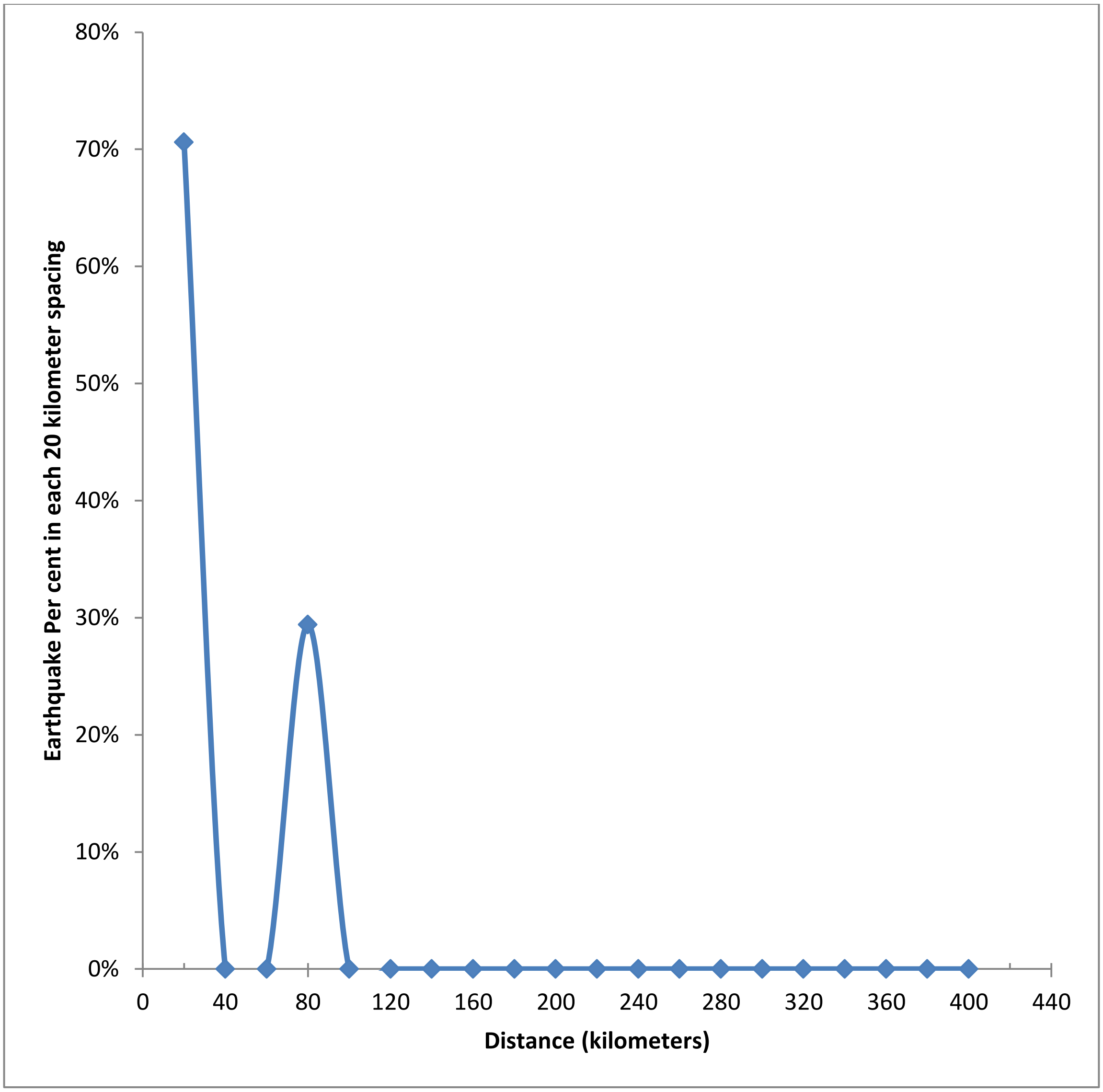

Figure 34 Divergent Boundary Segment 2 Side-A Results

Table 25
Divergent Boundary Segment 2 Side B

Distance from boundary	No. of earthquakes	No. of earthquakes in the 20km segment	Per cent %	Difference %
20	6	6	6.59	
40	21	15	16.48	9.89
60	23	2	2.20	14.29
80	23	0	0.00	2.20
100	23	0	0.00	0.00
120	23	0	0.00	0.00
140	23	0	0.00	0.00
160	23	0	0.00	0.00
180	26	3	3.30	3.30
200	27	1	1.10	2.20
220	27	0	0.00	1.10
240	29	2	2.20	2.20
260	46	17	18.68	16.48
280	56	10	10.99	7.69
300	71	15	16.48	5.49
320	83	12	13.19	3.30
340	87	4	4.40	8.79
360	89	2	2.20	2.20
380	89	0	0.00	2.20
400	91	2	2.20	2.20

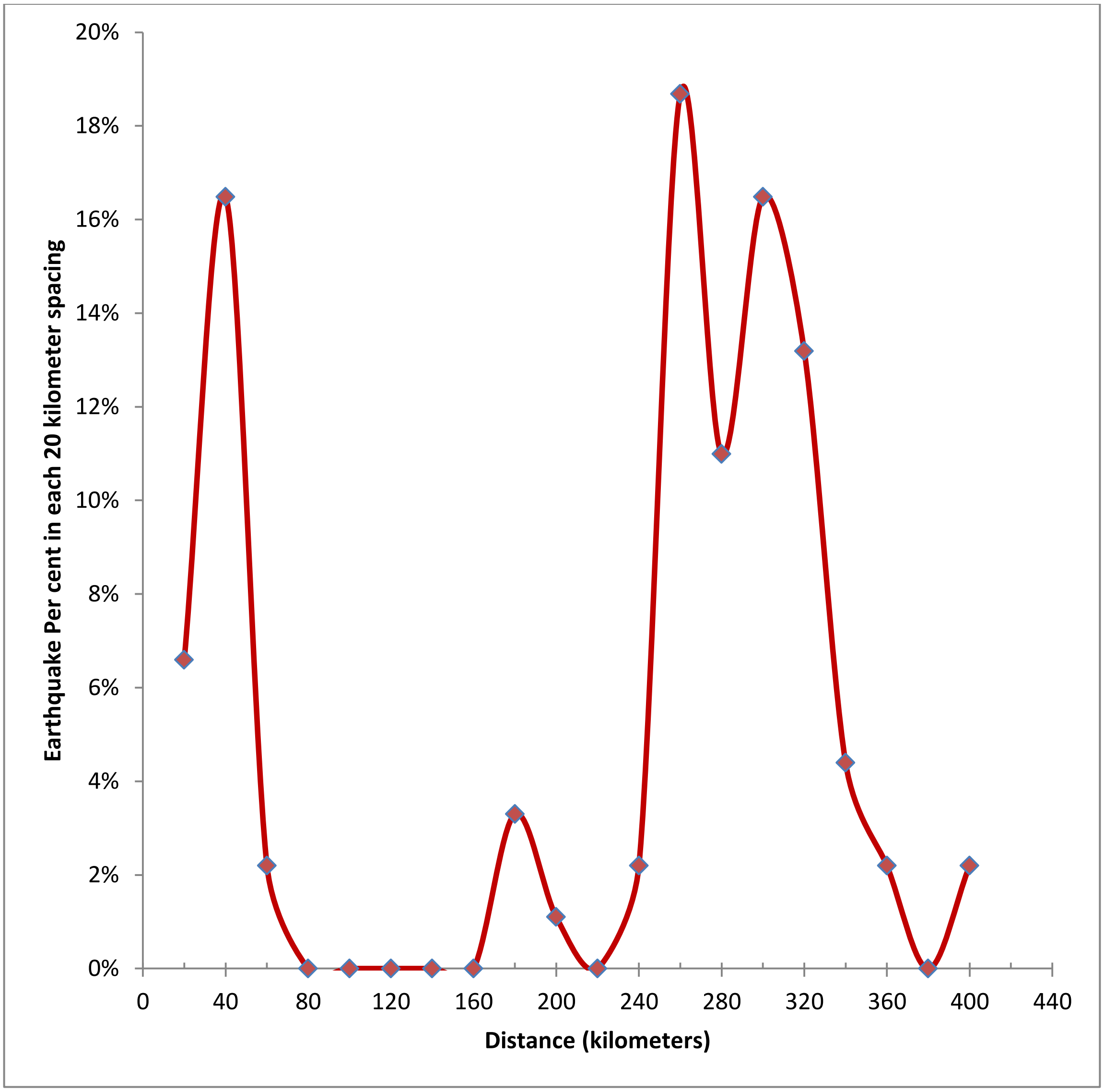

Figure 35 Divergent Boundary Segment 2 Side-B Results

Divergent Boundary Set Three

The data is shown in Table 26 and Table 27 for Side A and Side B respectively.

Table 26
Divergent Boundary Segment 3 Side A

Distance from boundary	No. of earthquakes	No. of earthquakes in the 20km segment	Per cent %	Difference %
20	33	33	64.71	
40	37	4	7.84	56.86
60	38	1	1.96	5.88
80	38	0	0.00	1.96
100	39	1	1.96	1.96
120	40	1	1.96	0.00
140	45	5	9.80	7.84
160	48	3	5.88	3.92
180	49	1	1.96	3.92
200	49	0	0.00	1.96
220	51	2	3.92	3.92
240	51	0	0.00	3.92
260	51	0	0.00	0.00
280	51	0	0.00	0.00
300	51	0	0.00	0.00
320	51	0	0.00	0.00
340	51	0	0.00	0.00
360	51	0	0.00	0.00
380	51	0	0.00	0.00
400	51	0	0.00	0.00

Figure 36 and Figure 37 show the results for Table 26 and Table 27 plotted with the distance from the nominal centerline of the boundary as the independent variable.

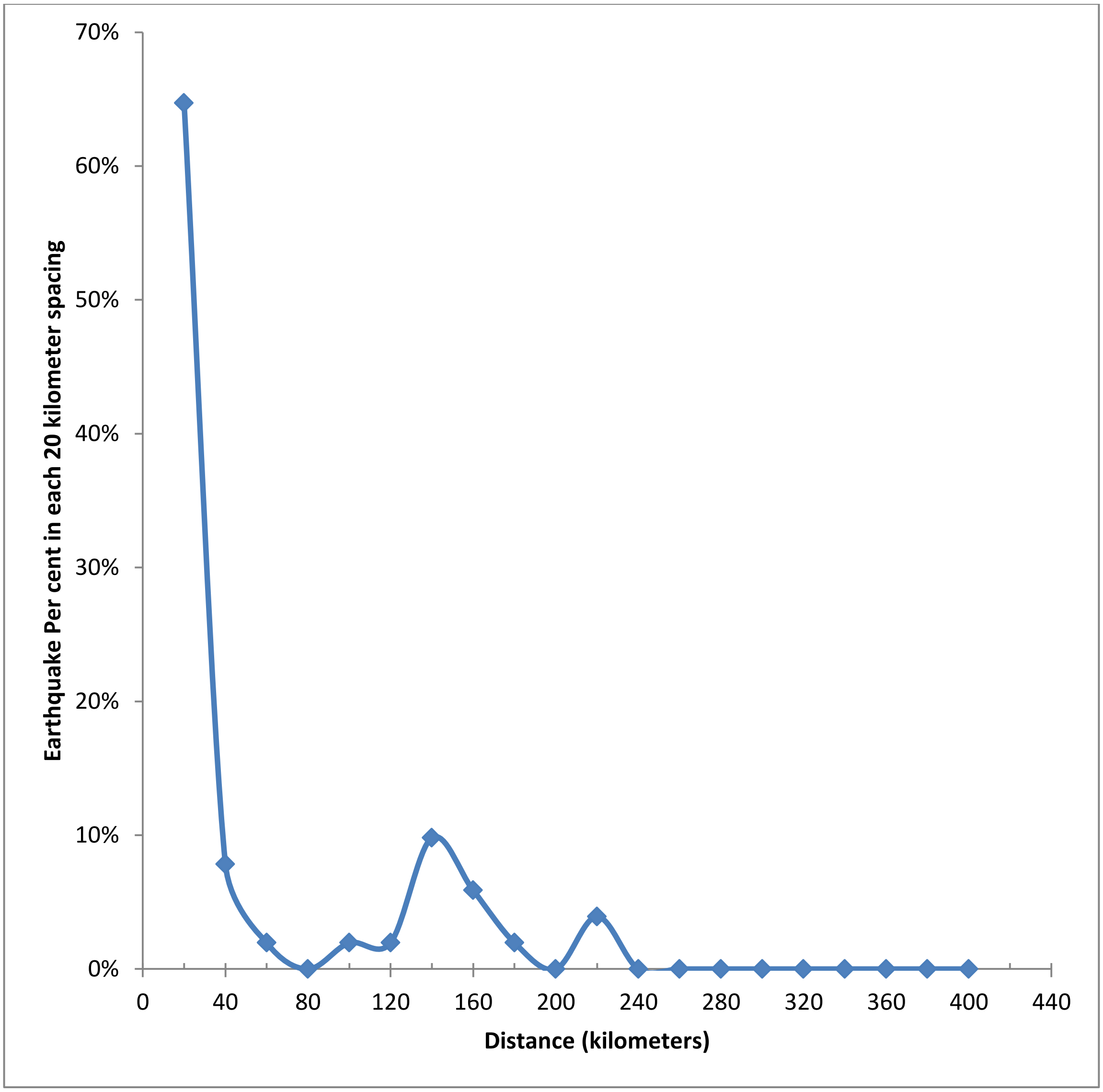

Figure 36 Divergent Boundary Segment 3 Side-A Results

Table 27
Divergent Boundary Segment 3 Side B

Distance from boundary	No. of earthquakes	No. of earthquakes in the 20km segment	Per cent %	Difference %
20	53	53	72.60	
40	58	5	6.85	65.75
60	60	2	2.74	4.11
80	60	0	0.00	2.74
100	61	1	1.37	1.37
120	63	2	2.74	1.37
140	67	4	5.48	2.74
160	69	2	2.74	2.74
180	71	2	2.74	0.00
200	72	1	1.37	1.37
220	73	1	1.37	0.00
240	73	0	0.00	1.37
260	73	0	0.00	0.00
280	73	0	0.00	0.00
300	73	0	0.00	0.00
320	73	0	0.00	0.00
340	73	0	0.00	0.00
360	73	0	0.00	0.00
380	73	0	0.00	0.00
400	73	0	0.00	0.00

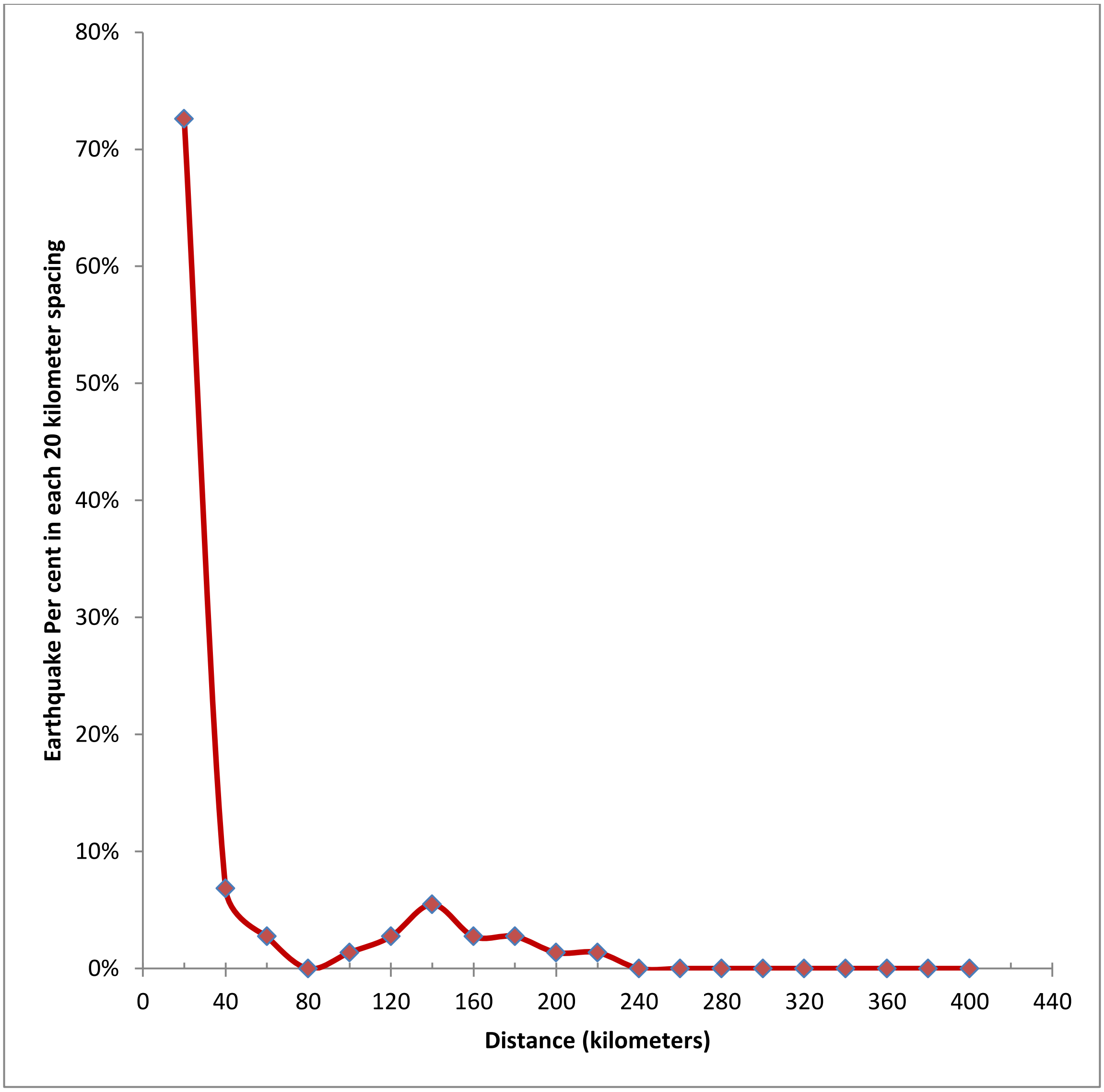

Figure 37 Divergent Boundary Segment 3 Side-B Results

Divergent Boundary Set Four

The data is shown in Table 28 and Table 29 for Side A and Side B respectively.

Table 28
Divergent Boundary Segment 4 Side A

Distance from boundary	No. of earthquakes	No. of earthquakes in the 20km segment	Per cent %	Difference %
20	13	13	92.86	
40	14	1	7.14	85.71
60	14	0	0.00	7.14
80	14	0	0.00	0.00
100	14	0	0.00	0.00
120	14	0	0.00	0.00
140	14	0	0.00	0.00
160	14	0	0.00	0.00
180	14	0	0.00	0.00
200	14	0	0.00	0.00
220	14	0	0.00	0.00
240	14	0	0.00	0.00
260	14	0	0.00	0.00
280	14	0	0.00	0.00
300	14	0	0.00	0.00
320	14	0	0.00	0.00
340	14	0	0.00	0.00
360	14	0	0.00	0.00
380	14	0	0.00	0.00
400	14	0	0.00	0.00

Figure 38 and Figure 39 show the results for Table 28 and Table 29 plotted with the distance from the nominal centerline of the boundary as the independent variable.

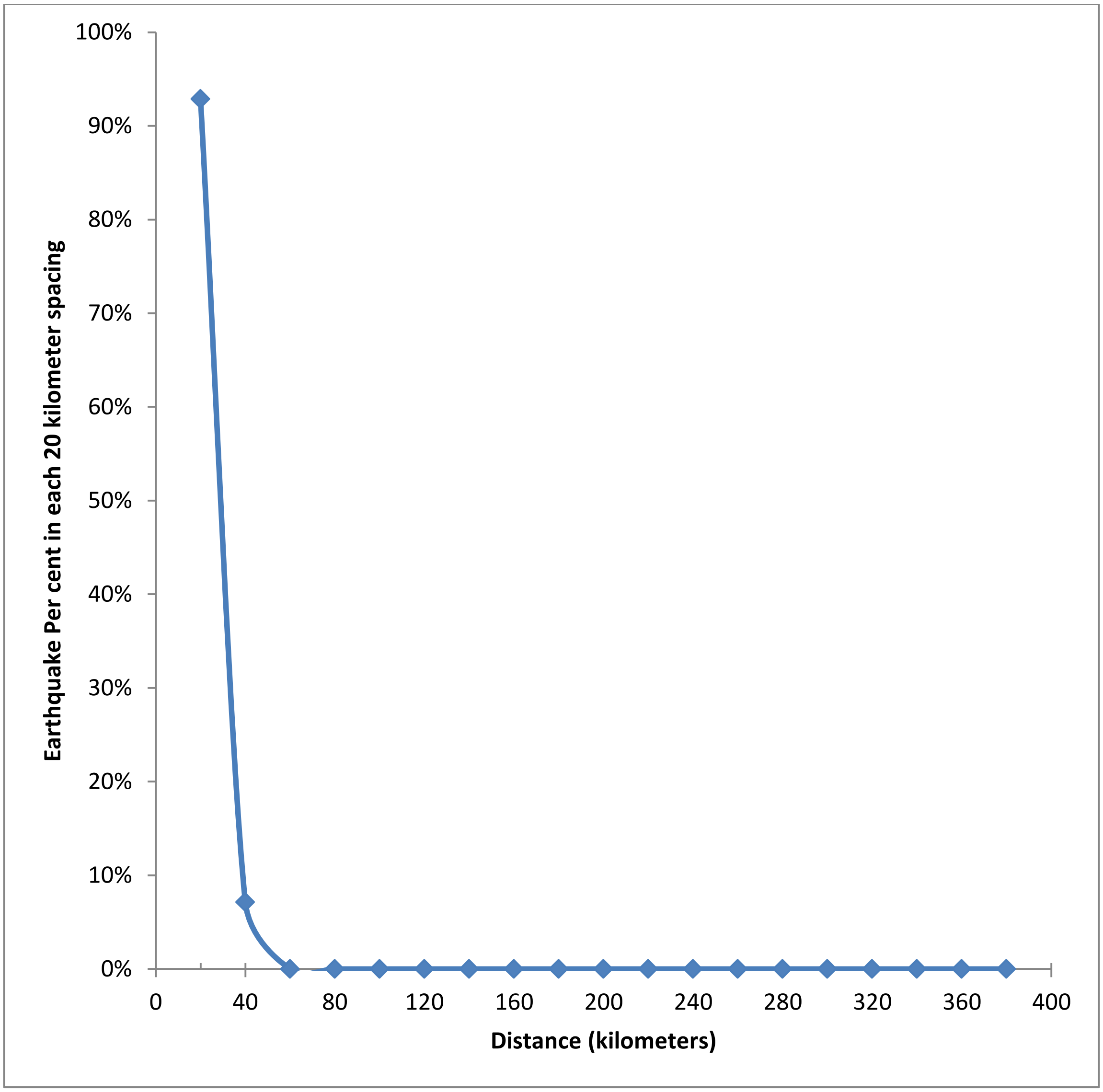

Figure 38 Divergent Boundary Segment 4 Side-A Results

Table 29
Divergent Boundary Segment 4 Side B

Distance from boundary	No. of earthquakes	No. of earthquakes in the 20km segment	Per cent %	Difference %
20	6	6	85.71	
40	6	0	0.00	85.71
60	7	1	14.29	14.29
80	7	0	0.00	14.29
100	7	0	0.00	0.00
120	7	0	0.00	0.00
140	7	0	0.00	0.00
160	7	0	0.00	0.00
180	7	0	0.00	0.00
200	7	0	0.00	0.00
220	7	0	0.00	0.00
240	7	0	0.00	0.00
260	7	0	0.00	0.00
280	7	0	0.00	0.00
300	7	0	0.00	0.00
320	7	0	0.00	0.00
340	7	0	0.00	0.00
360	7	0	0.00	0.00
380	7	0	0.00	0.00
400	7	0	0.00	0.00

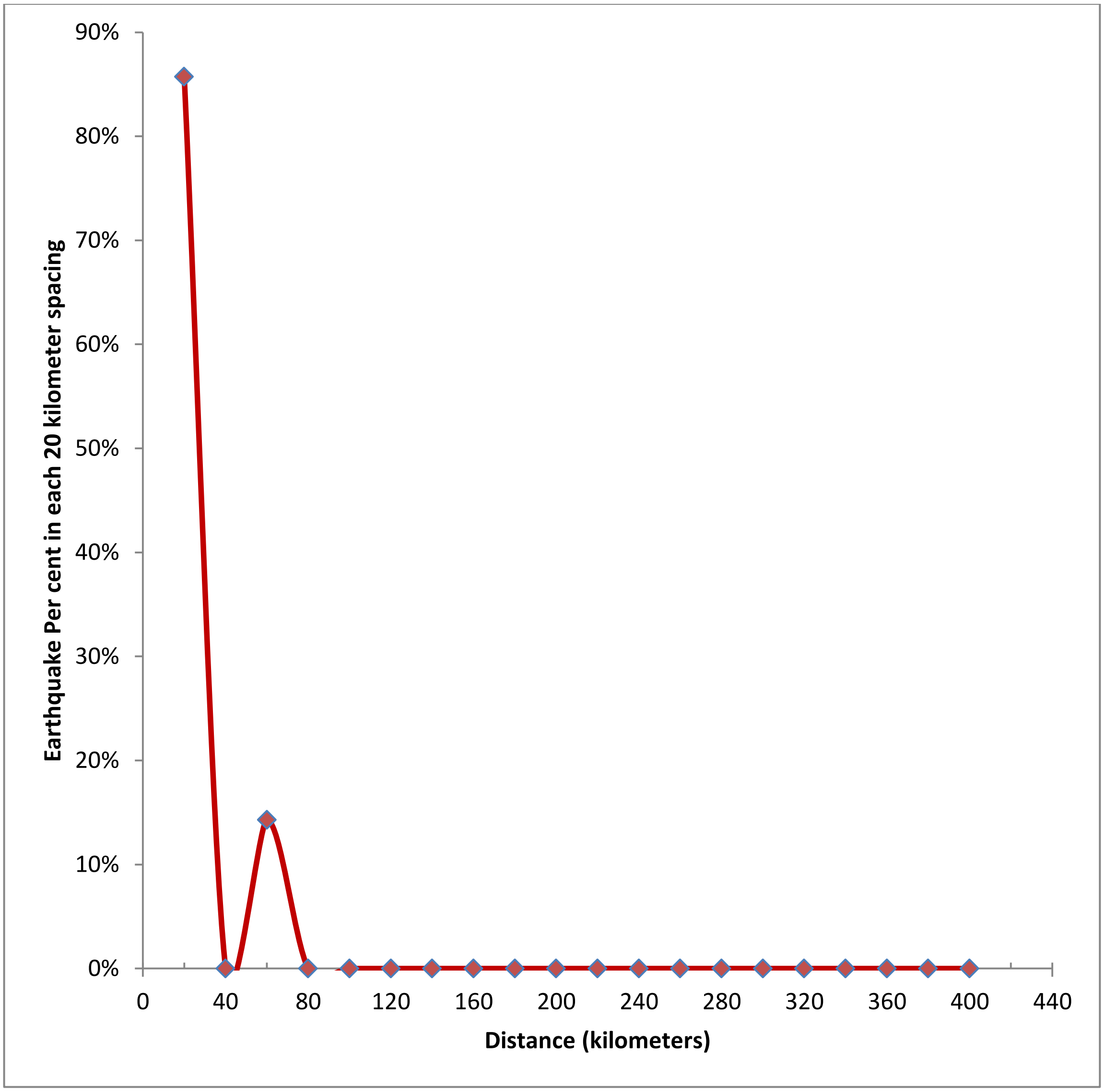

Figure 39 Divergent Boundary Segment 4 Side-B Results

Divergent Boundary Set Five

The data is shown in Table 30 and Table 31 for Side A and Side B respectively.

Table 30
Divergent Boundary Segment 5 Side A

Distance from boundary	No. of earthquakes	No. of earthquakes in the 20km segment	Per cent %	Difference %
20	14	14	82.35	
40	17	3	17.65	64.71
60	17	0	0.00	17.65
80	17	0	0.00	0.00
100	17	0	0.00	0.00
120	17	0	0.00	0.00
140	17	0	0.00	0.00
160	17	0	0.00	0.00
180	17	0	0.00	0.00
200	17	0	0.00	0.00
220	17	0	0.00	0.00
240	17	0	0.00	0.00
260	17	0	0.00	0.00
280	17	0	0.00	0.00
300	17	0	0.00	0.00
320	17	0	0.00	0.00
340	17	0	0.00	0.00
360	17	0	0.00	0.00
380	17	0	0.00	0.00
400	17	0	0.00	0.00

Figure 40 and Figure 41 show the results for Table 30 and Table 31 plotted with the distance from the nominal centerline of the boundary as the independent variable.

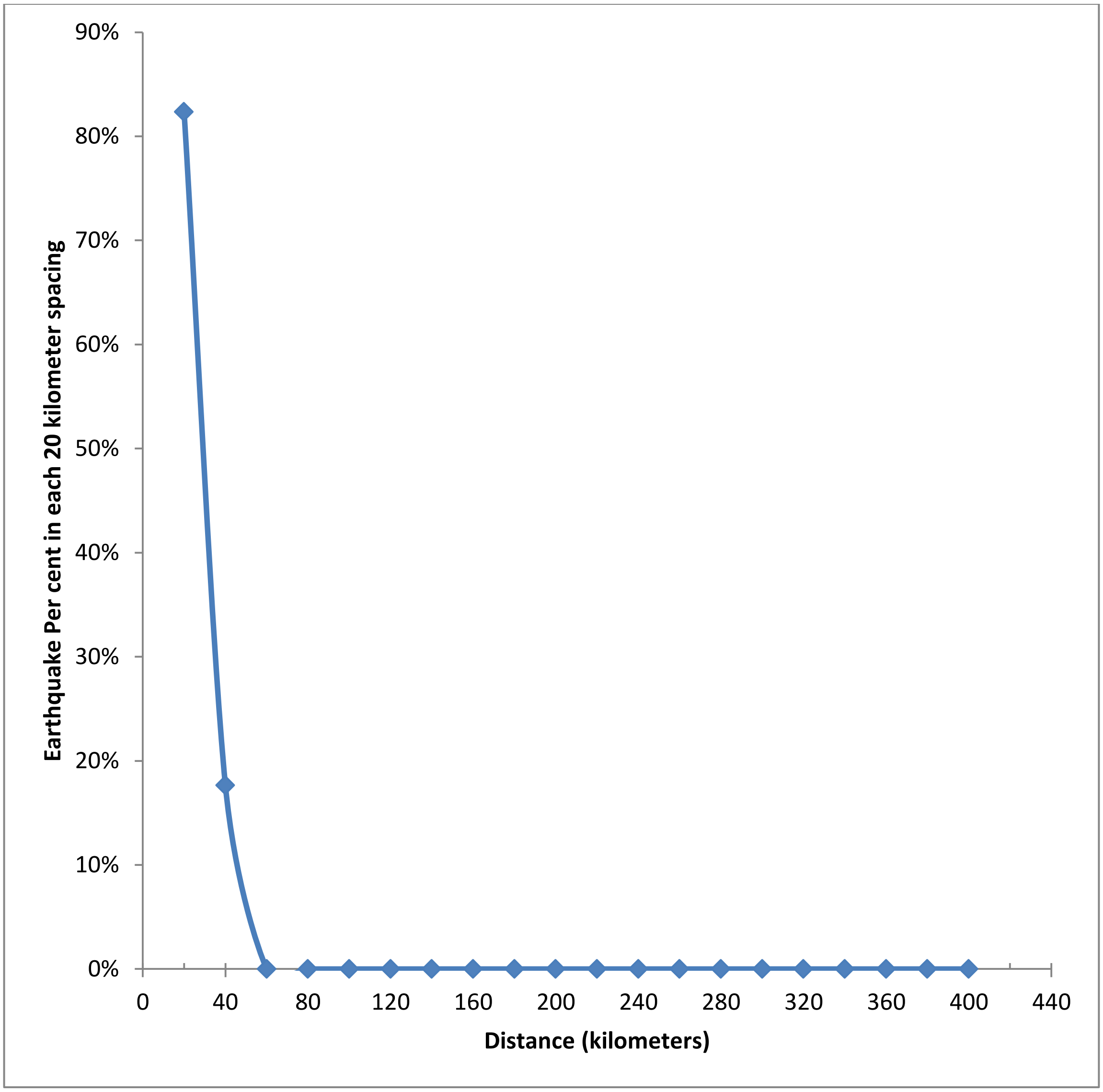

Figure 40 Divergent Boundary Segment 5 Side-A Results

Table 31
Divergent Boundary Segment 5 Side B

Distance from boundary	No. of earthquakes	No. of earthquakes in the 20km segment	Per cent %	Difference %
20	27	27	48.21	
40	54	27	48.21	0.00
60	55	1	1.79	46.43
80	56	1	1.79	0.00
100	56	0	0.00	1.79
120	56	0	0.00	0.00
140	56	0	0.00	0.00
160	56	0	0.00	0.00
180	56	0	0.00	0.00
200	56	0	0.00	0.00
220	56	0	0.00	0.00
240	56	0	0.00	0.00
260	56	0	0.00	0.00
280	56	0	0.00	0.00
300	56	0	0.00	0.00
320	56	0	0.00	0.00
340	56	0	0.00	0.00
360	56	0	0.00	0.00
380	56	0	0.00	0.00
400	56	0	0.00	0.00

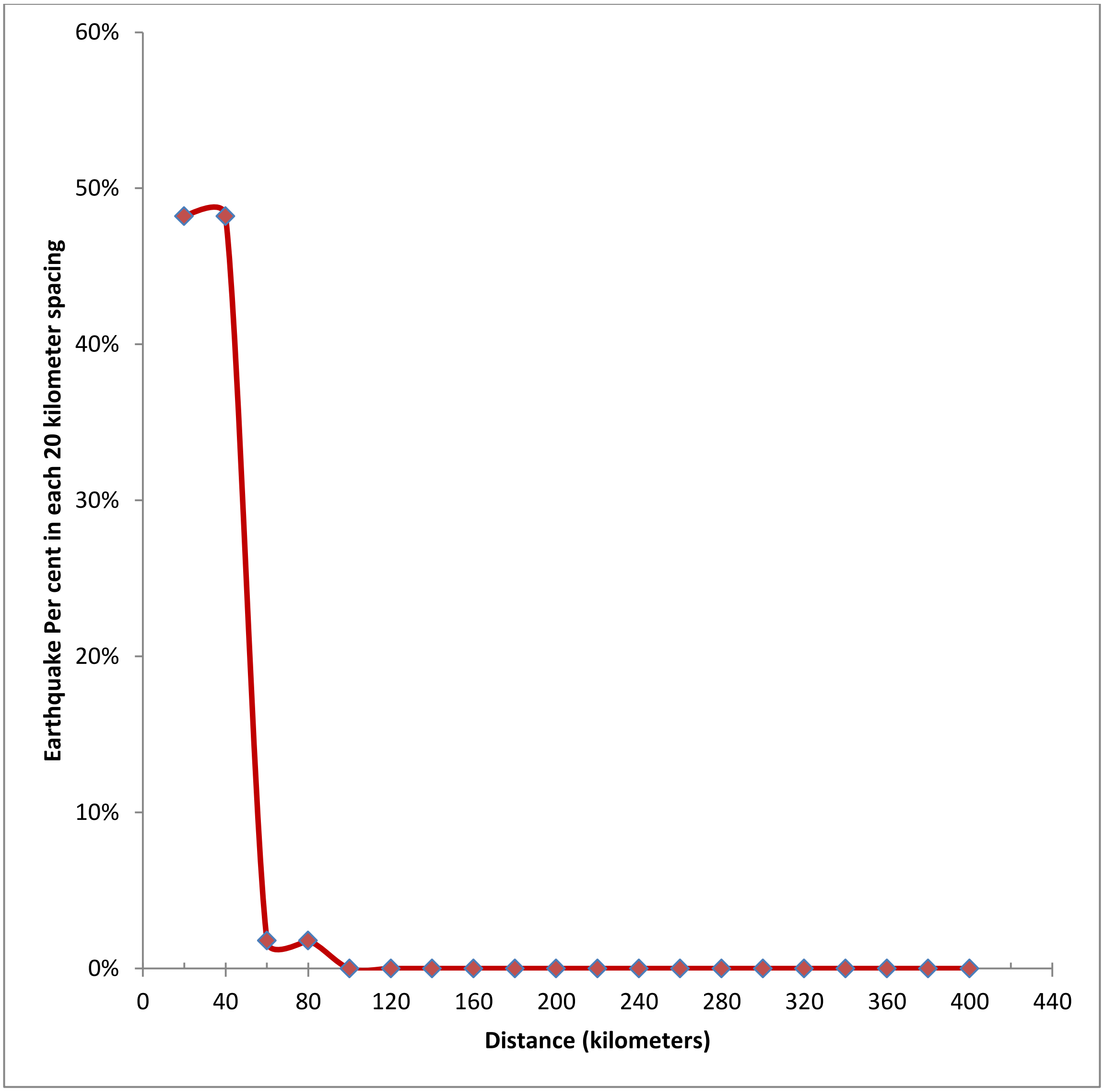

Figure 41 Divergent Boundary Segment 5 Side-B Results

Divergent Boundary Set Six

The data is shown in Table 32 and Table 33 for Side A and Side B respectively.

Table 32
Divergent Boundary Segment 6 Side A

Distance from boundary	No. of earthquakes	No. of earthquakes in the 20km segment	Per cent %	Difference %
20	2	2	25.00	
40	5	3	37.50	12.50
60	8	3	37.50	0.00
80	8	0	0.00	37.50
100	8	0	0.00	0.00
120	8	0	0.00	0.00
140	8	0	0.00	0.00
160	8	0	0.00	0.00
180	8	0	0.00	0.00
200	8	0	0.00	0.00
220	8	0	0.00	0.00
240	8	0	0.00	0.00
260	8	0	0.00	0.00
280	8	0	0.00	0.00
300	8	0	0.00	0.00
320	8	0	0.00	0.00
340	8	0	0.00	0.00
360	8	0	0.00	0.00
380	8	0	0.00	0.00
400	8	0	0.00	0.00

Figure 42 and Figure 43 show the results for Table 32and Table 33 plotted with the distance from the nominal centerline of the boundary as the independent variable.

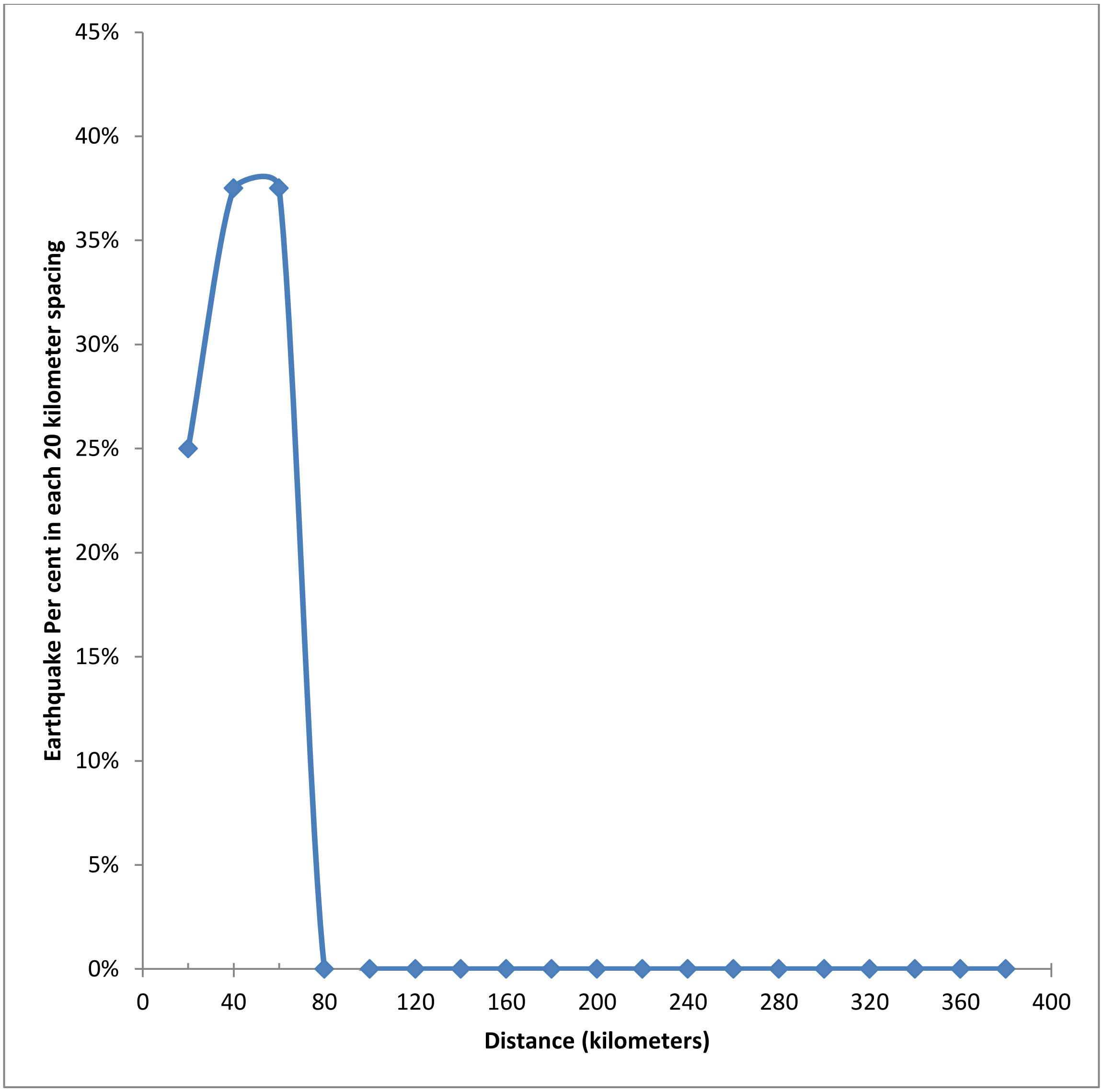

Figure 42 Divergent Boundary Segment 6 Side-A Results

Table 33
Divergent Boundary Segment 6 Side B

Distance from boundary	No. of earthquakes	No. of earthquakes in the 20km segment	Per cent %	Difference %
20	2	2	14.29	
40	7	5	35.71	21.43
60	12	5	35.71	0.00
80	13	1	7.14	28.57
100	14	1	7.14	0.00
120	14	0	0.00	7.14
140	14	0	0.00	0.00
160	14	0	0.00	0.00
180	14	0	0.00	0.00
200	14	0	0.00	0.00
220	14	0	0.00	0.00
240	14	0	0.00	0.00
260	14	0	0.00	0.00
280	14	0	0.00	0.00
300	14	0	0.00	0.00
320	14	0	0.00	0.00
340	14	0	0.00	0.00
360	14	0	0.00	0.00
380	14	0	0.00	0.00
400	14	0	0.00	0.00

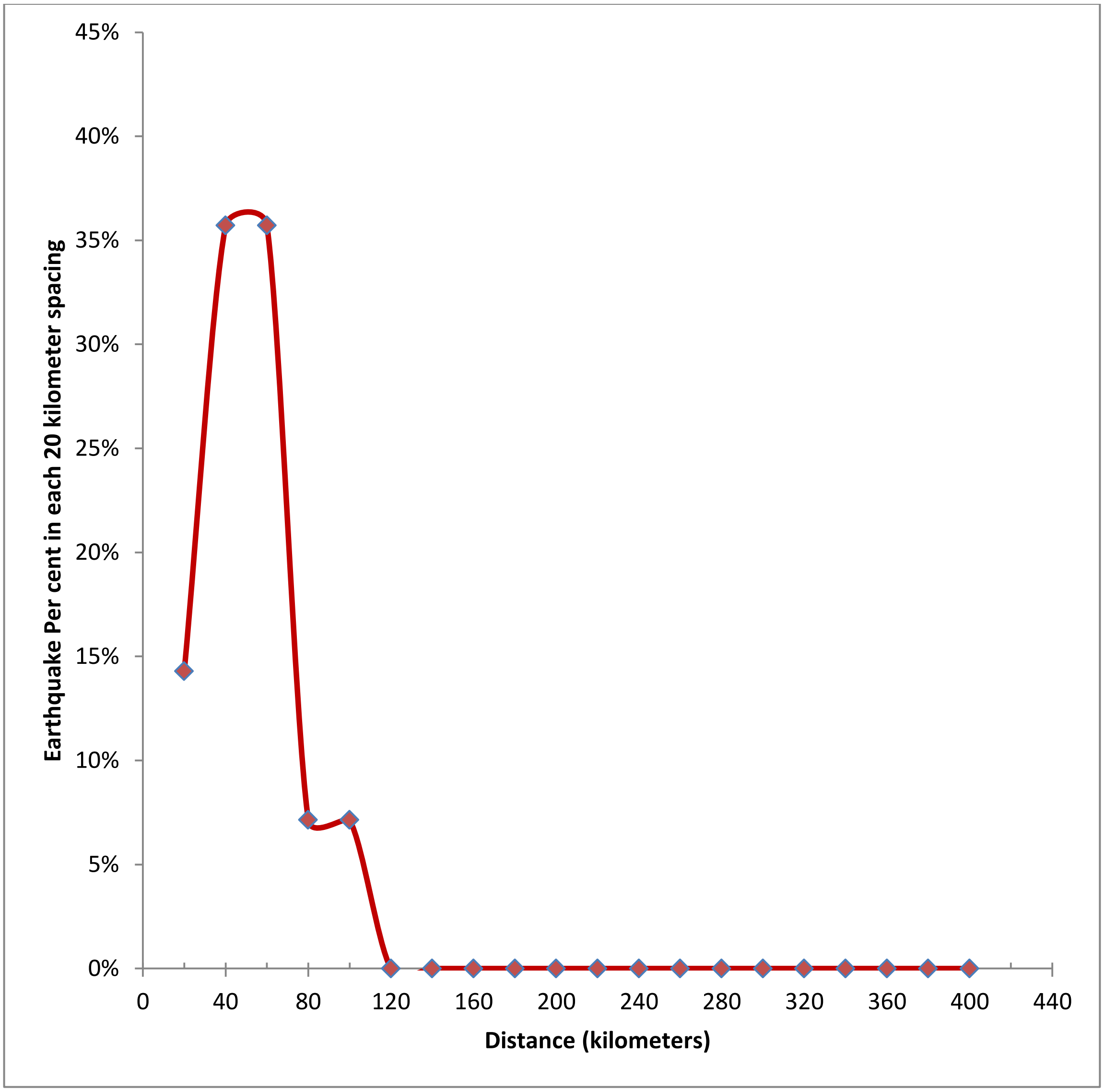

Figure 43 Divergent Boundary Segment 6 Side-B Results

APPENDIX C

TRANSFORM BOUNDARY DATA

Introduction

Six boundary segments were selected for the analysis of the distribution of earthquakes on the divergent boundary. The six groups were placed into four data sets as shown in Table 34.

Table 34
Transform Boundary Data Sets One to Six

Set Number	Segment	Comments
1	D1	Represents the minor plate boundaries in the African plate
2	D2	Represents the juncture between the Pacific plate and the North American plate
3	D3	Represents the juncture between the Arabian plate and the African plate
4	D4	Represents the juncture between the Australian plate and the Antarctic plate
5	D5	Represents the juncture between the Eurasian plate and the North American plate
6	D6	Represents the juncture between the Eurasian plate and the North American plate

Transform boundary study data contains 232 earthquakes with a magnitude M_w of five or greater on Side B and 250 earthquakes on Side A. Table 35 summarizes the number of earthquakes recorded in each of the segments.

Table 35
Earthquake Numbers Counted in Transform Segments

Segments	Earthquake Numbers Side H	Earthquake Numbers Side L	Ratio
T1	85	94	1.11
T2	23	37	1.61
T3	19	21	1.11
T4	67	51	0.76
T5	39	14	0.36
T6	17	15	0.88

Figure 44 show a plot of the data for side A and Side B earthquake numbers.

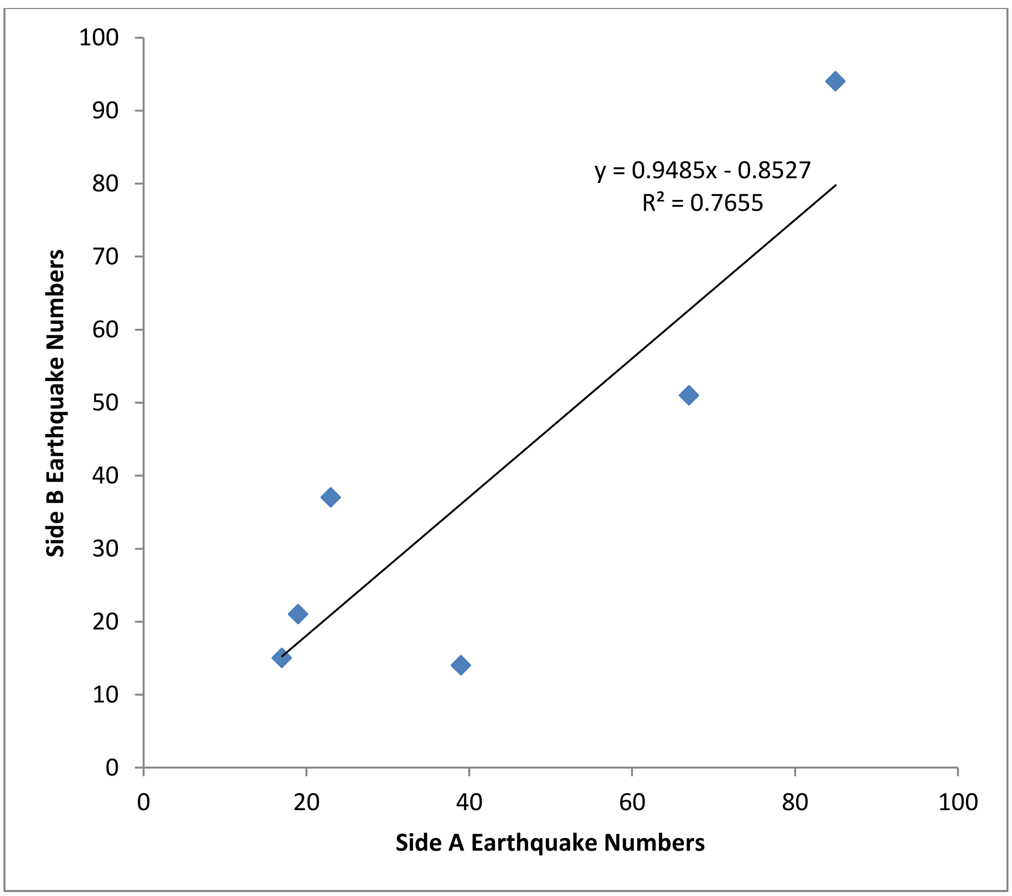

Figure 44 Transform - Number of Earthquakes on Each Side of the Boundary

Transform Boundary Set One

The data is shown in Table 36 and Table 37 for Side A and Side B respectively.

Table 36
Transform Boundary Segment 1 Side A

Distance from boundary	No. of earthquakes	No. of earthquakes in the 20km segment	Per cent %	Difference %
20	32	32	37.65	
40	61	29	34.12	3.53
60	71	10	11.76	22.35
80	78	7	8.24	3.53
100	83	5	5.88	2.35
120	84	1	1.18	4.71
140	84	0	0.00	1.18
160	84	0	0.00	0.00
180	84	0	0.00	0.00
200	85	1	1.18	1.18
220	85	0	0.00	1.18
240	85	0	0.00	0.00
260	85	0	0.00	0.00
280	85	0	0.00	0.00
300	85	0	0.00	0.00
320	85	0	0.00	0.00
340	85	0	0.00	0.00
360	85	0	0.00	0.00
380	85	0	0.00	0.00
400	85	0	0.00	0.00

Figure 45 and Figure 46 show the results for Figure 36and Figure 37 plotted with the distance from the nominal centerline of the boundary as the independent variable.

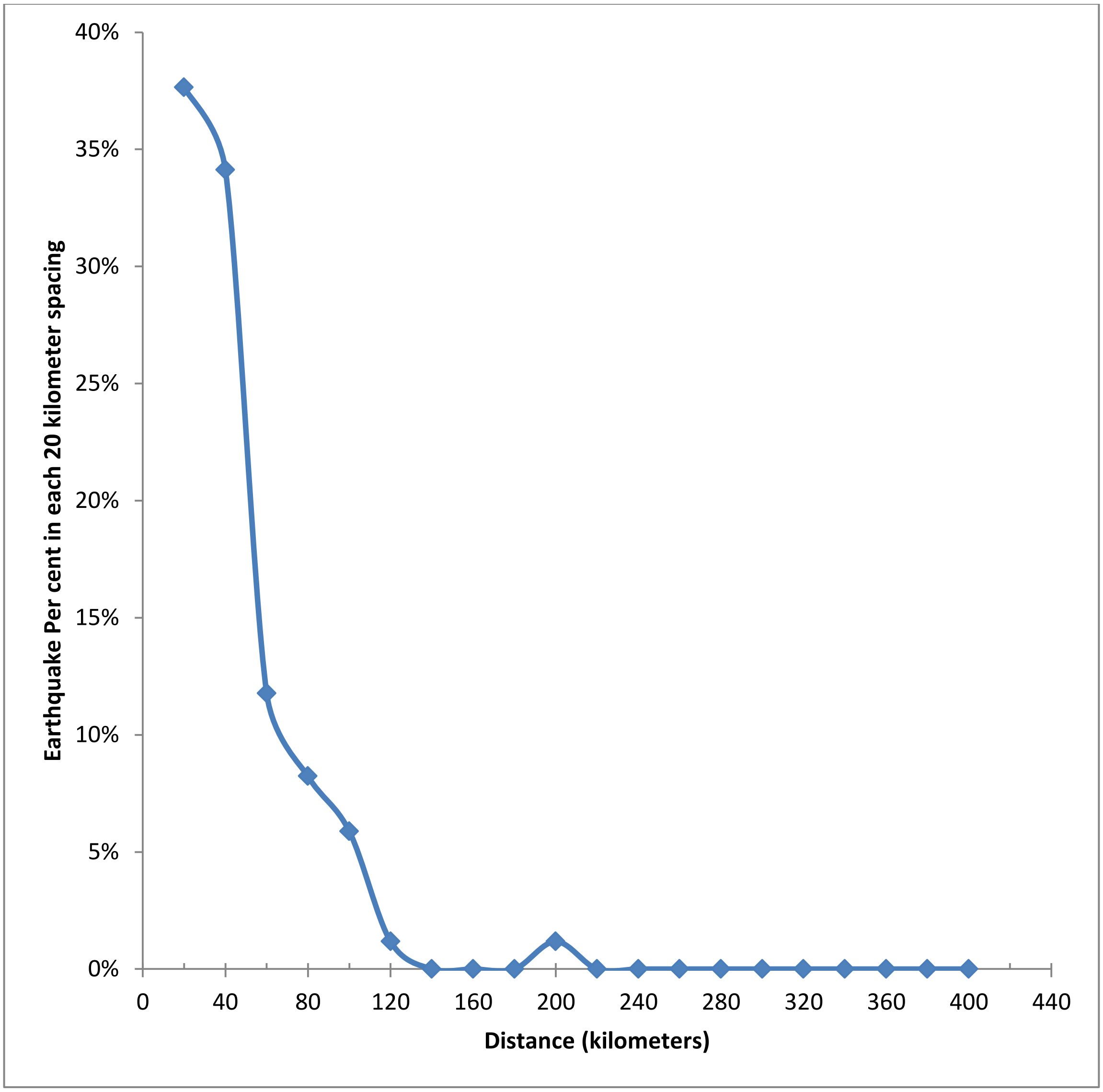

Figure 45 Transform Boundary Segment 1 Side A Results

Table 37
Transform Boundary Segment 1 Side B

Distance from boundary	No. of earthquakes	No. of earthquakes in the 20km segment	Per cent %	Difference %
20	63	63	67.02	
40	89	26	27.66	39.36
60	90	1	1.06	26.60
80	92	2	2.13	1.06
100	93	1	1.06	1.06
120	93	0	0.00	1.06
140	93	0	0.00	0.00
160	94	1	1.06	1.06
180	94	0	0.00	1.06
200	94	0	0.00	0.00
220	94	0	0.00	0.00
240	94	0	0.00	0.00
260	94	0	0.00	0.00
280	94	0	0.00	0.00
300	94	0	0.00	0.00
320	94	0	0.00	0.00
340	94	0	0.00	0.00
360	94	0	0.00	0.00
380	94	0	0.00	0.00
400	94	0	0.00	0.00

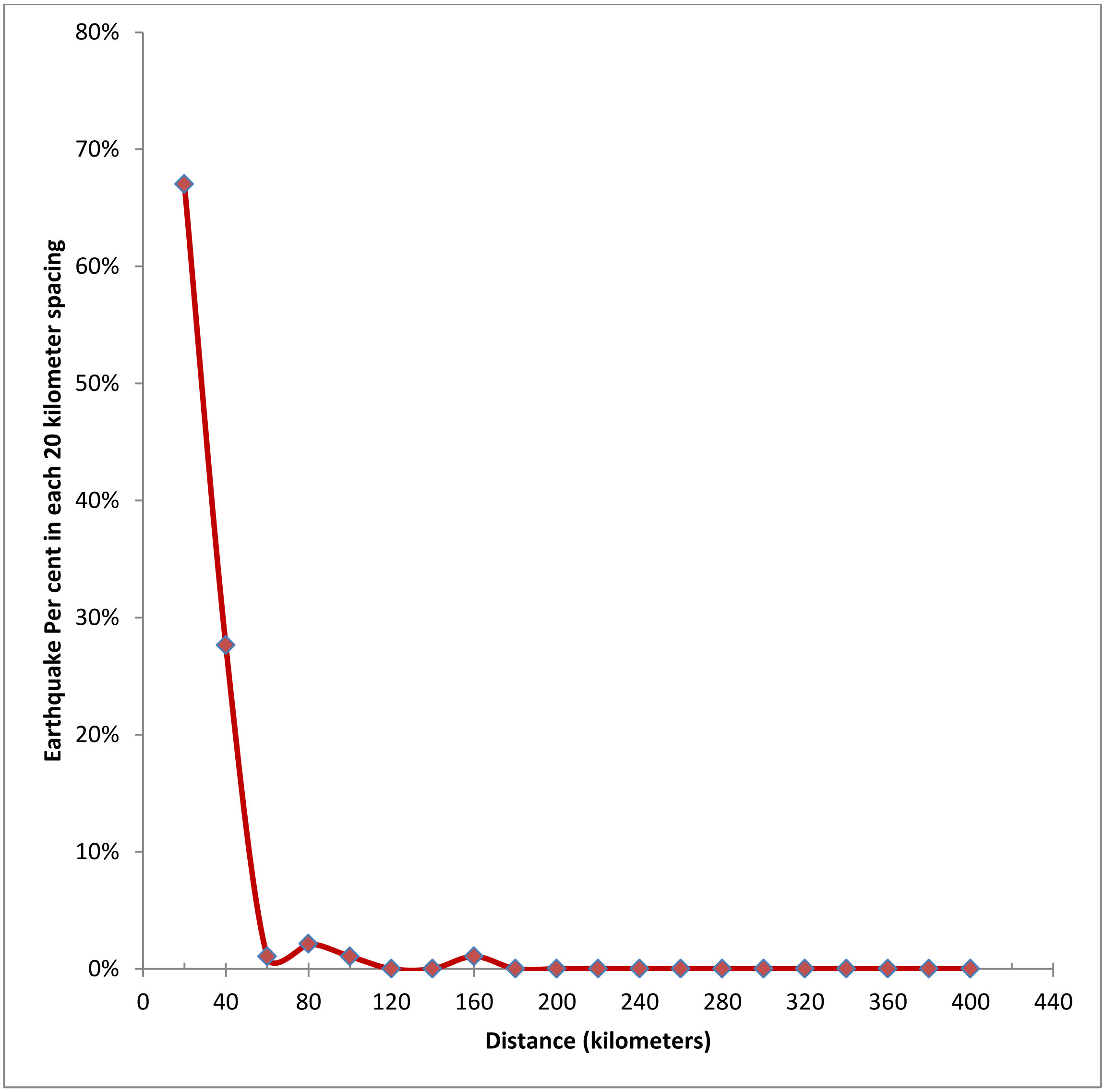

Figure 46 Transform Boundary Segment 1 Side B Results

Transform Boundary Set Two

The data is shown in Table 38 and Table 39 for Side A and Side B respectively.

Table 38
Transform Boundary Segment 2 Side A

Distance from boundary	No. of earthquakes	No. of earthquakes in the 20km segment	Per cent %	Difference %
20	11	11	47.83	
40	18	7	30.43	17.39
60	19	1	4.35	26.09
80	22	3	13.04	8.70
100	22	0	0.00	13.04
120	22	0	0.00	0.00
140	23	1	4.35	4.35
160	23	0	0.00	4.35
180	23	0	0.00	0.00
200	23	0	0.00	0.00
220	23	0	0.00	0.00
240	23	0	0.00	0.00
260	23	0	0.00	0.00
280	23	0	0.00	0.00
300	23	0	0.00	0.00
320	23	0	0.00	0.00
340	23	0	0.00	0.00
360	23	0	0.00	0.00
380	23	0	0.00	0.00
400	23	0	0.00	0.00

Figure 47 and Figure 48 show the results for Table 38 and Table 39 plotted with the distance from the nominal centerline of the boundary as the independent variable.

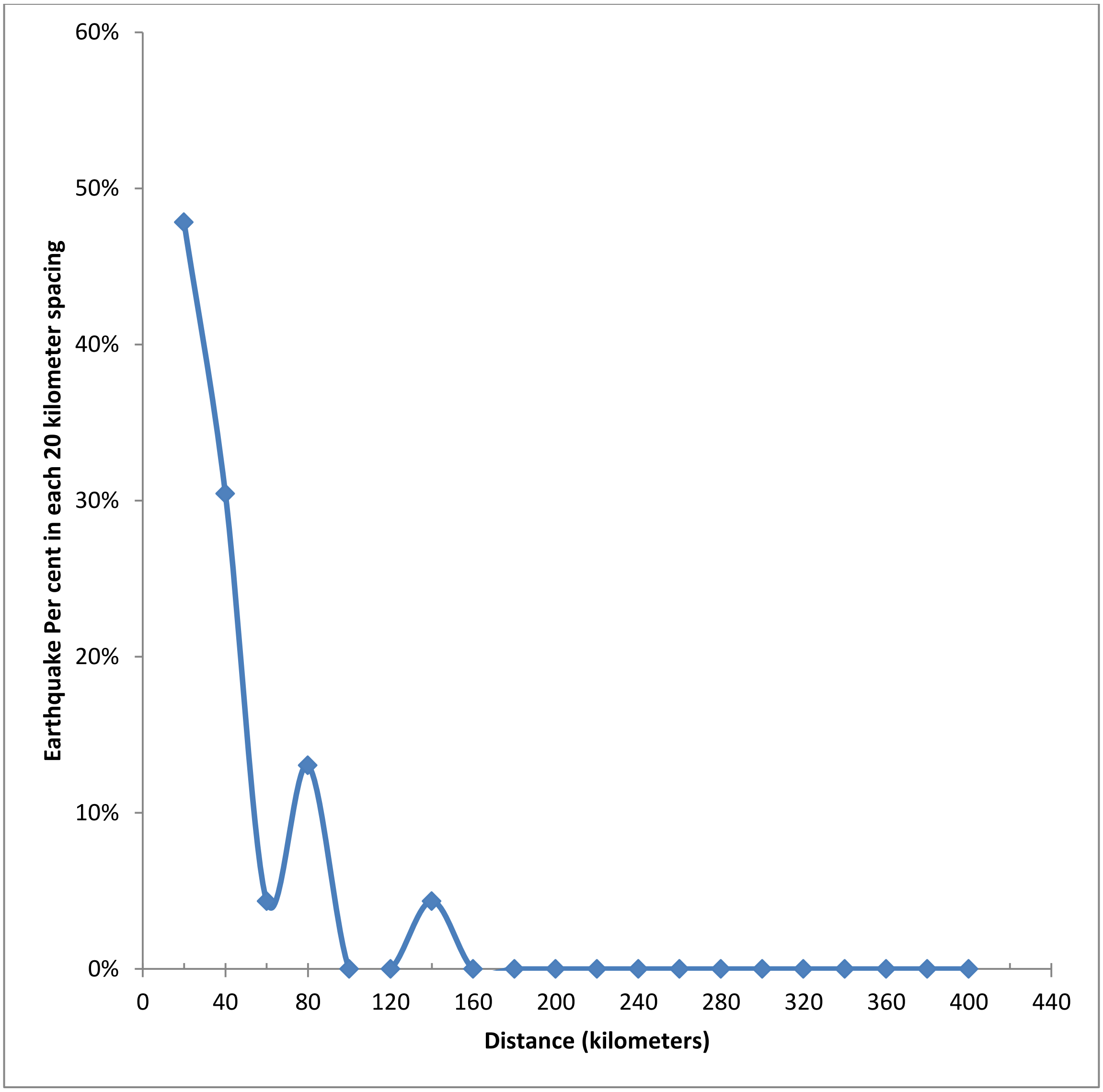

Figure 47 Transform Boundary Segment 2 Side A Results

Table 39
Transform Boundary Segment 2 Side B

Distance from boundary	No. of earthquakes	No. of earthquakes in the 20km segment	Per cent %	Difference %
20	29	29	78.38	
40	35	6	16.22	62.16
60	36	1	2.70	13.51
80	37	1	2.70	0.00
100	37	0	0.00	2.70
120	37	0	0.00	0.00
140	37	0	0.00	0.00
160	37	0	0.00	0.00
180	37	0	0.00	0.00
200	37	0	0.00	0.00
220	37	0	0.00	0.00
240	37	0	0.00	0.00
260	37	0	0.00	0.00
280	37	0	0.00	0.00
300	37	0	0.00	0.00
320	37	0	0.00	0.00
340	37	0	0.00	0.00
360	37	0	0.00	0.00
380	37	0	0.00	0.00
400	37	0	0.00	0.00

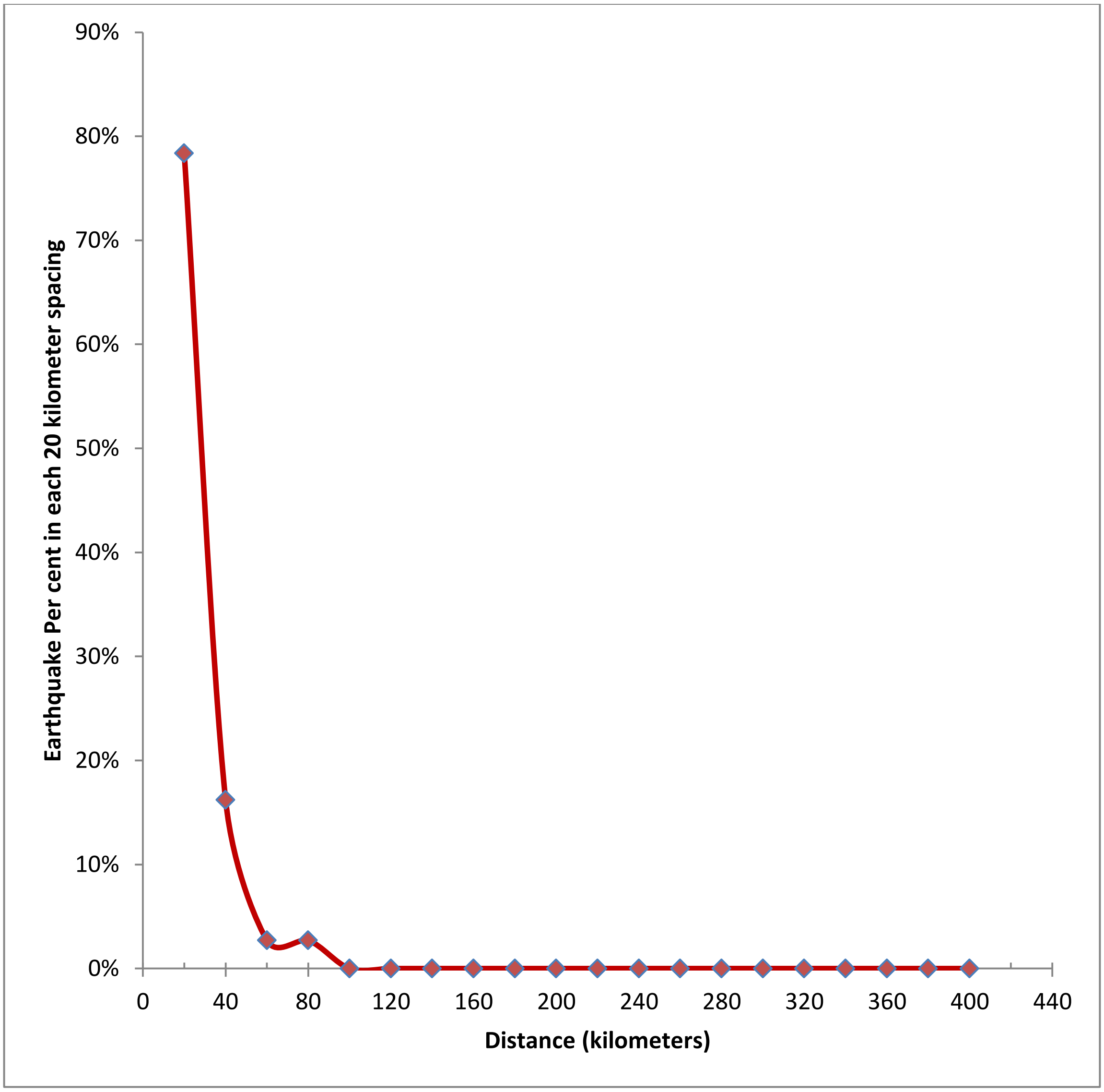

Figure 48 Transform Boundary Segment 2 Side B Results

Transform Boundary Set Three

The data is shown in Table 40 and Table 41 for Side A and Side B respectively.

Table 40
Transform Boundary Segment 3 Side A

Distance from boundary	No. of earthquakes	No. of earthquakes in the 20km segment	Per cent %	Difference %
20	17	17	89.47	
40	17	0	0.00	89.47
60	18	1	5.26	5.26
80	18	0	0.00	5.26
100	19	1	5.26	5.26
120	19	0	0.00	5.26
140	19	0	0.00	0.00
160	19	0	0.00	0.00
180	19	0	0.00	0.00
200	19	0	0.00	0.00
220	19	0	0.00	0.00
240	19	0	0.00	0.00
260	19	0	0.00	0.00
280	19	0	0.00	0.00
300	19	0	0.00	0.00
320	19	0	0.00	0.00
340	19	0	0.00	0.00
360	19	0	0.00	0.00
380	19	0	0.00	0.00
400	19	0	0.00	0.00

Figure 49 and Figure 50 show the results for Table 40 and Table 41 plotted with the distance from the nominal centerline of the boundary as the independent variable.

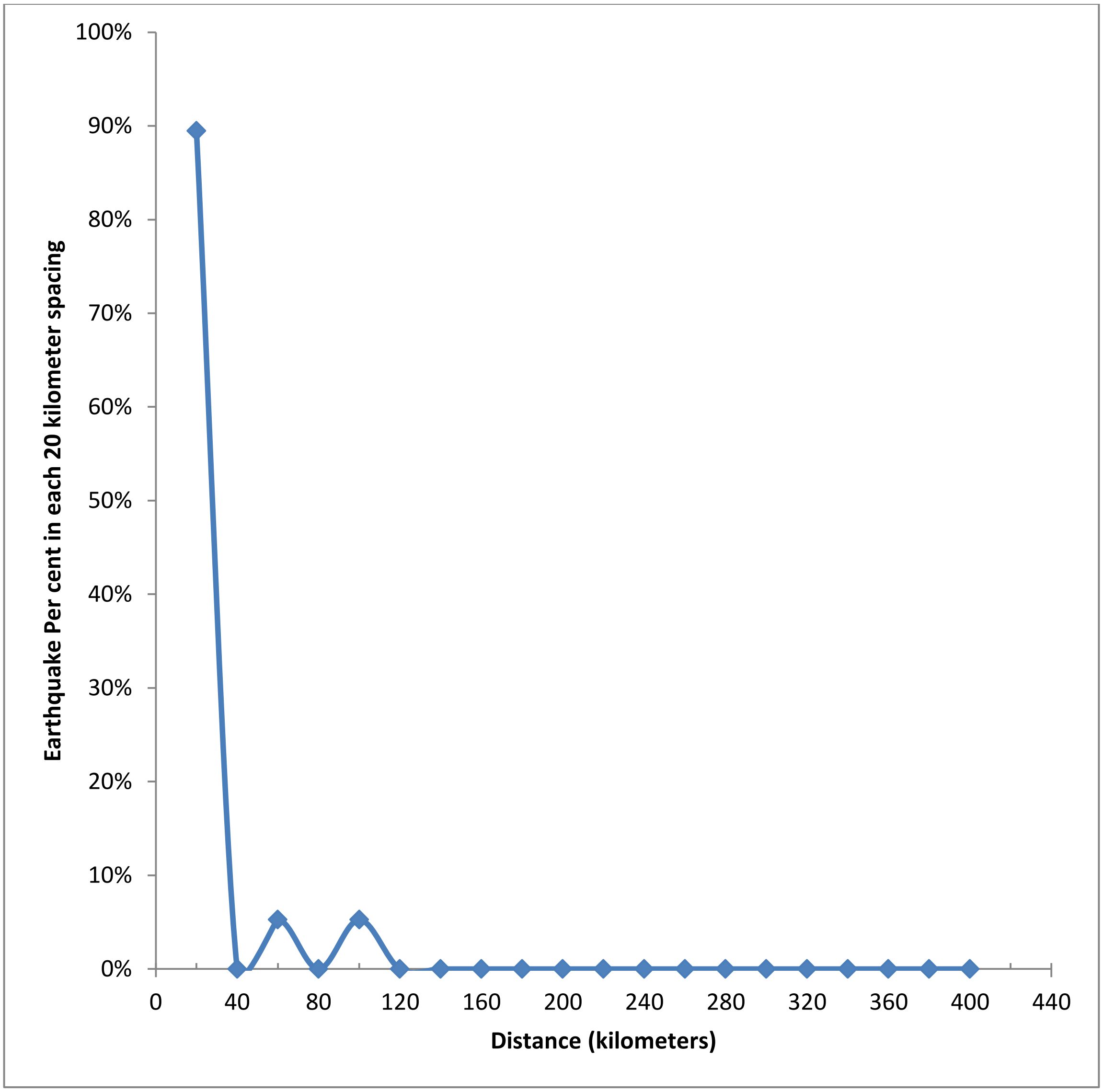

Figure 49 Transform Boundary Segment 3 Side A Results

Table 41
Transform Boundary Segment 3 Side B

Distance from boundary	No. of earthquakes	No. of earthquakes in the 20km segment	Per cent %	Difference %
20	15	15	71.43	
40	16	1	4.76	66.67
60	17	1	4.76	0.00
80	19	2	9.52	4.76
100	19	0	0.00	9.52
120	19	0	0.00	0.00
140	19	0	0.00	0.00
160	20	1	4.76	4.76
180	21	1	4.76	0.00
200	21	0	0.00	4.76
220	21	0	0.00	0.00
240	21	0	0.00	0.00
260	21	0	0.00	0.00
280	21	0	0.00	0.00
300	21	0	0.00	0.00
320	21	0	0.00	0.00
340	21	0	0.00	0.00
360	21	0	0.00	0.00
380	21	0	0.00	0.00
400	21	0	0.00	0.00

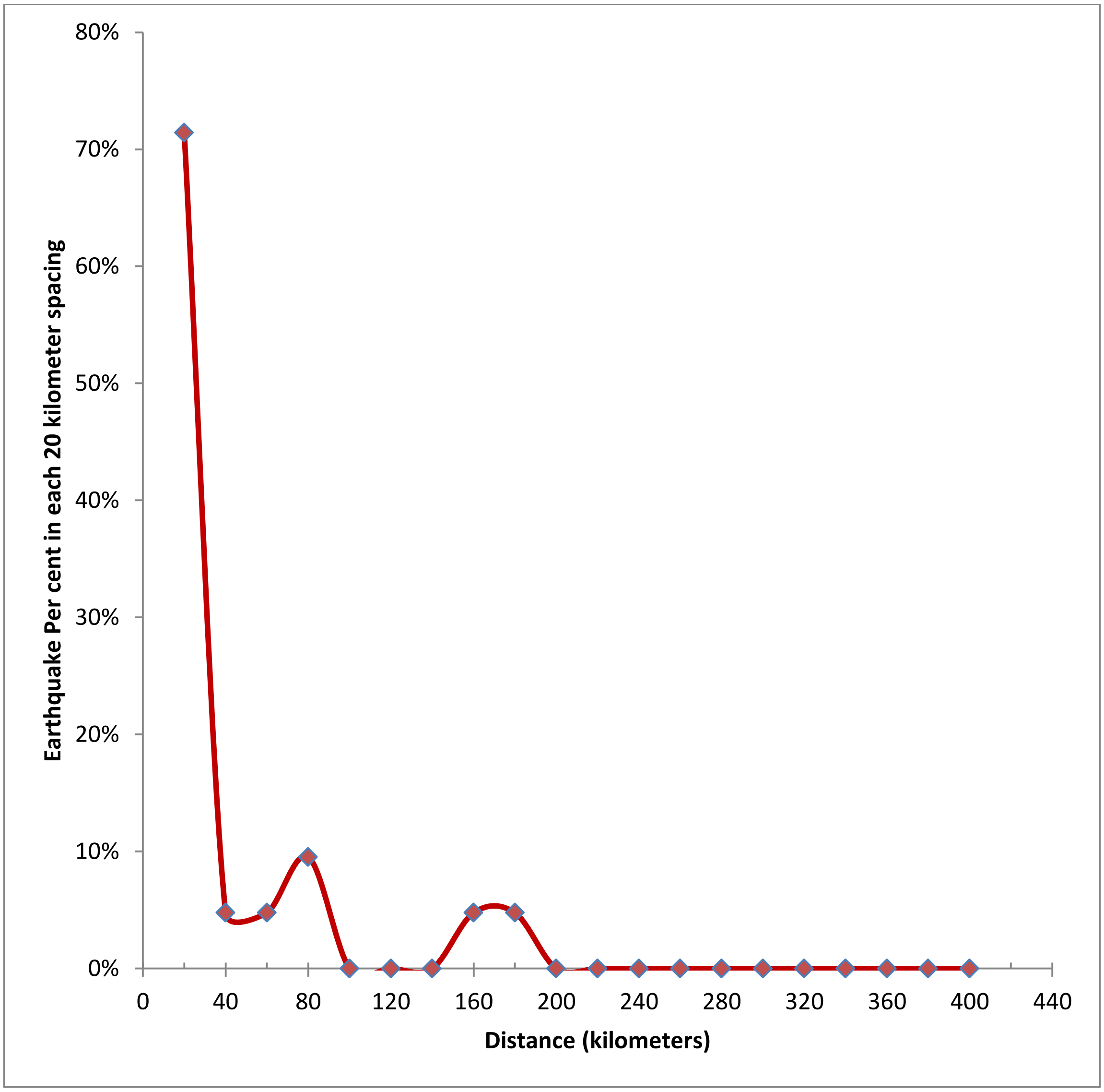

Figure 50 Transform Boundary Segment 3 Side B Results

Transform Boundary Set Four

The data is shown in Table 42 and Table 43 for Side A and Side B respectively.

Table 42
Transform Boundary Segment 4 Side A

Distance from boundary	No. of earthquakes	No. of earthquakes in the 20km segment	Per cent %	Difference %
20	43	43	64.18	
40	59	16	23.88	40.30
60	64	5	7.46	16.42
80	65	1	1.49	5.97
100	65	0	0.00	1.49
120	66	1	1.49	1.49
140	67	1	1.49	0.00
160	67	0	0.00	1.49
180	67	0	0.00	0.00
200	67	0	0.00	0.00
220	67	0	0.00	0.00
240	67	0	0.00	0.00
260	67	0	0.00	0.00
280	67	0	0.00	0.00
300	67	0	0.00	0.00
320	67	0	0.00	0.00
340	67	0	0.00	0.00
360	67	0	0.00	0.00
380	67	0	0.00	0.00
400	67	0	0.00	0.00

Figure 51 and Figure 52 show the results for Table 42 and Table 43 plotted with the distance from the nominal centerline of the boundary as the independent variable.

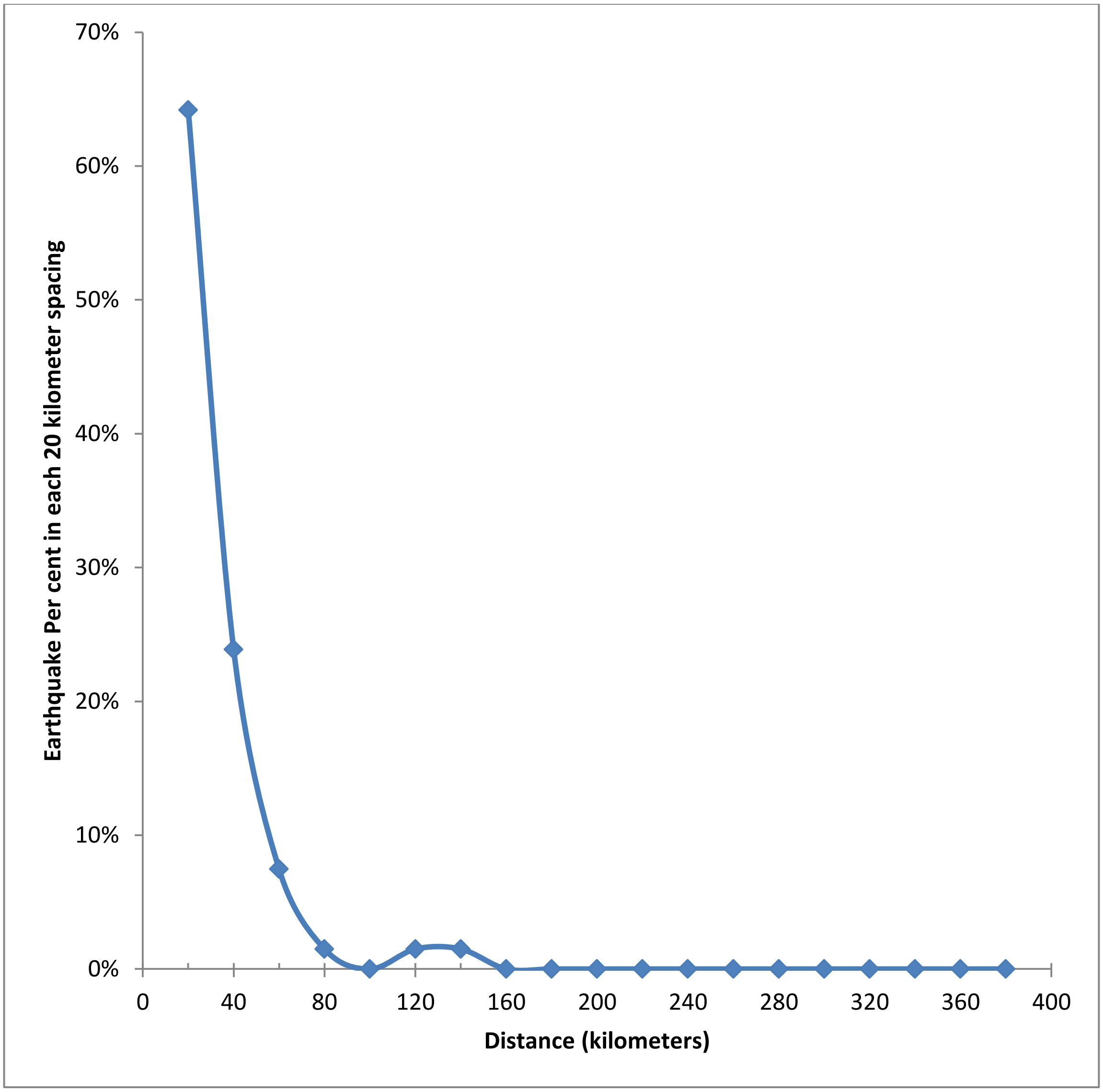

Figure 51 Transform Boundary Segment 4 Side A Results

Table 43
Transform Boundary Segment 4 Side B

Distance from boundary	No. of earthquakes	No. of earthquakes in the 20km segment	Per cent %	Difference %
20	32	32	62.75	
40	45	13	25.49	37.25
60	48	3	5.88	19.61
80	50	2	3.92	1.96
100	51	1	1.96	1.96
120	51	0	0.00	1.96
140	51	0	0.00	0.00
160	51	0	0.00	0.00
180	51	0	0.00	0.00
200	51	0	0.00	0.00
220	51	0	0.00	0.00
240	51	0	0.00	0.00
260	51	0	0.00	0.00
280	51	0	0.00	0.00
300	51	0	0.00	0.00
320	51	0	0.00	0.00
340	51	0	0.00	0.00
360	51	0	0.00	0.00
380	51	0	0.00	0.00
400	51	0	0.00	0.00

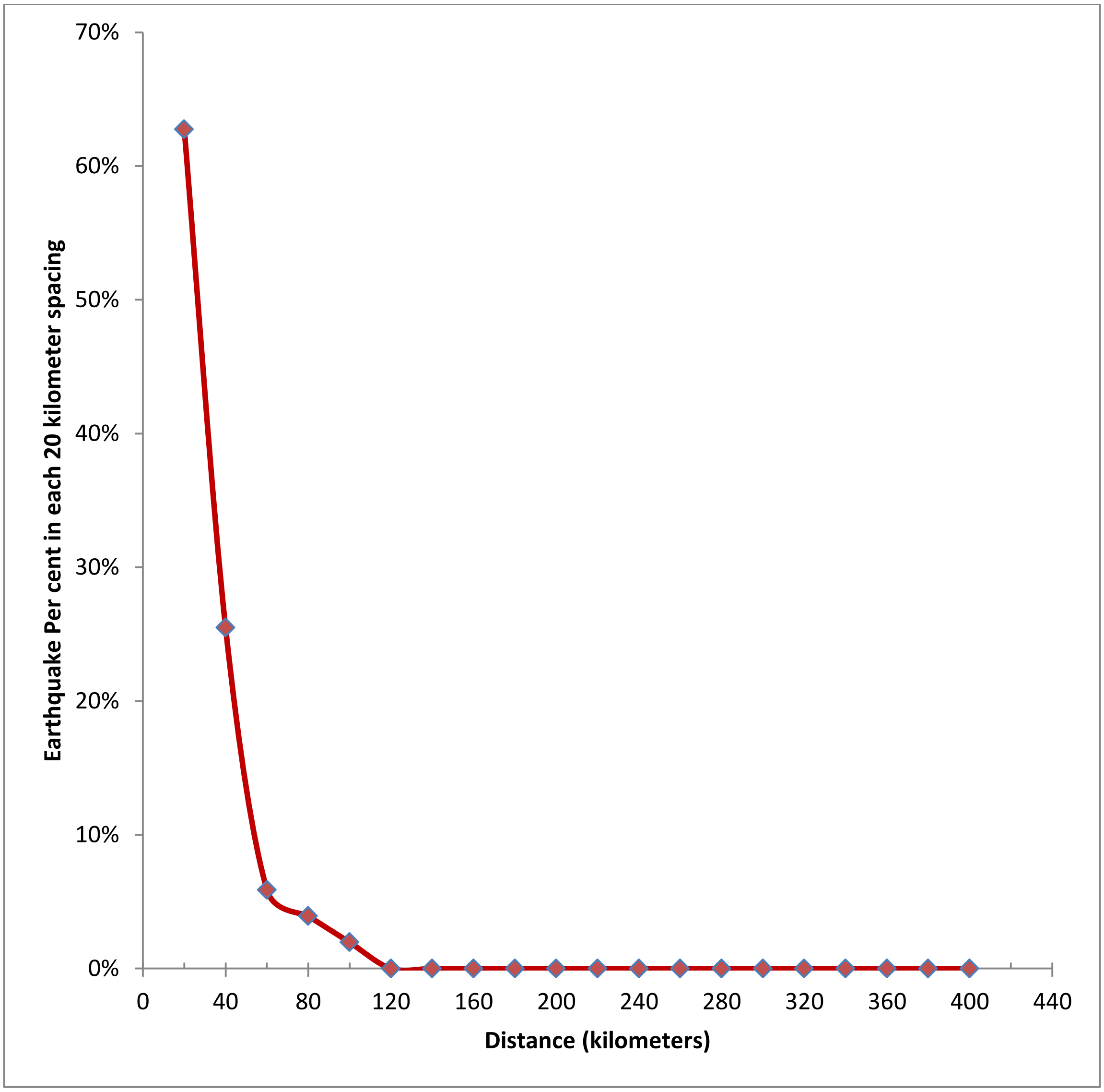

Figure 52 Transform Boundary Segment 4 Side-B Results

Transform Boundary Set Five

The data is shown in Table 44 and Table 45 for Side A and Side B respectively.

Table 44
Transform Boundary Segment 5 Side A

Distance from boundary	No. of earthquakes	No. of earthquakes in the 20km segment	Per cent %	Difference %
20	18	18	46.15	
40	29	11	28.21	17.95
60	37	8	20.51	7.69
80	39	2	5.13	15.38
100	39	0	0.00	5.13
120	39	0	0.00	0.00
140	39	0	0.00	0.00
160	39	0	0.00	0.00
180	39	0	0.00	0.00
200	39	0	0.00	0.00
220	39	0	0.00	0.00
240	39	0	0.00	0.00
260	39	0	0.00	0.00
280	39	0	0.00	0.00
300	39	0	0.00	0.00
320	39	0	0.00	0.00
340	39	0	0.00	0.00
360	39	0	0.00	0.00
380	39	0	0.00	0.00
400	39	0	0.00	0.00

Figure 53 and Figure 54 show the results for Table 44 and Table 45 plotted with the distance from the nominal centerline of the boundary as the independent variable.

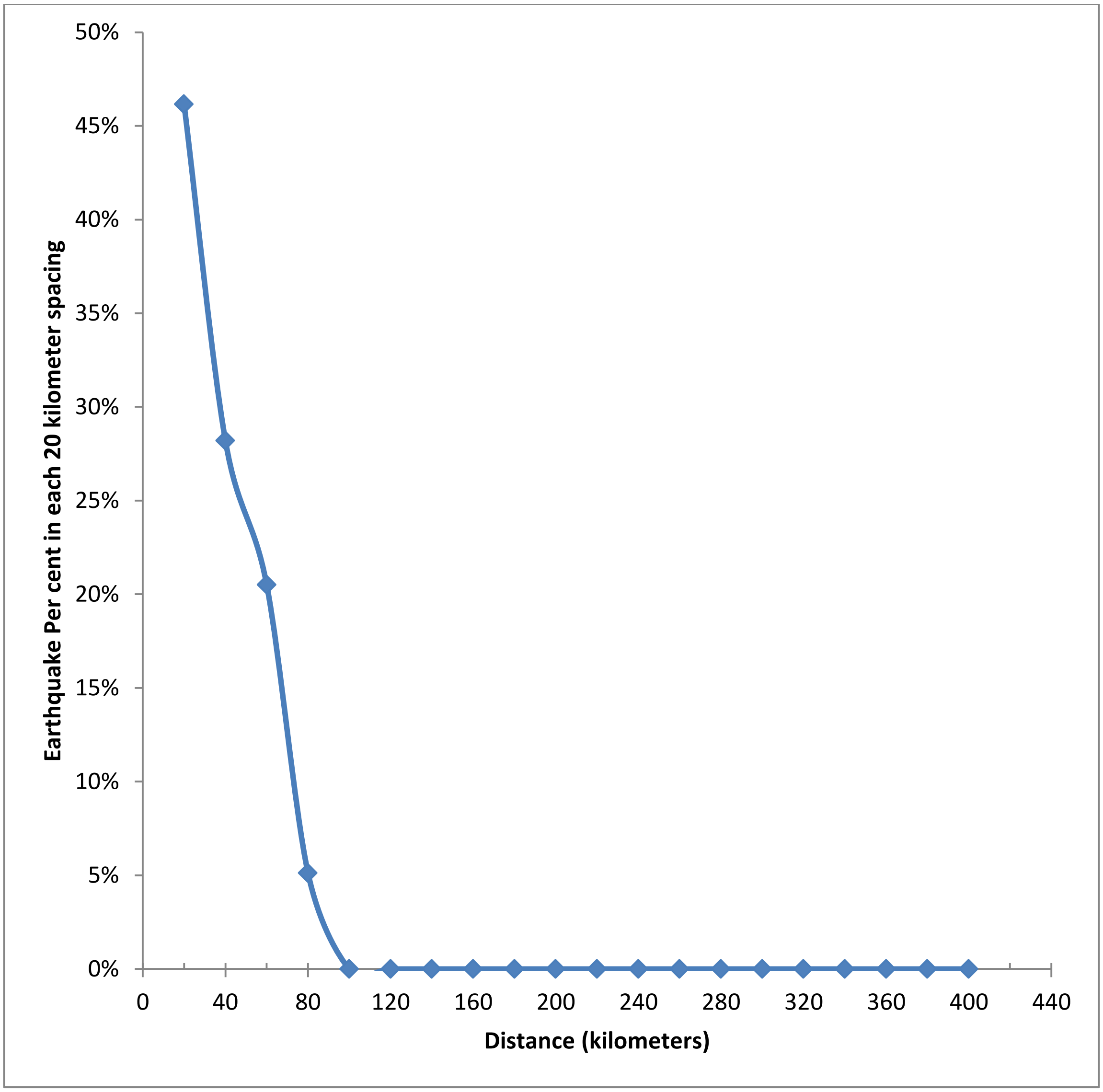

Figure 53 Transform Boundary Segment 5 Side A Results

Table 45
Transform Boundary Segment 5 Side B

Distance from boundary	No. of earthquakes	No. of earthquakes in the 20km segment	Per cent %	Difference %
20	9	9	64.29	
40	11	2	14.29	50.00
60	13	2	14.29	0.00
80	14	1	7.14	7.14
100	14	0	0.00	7.14
120	14	0	0.00	0.00
140	14	0	0.00	0.00
160	14	0	0.00	0.00
180	14	0	0.00	0.00
200	14	0	0.00	0.00
220	14	0	0.00	0.00
240	14	0	0.00	0.00
260	14	0	0.00	0.00
280	14	0	0.00	0.00
300	14	0	0.00	0.00
320	14	0	0.00	0.00
340	14	0	0.00	0.00
360	14	0	0.00	0.00
380	14	0	0.00	0.00
400	14	0	0.00	0.00

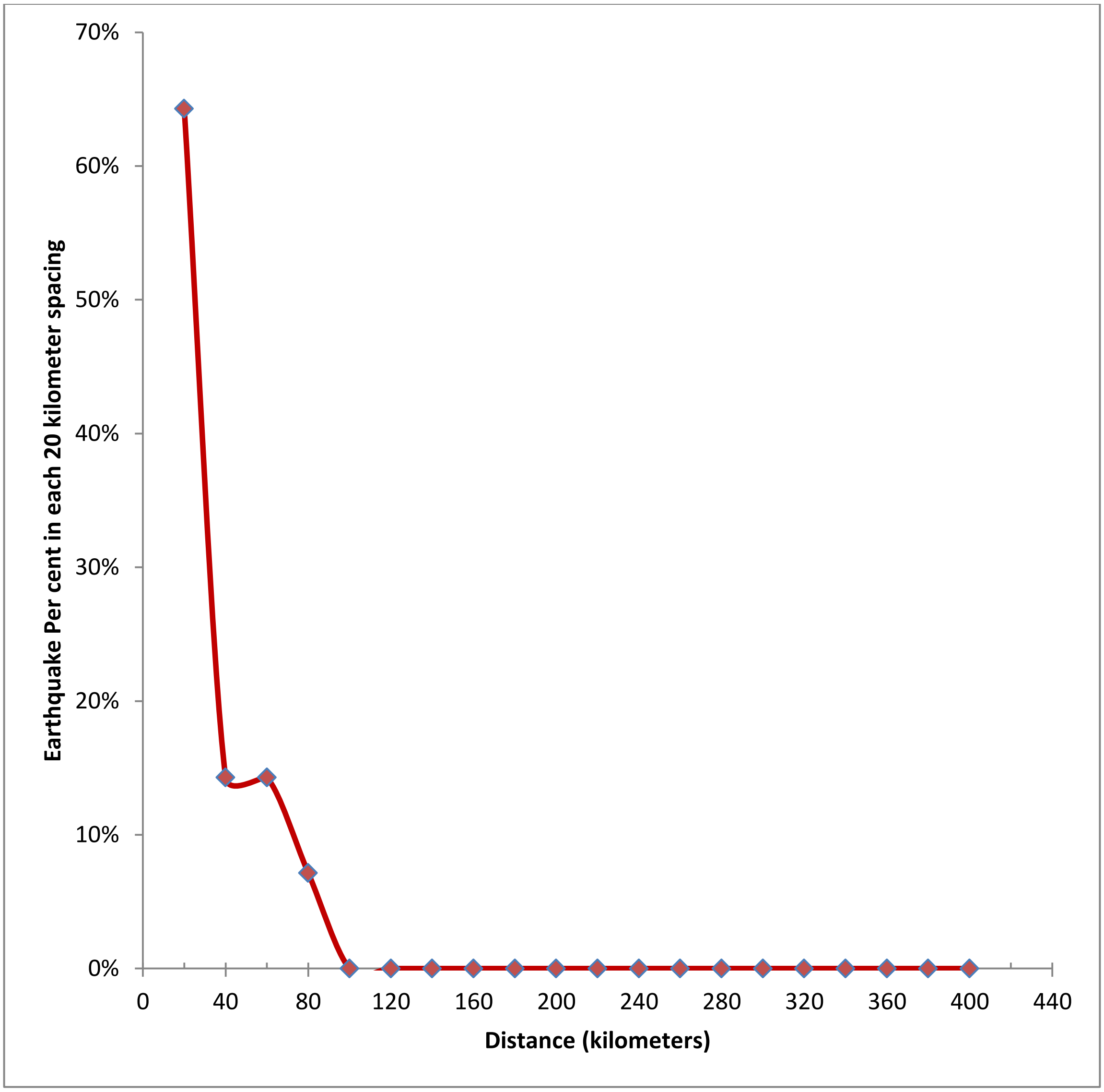

Figure 54 Transform Boundary Segment 5 Side B Results

Transform Boundary Set Six

The data is shown in Table 46 and Table 47 for Side A and Side B respectively.

Table 46
Transform Boundary Segment 6 Side A

Distance from boundary	No. of earthquakes	No. of earthquakes in the 20km segment	Per cent %	Difference %
20	15	15	88.24	
40	17	2	11.76	76.47
60	17	0	0.00	11.76
80	17	0	0.00	0.00
100	17	0	0.00	0.00
120	17	0	0.00	0.00
140	17	0	0.00	0.00
160	17	0	0.00	0.00
180	17	0	0.00	0.00
200	17	0	0.00	0.00
220	17	0	0.00	0.00
240	17	0	0.00	0.00
260	17	0	0.00	0.00
280	17	0	0.00	0.00
300	17	0	0.00	0.00
320	17	0	0.00	0.00
340	17	0	0.00	0.00
360	17	0	0.00	0.00
380	17	0	0.00	0.00
400	17	0	0.00	0.00

Figure 55 and Figure 56 show the results for Table 46 and Table 47 plotted with the distance from the nominal centerline of the boundary as the independent variable.

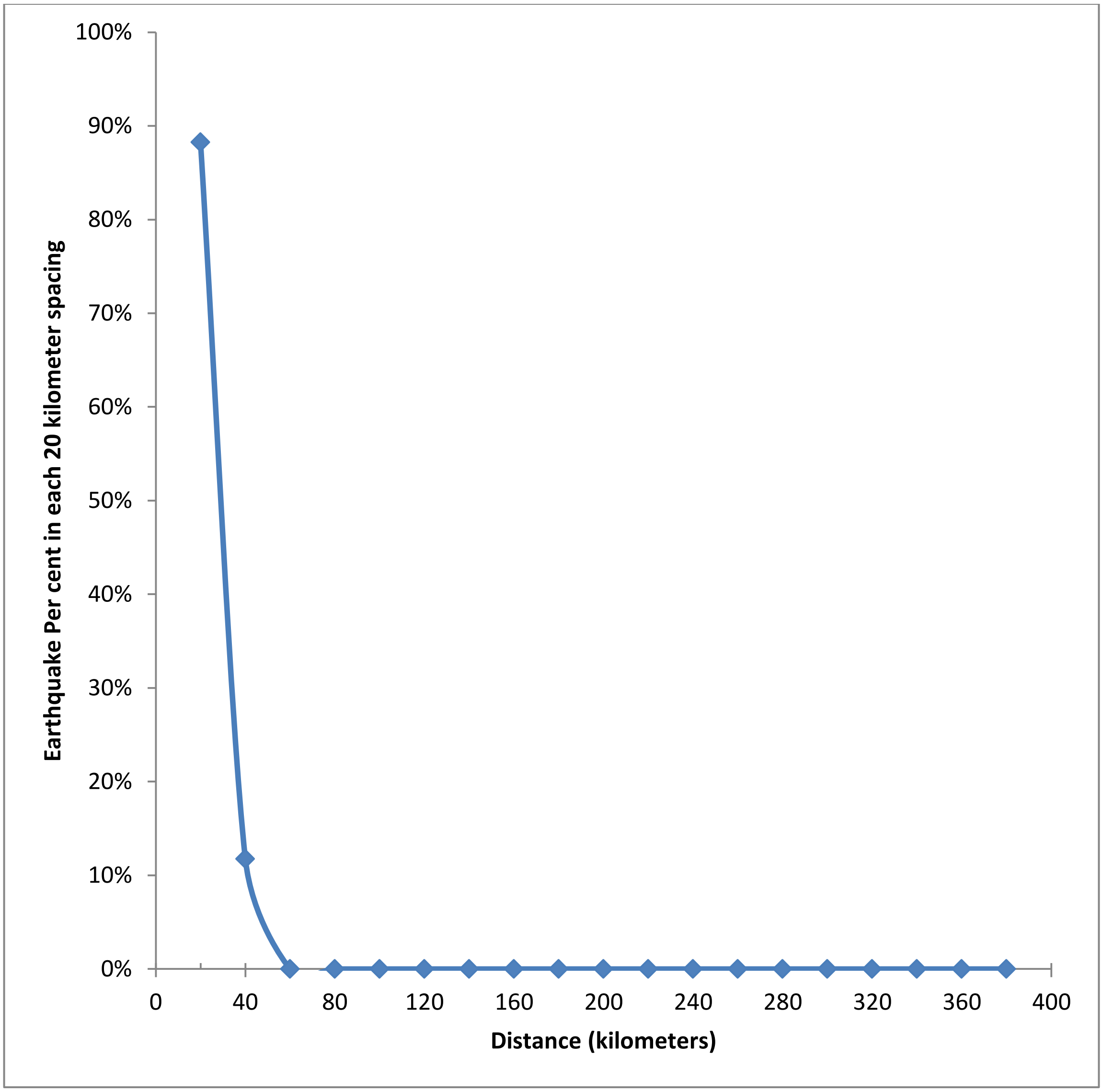

Figure 55 Transform Boundary Segment 6 Side A Results

Table 47
Transform Boundary Segment 6 Side B

Distance from boundary	No. of earthquakes	No. of earthquakes in the 20km segment	Per cent %	Difference %
20	12	12	80.00	
40	14	2	13.33	66.67
60	15	1	6.67	6.67
80	15	0	0.00	6.67
100	15	0	0.00	0.00
120	15	0	0.00	0.00
140	15	0	0.00	0.00
160	15	0	0.00	0.00
180	15	0	0.00	0.00
200	15	0	0.00	0.00
220	15	0	0.00	0.00
240	15	0	0.00	0.00
260	15	0	0.00	0.00
280	15	0	0.00	0.00
300	15	0	0.00	0.00
320	15	0	0.00	0.00
340	15	0	0.00	0.00
360	15	0	0.00	0.00
380	15	0	0.00	0.00
400	15	0	0.00	0.00

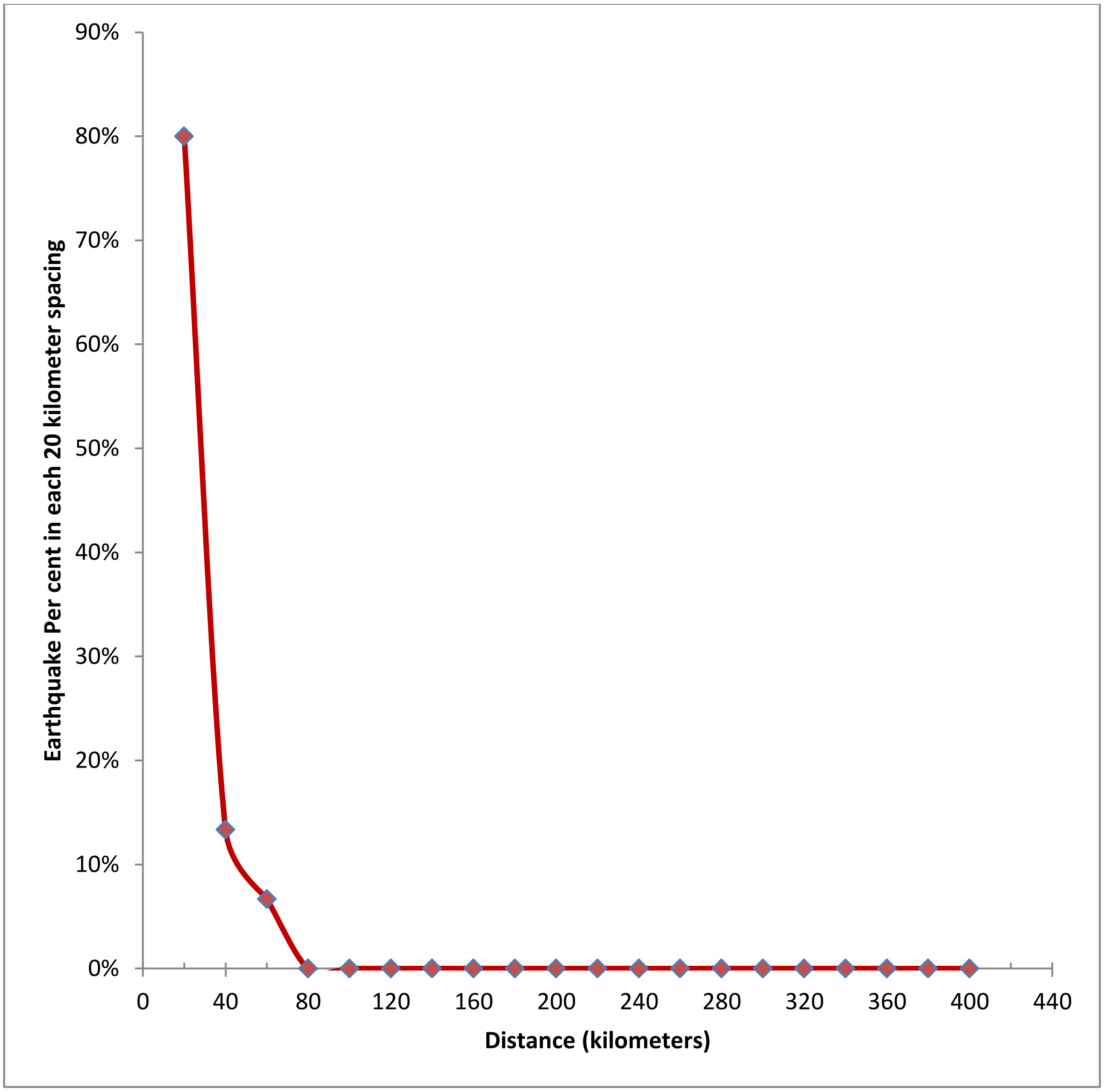

Figure 56 Transform Boundary Segment 6 Side B Results

APPENDIX D

WORLD DATA AVERAGE

Introduction

The study performed on the entire population yielded the results as depicted in this appendix, which presents the frequency of earthquakes distributed as a function of distance from the plate boundaries for Side A and Side B.

Linear Width

Table 48 and Table 49 represent the summary of the data presented in the graphical format in Figure 57 and Figure 58 respectively.

Table 48
Linear Width World Map Calculation Side A Results

Distance from boundary	No. of earthquakes	No. of earthquakes in the 20km segment	Per cent %	Difference %
20	8159	8159	15.63	
40	13517	5358	10.26	2.06
60	17802	4285	8.21	1.89
80	21099	3297	6.32	1.75
100	23482	2383	4.56	1.23
120	25221	1739	3.33	0.86
140	26513	1292	2.47	0.73
160	27422	909	1.74	0.35
180	28148	726	1.39	0.32
200	28707	559	1.07	0.04
220	29247	540	1.03	0.36
240	29600	353	0.68	0.08
260	29912	312	0.60	0.08

Table 48 Continued

Distance from boundary	No. of earthquakes	No. of earthquakes in the 20km segment	Per cent %	Difference %
280	30184	272	0.52	0.05
300	30484	300	0.57	0.04
320	30762	278	0.53	0.26
340	30904	142	0.27	0.06
360	31013	109	0.21	0.02
380	31132	119	0.23	0.03
400	31237	105	0.20	0.20

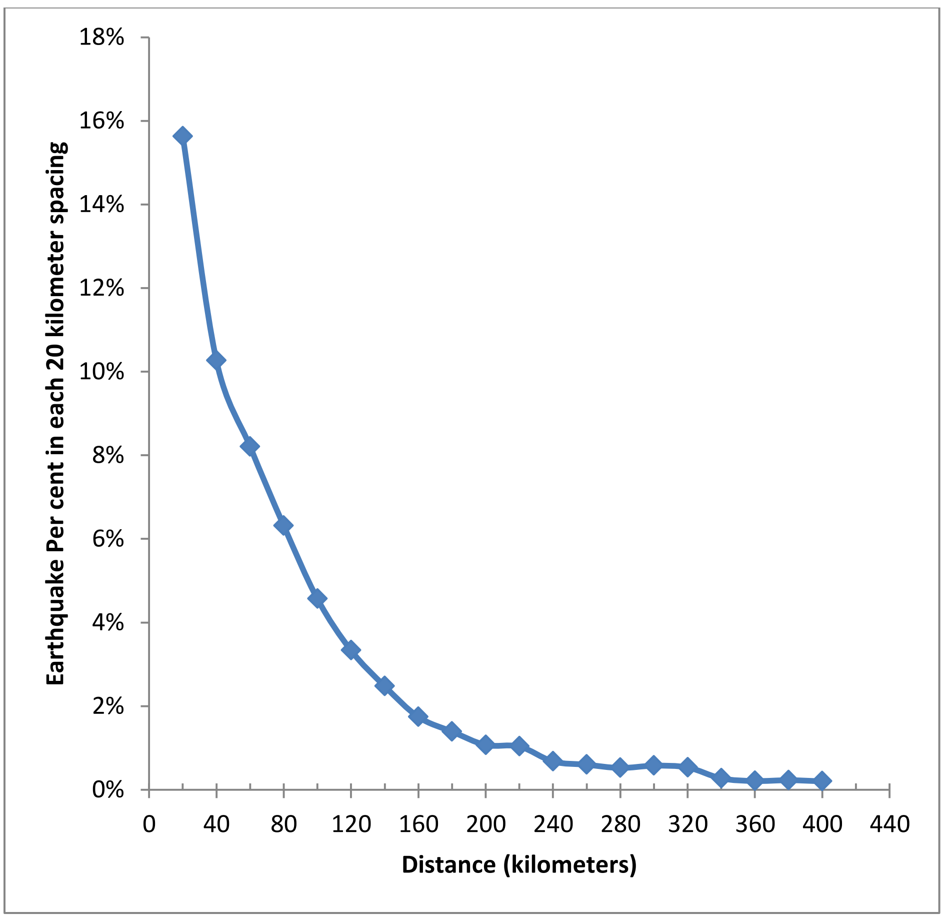

Figure 57 Linear Width Calculations Side A Results

Table 49
Linear Width World Map Calculation Side A Results

Distance from boundary	No. of earthquakes	No. of earthquakes in the 20km segment	Per cent %	Difference %
20	11883	11883	22.76	
40	18365	6482	12.42	10.35
60	24763	6398	12.26	0.16
80	31033	6270	12.01	0.25
100	35973	4940	9.46	2.55
120	40165	4192	8.03	1.43
140	43134	2969	5.69	2.34
160	45023	1889	3.62	2.07
180	46448	1425	2.73	0.89
200	47587	1139	2.18	0.55
220	48671	1084	2.08	0.11
240	49475	804	1.54	0.54
260	50157	682	1.31	0.23
280	50757	600	1.15	0.16
300	51143	386	0.74	0.41
320	51378	235	0.45	0.29
340	51625	247	0.47	0.02
360	51914	289	0.55	0.08
380	52073	159	0.30	0.25
400	52205	132	0.25	0.05

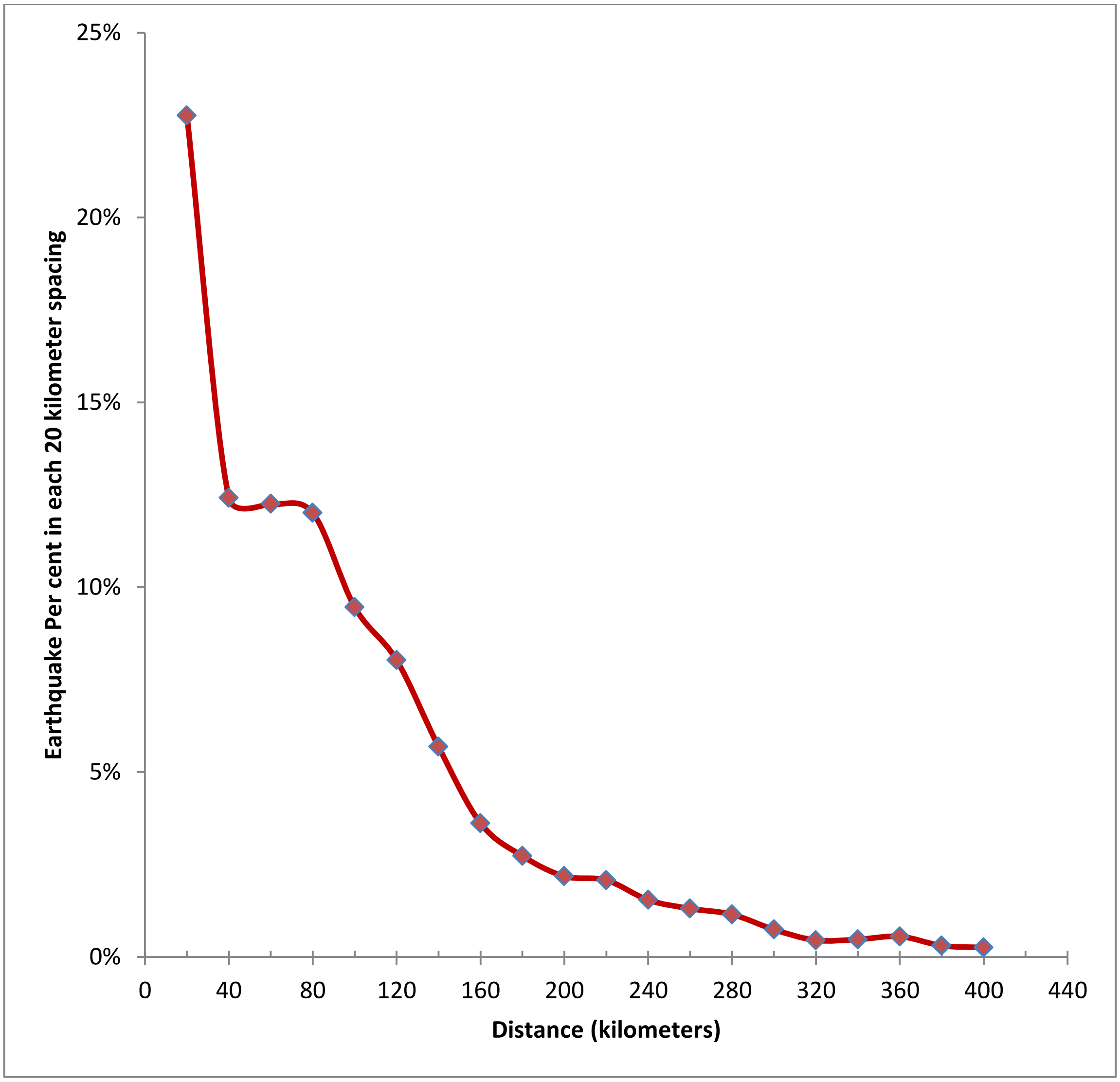

Figure 58 Linear Width calculations Side B Results

Angular Width

Table 50 and Table 51 represent the summary of the data presented in the graphical format in Figure 59 and Figure 60 respectively.

Table 50
Angular Width World Map Calculation Side A Results

Distance from boundary	No. of earthquakes	No. of earthquakes in the 20km segment	Per cent %	Difference %
0.2	9011	9011	18.43	
0.4	14831	5820	11.90	2.62
0.6	19369	4538	9.28	2.55
0.8	22659	3290	6.73	1.95
1.0	24996	2337	4.78	1.41
1.2	26641	1645	3.36	0.99
1.4	27803	1162	2.38	0.63
1.6	28655	852	1.74	0.35
1.8	29334	679	1.39	0.12
2.0	29952	618	1.26	0.51
2.2	30320	368	0.75	0.03
2.4	30674	354	0.72	0.08
2.6	30989	315	0.64	0.03
2.8	31318	329	0.67	0.25
3.0	31527	209	0.43	0.15
3.2	31662	135	0.28	0.03
3.4	31812	150	0.31	0.07
3.6	31928	116	0.24	0.07
3.8	32012	84	0.17	0.06
4.0	32065	53	0.11	0.11

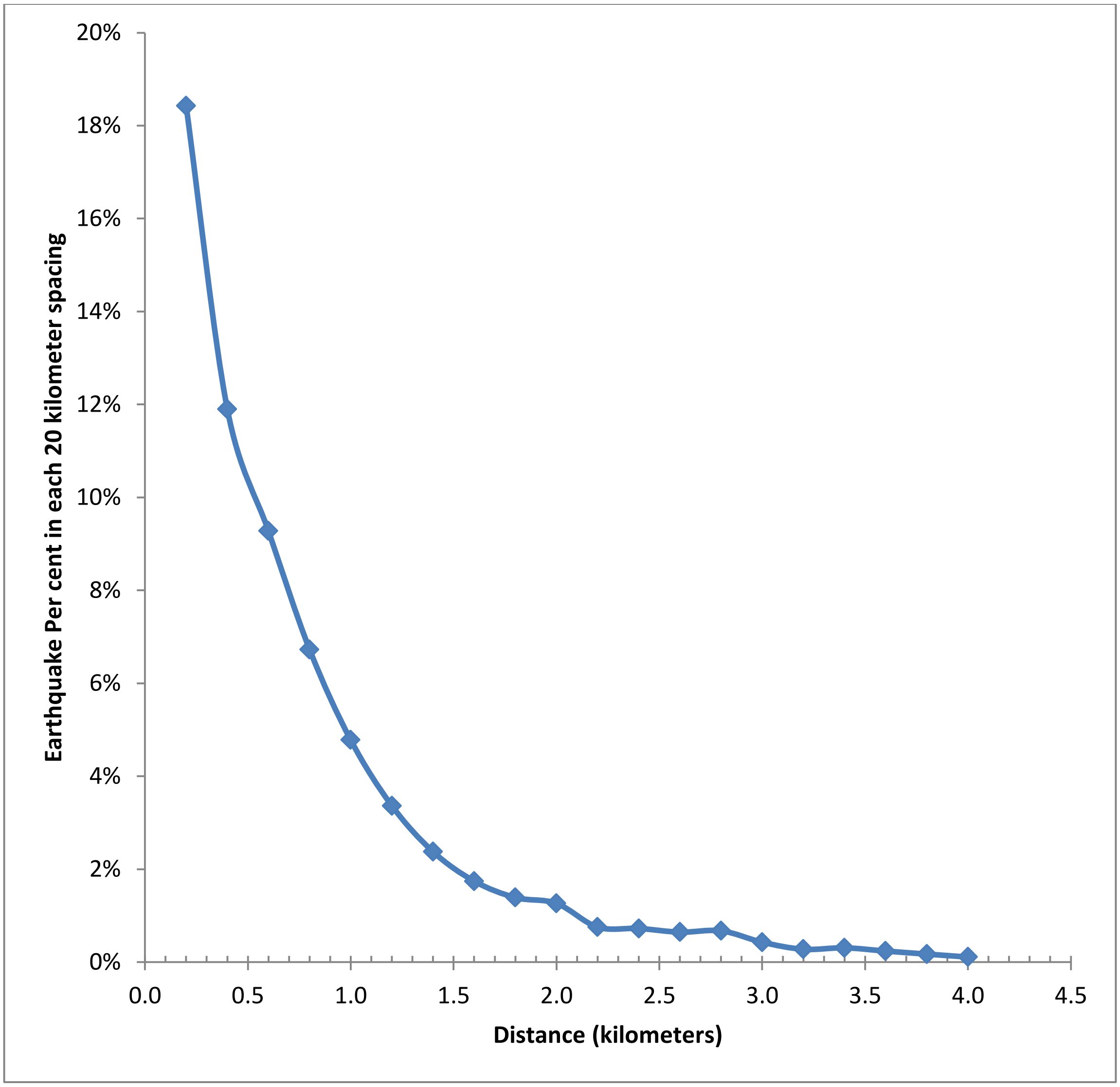

Figure 59 Angular Width Calculations Side A Results

Table 51
Angular Width World Map Calculation Side B Results

Distance from boundary	No. of earthquakes	No. of earthquakes in the 20km segment	Per cent %	Difference %
0.2	9588	9588	19.60	
0.4	16470	6882	14.07	5.53
0.6	23501	7031	14.38	0.30
0.8	29873	6372	13.03	1.35
1.0	34978	5105	10.44	2.59
1.2	38757	3779	7.73	2.71
1.4	41122	2365	4.84	2.89
1.6	42773	1651	3.38	1.46
1.8	44089	1316	2.69	0.68
2.0	45292	1203	2.46	0.23
2.2	46163	871	1.78	0.68
2.4	46881	718	1.47	0.31
2.6	47461	580	1.19	0.28
2.8	47763	302	0.62	0.57
3.0	48037	274	0.56	0.06
3.2	48373	336	0.69	0.13
3.4	48557	184	0.38	0.31
3.6	48706	149	0.30	0.07
3.8	48817	111	0.23	0.08
4.0	48906	89	0.18	0.04

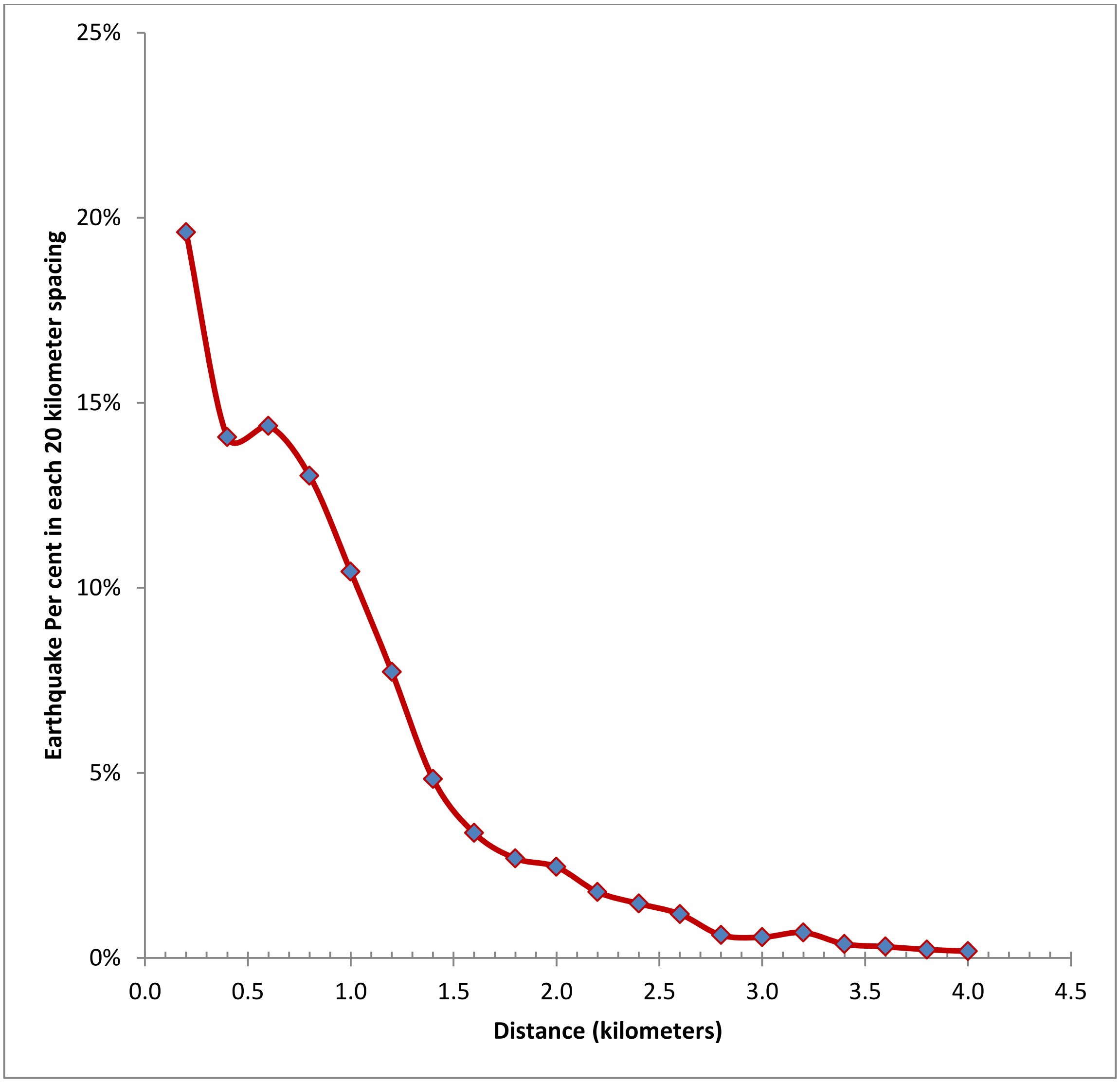

Figure 60 Angular Width Calculations Side B Results

APPENDIX E

DATA SUMMARY FOR THE THREE TECTONIC PLATE BOUNDARIES

Introduction

The study performed on the three types of plate boundaries, namely, convergent, divergent and transform tectonic plate boundaries, is summarized and averaged to yield the results as depicted in this appendix, which presents the frequency of earthquakes distributed as a function of distance from the plate boundaries for Side A and Side B.

Convergent Plate Boundary

Table 52 and Table 53 represent the data on the convergent plate boundary for Side A and Side B respectively.

Table 52
Table Showing the Percentage Values for the Number of Earthquakes at Segmented Distances from the Convergent Plate Boundary With Respect to the Total Number of Earthquakes in That Particular Segment for Side A

Distance from boundary	Average Percentile	Difference
20	25.74	
40	26.11	-0.37
60	16.27	9.84
80	9.24	7.03
100	5.50	3.74
120	1.91	3.59
140	1.18	0.73

Table 52 Continued

Distance from boundary	Average Percentile	Difference
160	1.09	0.09
180	0.55	0.55
200	5.73	-5.19
220	6.04	-0.31
240	0.06	5.98
260	0.18	-0.12
280	0.18	0.00
300	0.00	0.18
320	0.00	0.00
340	0.00	0.00
360	0.06	-0.06
380	0.18	-0.12
400	0.00	0.18

Figure 61 and Figure 62 show the results for Table 52 and Table 53 represent the data on the convergent plate boundary for Side A and Side B respectively. Table 52 plotted with the distance from the nominal centerline of the boundary as the independent variable.

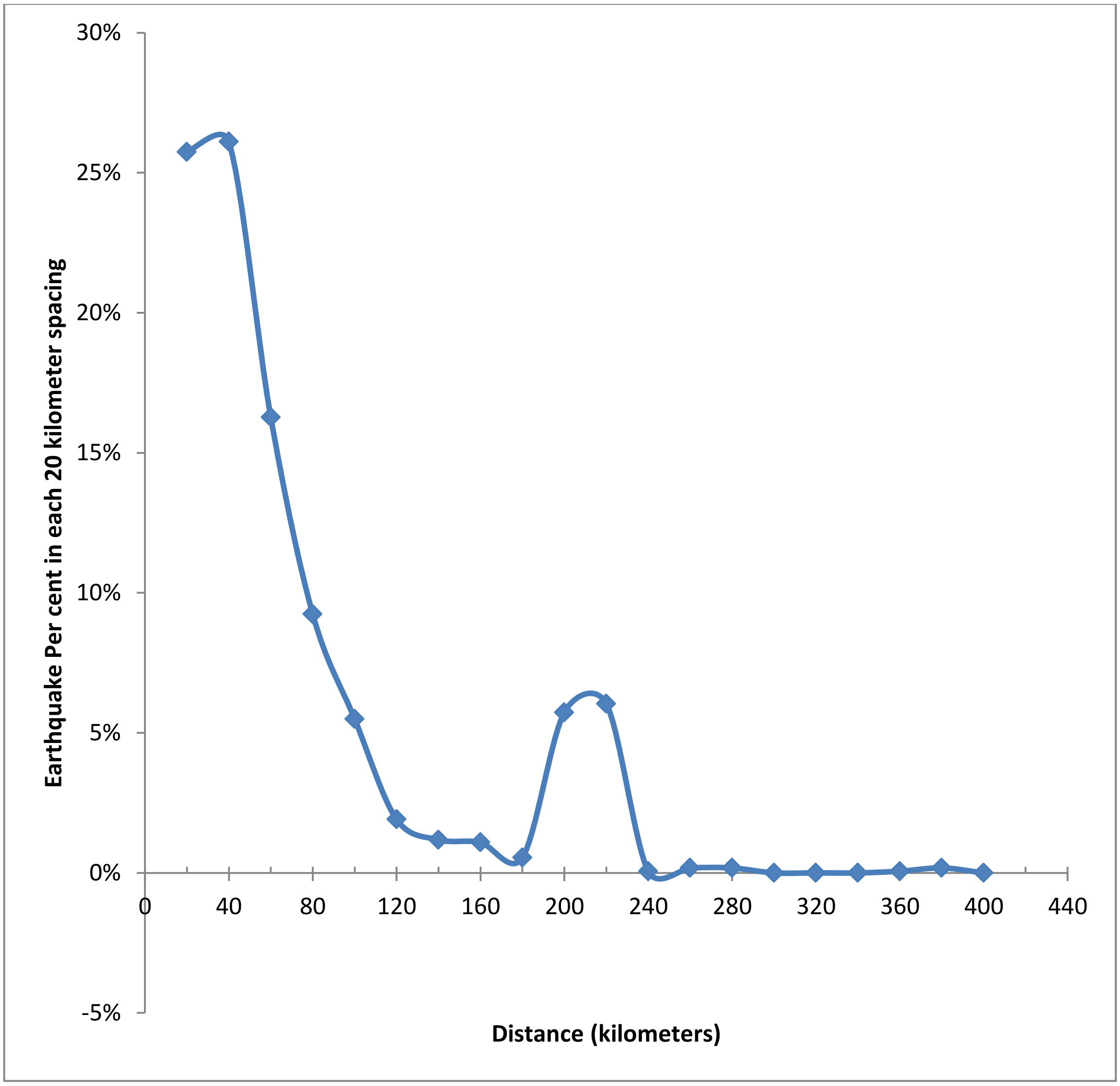

Figure 61 Graph Plotted for Linear Distance of the Earthquakes From the Plate Boundaries Against the Percentage of the Number of Earthquakes Out of the Total Number of Earthquakes in for Convergent Plate Boundary for Side A

Bivariate Fit of Convergent By Distance Set=A

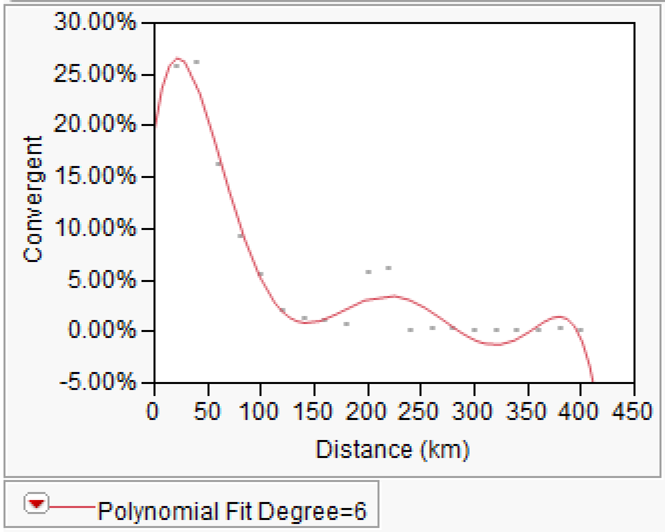

Polynomial Fit Degree=6

Convergent = -0.003067 + 0.0001779*Distance - 9.51e-6*(Distance-210)^2 - 4.5317e-8*(Distance-210)^3 + 8.537e-10*(Distance-210)^4 + 5.674e-13*(Distance-210)^5 - 1.433e-14*(Distance-210)^6

Summary of Fit

RSquare	0.968034
RSquare Adj	0.953281
Root Mean Square Error	0.017879
Mean of Response	0.05
Observations (or Sum Wgts)	20

Analysis of Variance

Source	DF	Sum of Squares	Mean Square	F Ratio
Model	6	0.12585085	0.020975	65.6140
Error	13	0.00415577	0.000320	**Prob > F**
C. Total	19	0.13000662		<.0001*

Parameter Estimates

Term	Estimate	Std Error	t Ratio	Prob>|t|
Intercept	-0.003067	0.033781	-0.09	0.9290
Distance	0.0001779	0.000155	1.15	0.2724
(Distance-210)^2	-9.51e-6	2.788e-6	-3.41	0.0046*
(Distance-210)^3	-4.532e-8	1.565e-8	-2.90	0.0125*
(Distance-210)^4	8.537e-10	1.97e-10	4.33	0.0008*
(Distance-210)^5	5.674e-13	3.5e-13	1.62	0.1291
(Distance-210)^6	-1.43e-14	3.66e-15	-3.92	0.0018*

Figure 62 Statistical Analysis of the Convergent Plate Boundary Using the JMP Software for Side A

Table 53
Table Showing the Percentage Values for the Number of Earthquakes at Segmented Distances from the Convergent Plate Boundary With Respect to the Total Number of Earthquakes in that Particular Segment for Side B

Distance from boundary	Average Percentile (%)	Difference (%)
20	1.80	
40	5.59	-3.80
60	12.91	-7.31
80	19.89	-6.98
100	14.70	5.19
120	11.45	3.24
140	7.91	3.54
160	5.68	2.23
180	4.06	1.62
200	3.75	0.32
220	2.80	0.94
240	2.51	0.29
260	1.94	0.57
280	1.51	0.43
300	0.93	0.58
320	0.82	0.11
340	0.56	0.26
360	0.39	0.17
380	0.31	0.08
400	0.48	-0.17

Figure 63 and Figure 64 show the results for Table 53 plotted with the distance from the nominal centerline of the boundary as the independent variable.

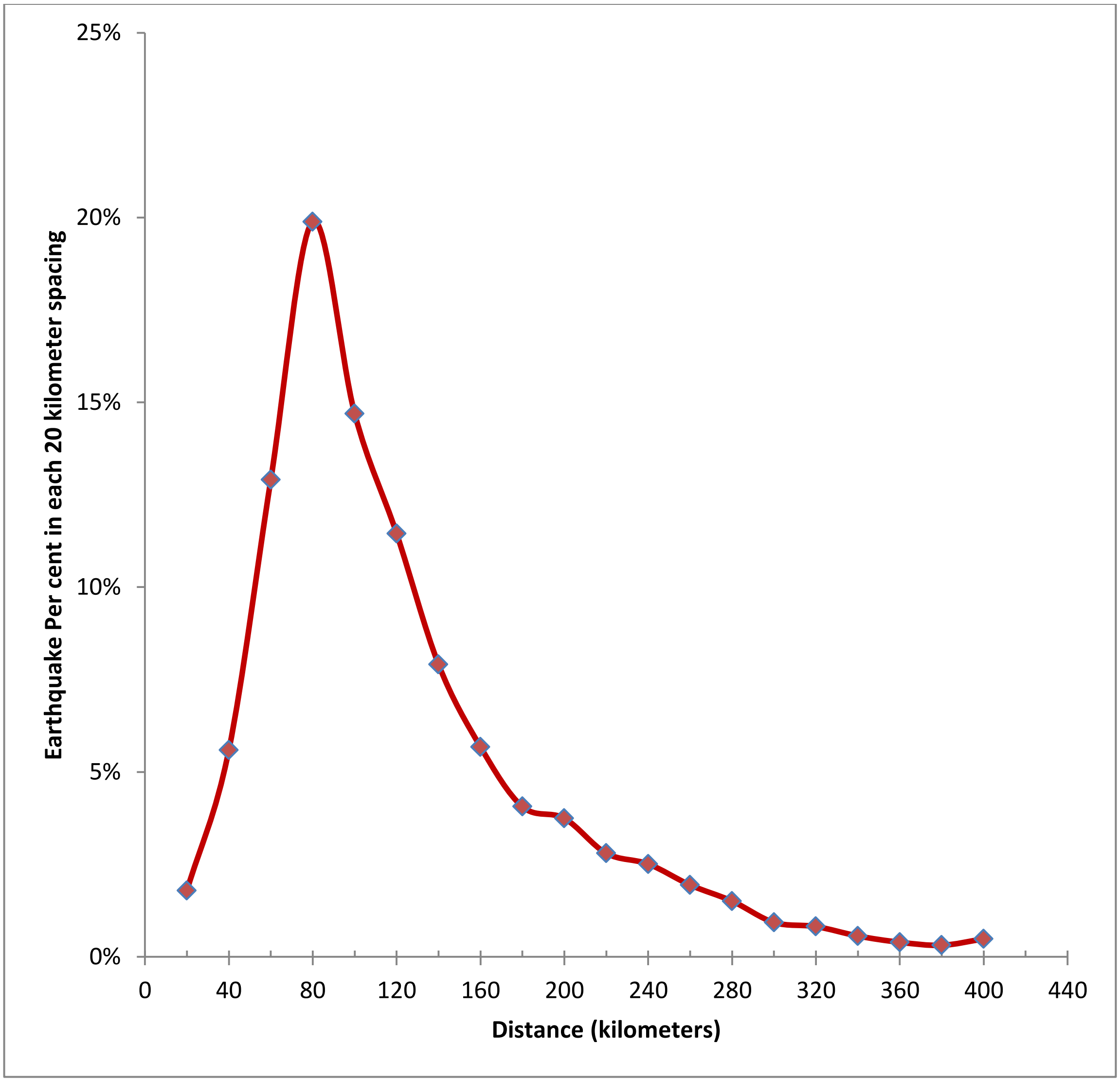

Figure 63 Graph Plotted for Linear Distance of the Earthquakes from the Plate Boundaries Against the Percentage of the Number of Earthquakes Out of the Total Number of Earthquakes in for Convergent Plate Boundary for Side B

Bivariate Fit of Convergent By Distance Set=B

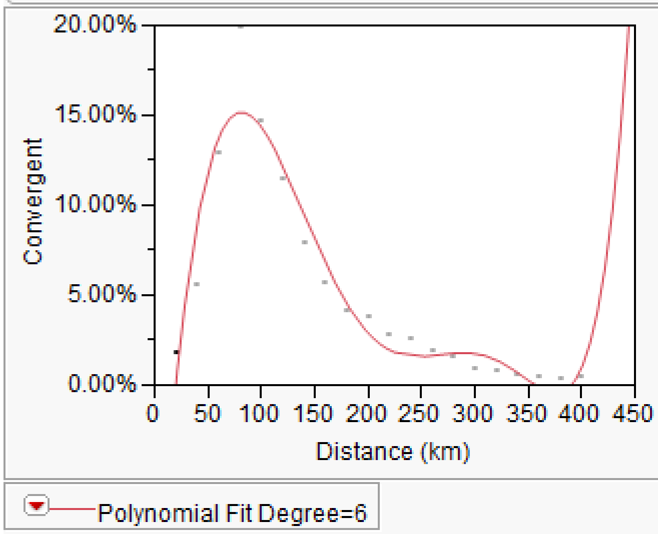

Polynomial Fit Degree=6

Convergent = 0.1217083 - 0.0004676*Distance + 8.3385e-6*(Distance-210)^2 - 2.1848e-8*(Distance-210)^3 - 3.442e-10*(Distance-210)^4 + 9.797e-13*(Distance-210)^5 + 2.76e-15*(Distance-210)^6

Summary of Fit

RSquare	0.92025
RSquare Adj	0.883442
Root Mean Square Error	0.019052
Mean of Response	0.05
Observations (or Sum Wgts)	20

Analysis of Variance

Source	DF	Sum of Squares	Mean Square	F Ratio
Model	6	0.05444979	0.009075	25.0015
Error	13	0.00471869	0.000363	**Prob > F**
C. Total	19	0.05916849		<.0001*

Parameter Estimates

Term	Estimate	Std Error	t Ratio	Prob>|t|
Intercept	0.1217083	0.035997	3.38	0.0049*
Distance	-0.000468	0.000165	-2.83	0.0143*
(Distance-210)^2	8.3385e-6	2.971e-6	2.81	0.0148*
(Distance-210)^3	-2.185e-8	1.668e-8	-1.31	0.2129
(Distance-210)^4	-3.44e-10	2.1e-10	-1.64	0.1256
(Distance-210)^5	9.797e-13	3.73e-13	2.63	0.0209*
(Distance-210)^6	2.76e-15	3.9e-15	0.71	0.4913

Figure 64 Statistical Analysis of the Convergent Plate Boundary Using the JMP Software for Side B

Divergent Plate Boundary

Table 54 and Table 55 represent the data on the divergent plate boundary for Side A and Side B respectively.

Table 54
Table Showing the Percentage Values for the Number of Earthquakes at Segmented Distances from the Divergent Plate Boundary With Respect to the Total Number of Earthquakes in that Particular Segment for Side A

Distance from boundary	Average Percentile (%)	Difference (%)
20	63.39	
40	14.56	48.83
60	7.15	7.41
80	5.67	1.48
100	1.67	4.00
120	0.52	1.15
140	1.83	-1.31
160	1.36	0.46
180	0.71	0.65
200	0.19	0.52
220	0.65	-0.46
240	0.96	-0.30
260	0.19	0.77
280	0.00	0.19
300	0.00	0.00
320	0.38	-0.38
340	0.77	-0.38
360	0.00	0.77
380	0.00	0.00
400	0.00	0.00

Figure 65 and Figure 66 show the results for Table 54 and Table 55 represent the data on the divergent plate boundary for Side A and Side B respectively plotted with the distance from the nominal centerline of the boundary as the independent variable.

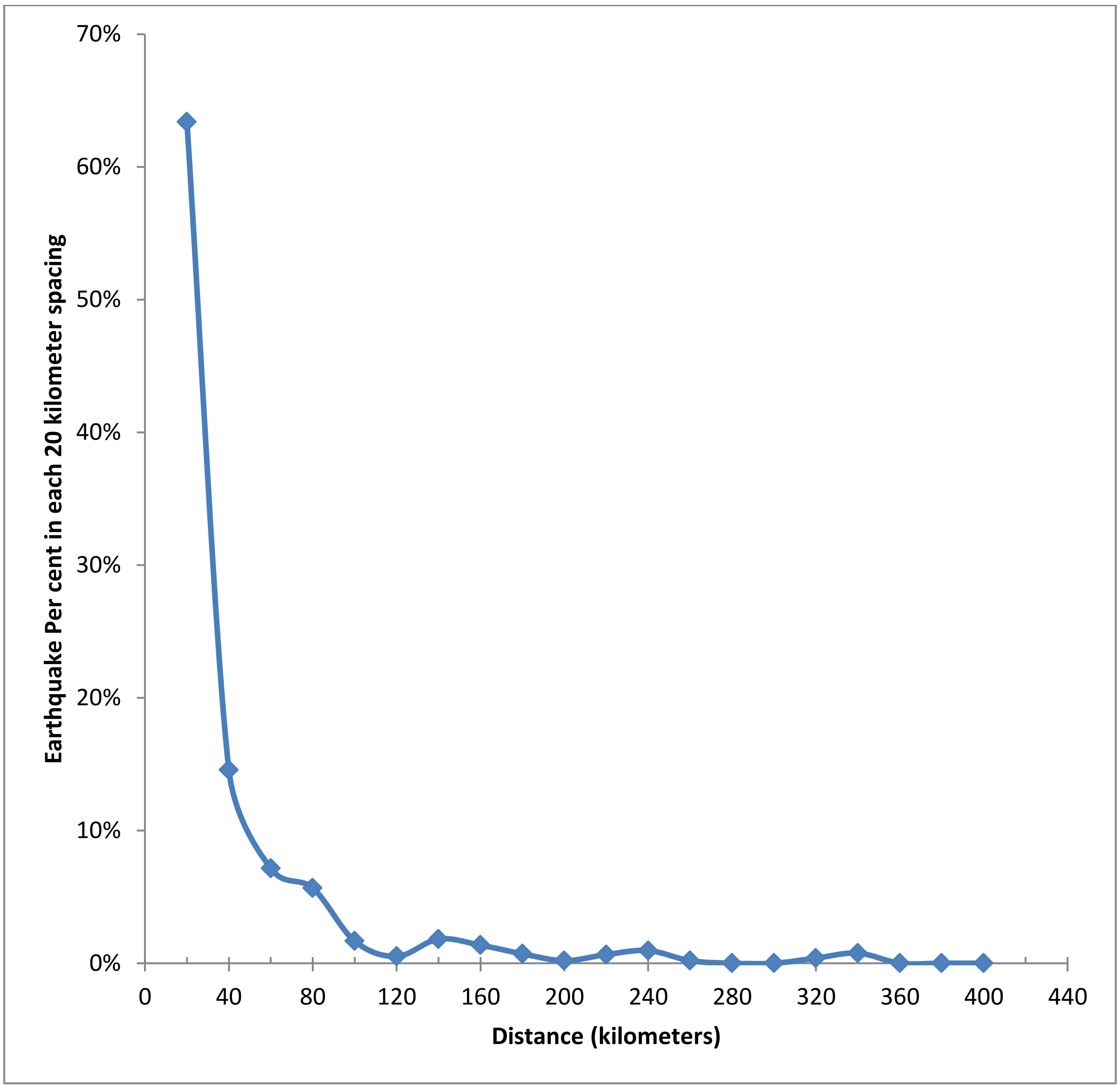

Figure 65 Graph Plotted for Linear Distance of the Earthquakes from the Plate Boundaries against the Percentage of the Number of Earthquakes Out of the Total Number of Earthquakes in for Divergent Plate Boundary for Side A

Bivariate Fit of Divergent By Distance Column 5=a

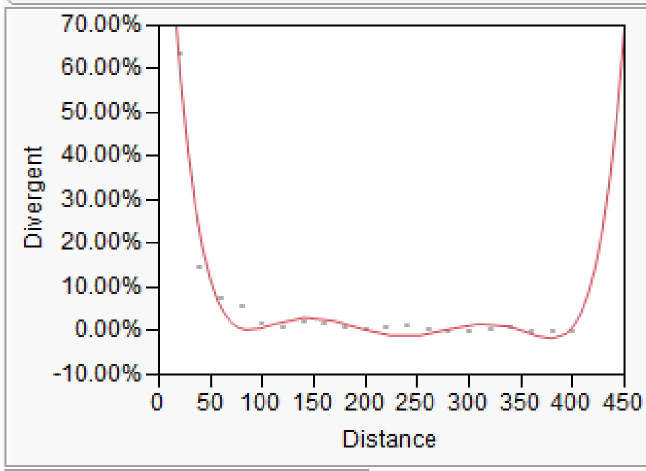

Polynomial Fit Degree=6

Polynomial Fit Degree=6

Divergent = 0.1112477 - 0.0005468*Distance + 7.7594e-6*(Distance-210)^2 + 8.7574e-8*(Distance-210)^3 - 8.104e-10*(Distance-210)^4 - 3.207e-12*(Distance-210)^5 + 2.311e-14*(Distance-210)^6

Summary of Fit

RSquare	0.969484
RSquare Adj	0.9554
Root Mean Square Error	0.029962
Mean of Response	0.05
Observations (or Sum Wgts)	20

Analysis of Variance

Source	DF	Sum of Squares	Mean Square	F Ratio
Model	6	0.37076498	0.061794	68.8345
Error	13	0.01167037	0.000898	**Prob > F**
C. Total	19	0.38243535		<.0001*

Parameter Estimates

Term	Estimate	Std Error	t Ratio	Prob>|t|
Intercept	0.1112477	0.05661	1.97	0.0711
Distance	-0.000547	0.00026	-2.10	0.0556
(Distance-210)^2	7.7594e-6	4.672e-6	1.66	0.1206
(Distance-210)^3	8.7574e-8	2.623e-8	3.34	0.0053*
(Distance-210)^4	-8.1e-10	3.31e-10	-2.45	0.0291*
(Distance-210)^5	-3.21e-12	5.87e-13	-5.47	0.0001*
(Distance-210)^6	2.311e-14	6.13e-15	3.77	0.0023*

Figure 66 Statistical Analysis of the Divergent Plate Boundary Using JMP Software for Side A

Table 55
Table Showing the Percentage Values for the number of Earthquakes at Segmented Distances from the Divergent Plate Boundary With Respect to the Total Number of Earthquakes in that Particular Segment for Side B

Distance from boundary	Average Percentile (%)	Difference (%)
20	46.06	
40	21.07	24.99
60	12.65	8.42
80	2.91	9.74
100	1.42	1.49
120	0.81	0.61
140	0.91	-0.10
160	0.46	0.46
180	1.01	-0.55
200	0.41	0.59
220	0.23	0.18
240	0.37	-0.14
260	3.11	-2.75
280	1.83	1.28
300	2.75	-0.92
320	2.20	0.55
340	1.09	1.11
360	0.37	0.72
380	0.00	0.37
400	0.37	-0.37

Figure 67 and Figure 68 show the results for Table 55 plotted with the distance from the nominal centerline of the boundary as the independent variable.

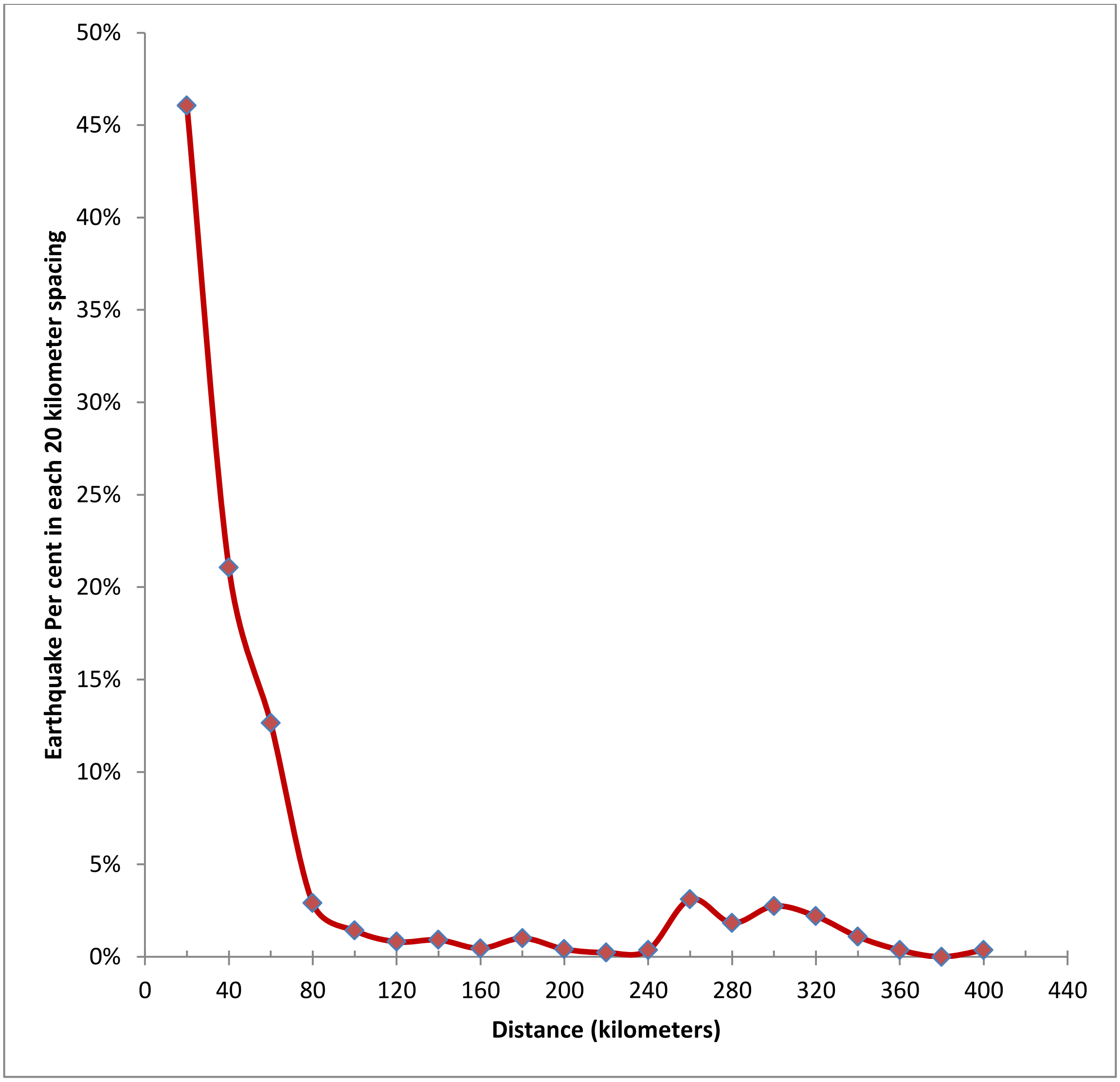

Figure 67 Graph Plotted for Linear Distance of the Earthquakes from the Plate Boundaries against the Percentage of the Number of Earthquakes Out of the Total Number of Earthquakes in for Divergent Plate Boundary for Side B

Bivariate Fit of Divergent By Distance Column 5=b

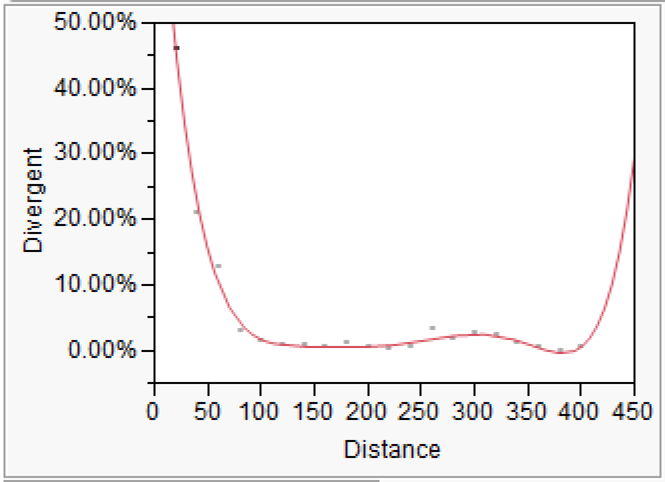

Polynomial Fit Degree=6

Polynomial Fit Degree=6

Divergent = -0.015974 + 0.000106*Distance + 2.4279e-6*(Distance-210)^2 + 8.2898e-9*(Distance-210)^3 - 2.16e-10*(Distance-210)^4 - 1.224e-12*(Distance-210)^5 + 8.903e-15*(Distance-210)^6

Summary of Fit

RSquare	0.993797
RSquare Adj	0.990934
Root Mean Square Error	0.010397
Mean of Response	0.05
Observations (or Sum Wgts)	20

Analysis of Variance

Source	DF	Sum of Squares	Mean Square	F Ratio
Model	6	0.22514535	0.037524	347.1322
Error	13	0.00140527	0.000108	**Prob > F**
C. Total	19	0.22655062		<.0001*

Parameter Estimates

Term	Estimate	Std Error	t Ratio	Prob>|t|
Intercept	-0.015974	0.019644	-0.81	0.4308
Distance	0.000106	9.028e-5	1.17	0.2616
(Distance-210)^2	2.4279e-6	1.621e-6	1.50	0.1581
(Distance-210)^3	8.2898e-9	9.102e-9	0.91	0.3790
(Distance-210)^4	-2.16e-10	1.15e-10	-1.88	0.0823
(Distance-210)^5	-1.22e-12	2.04e-13	-6.01	<.0001*
(Distance-210)^6	8.903e-15	2.13e-15	4.19	0.0011*

Figure 68 Statistical Analysis of the Divergent Plate Boundary Using JMP Software for Side B

Transform Plate Boundary

Table 56 and Table 57 represent the data on the convergent plate boundary for Side A and Side B respectively.

Table 56
Table Showing the Percentage Values for the Number of Earthquakes at Segmented Distances from the Transform Plate Boundary With Respect to the Total Number of Earthquakes in that Particular Segment for Side A

Distance from boundary	Average Percentile (%)	Difference (%)
20	62.25	
40	21.40	40.85
60	8.23	13.18
80	4.65	3.58
100	1.86	2.79
120	0.44	1.41
140	0.97	-0.53
160	0.00	0.97
180	0.00	0.00
200	0.20	-0.20
220	0.00	0.20
240	0.00	0.00
260	0.00	0.00
280	0.00	0.00
300	0.00	0.00
320	0.00	0.00
340	0.00	0.00
360	0.00	0.00
380	0.00	0.00
400	0.00	0.00

Figure 69 and Figure 70 show the results for Table 56 and Table 57 represent the data on the divergent plate boundary for Side A and Side B respectively plotted with the distance from the nominal centerline of the boundary as the independent variable.

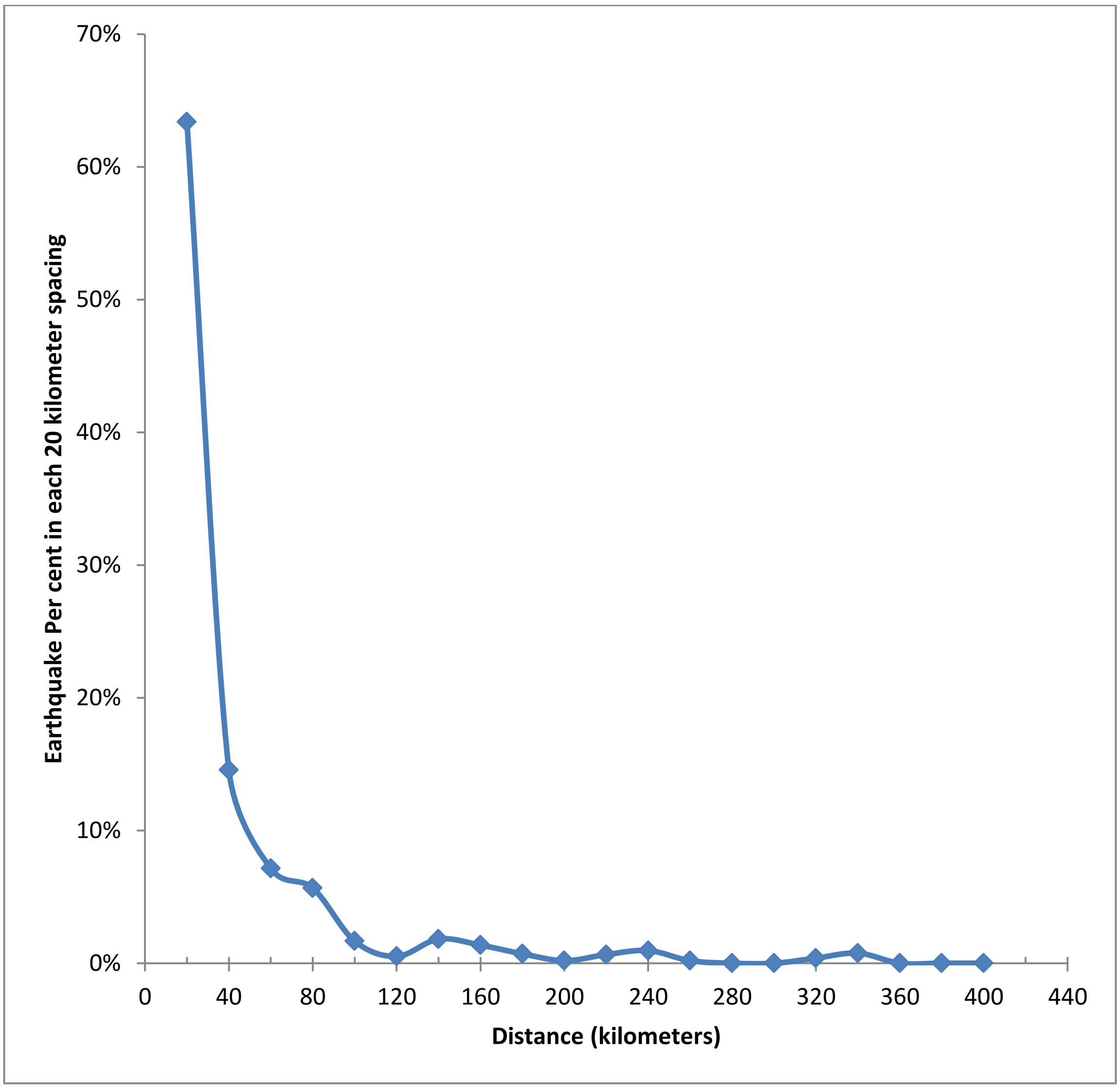

Figure 69 Graph Plotted for Linear Distance of the Earthquakes from the Plate Boundaries against the Percentage of the Number of Earthquakes Out of the Total Number of Earthquakes in for Transform Plate Boundary for Side A

Bivariate Fit of Transform By Distance Set=A

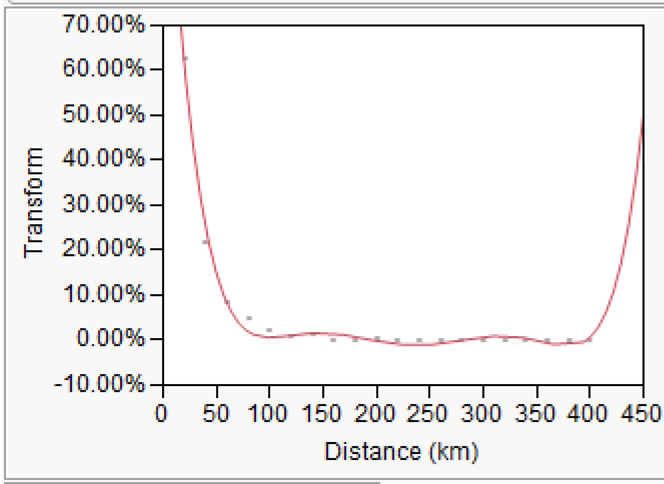

Polynomial Fit Degree=6

Polynomial Fit Degree=6

Transform = 0.071712 - 0.0003667*Distance + 4.9498e-6*(Distance-210)^2 + 6.4535e-8*(Distance-210)^3 - 5.27e-10*(Distance-210)^4 - 2.717e-12*(Distance-210)^5 + 1.744e-14*(Distance-210)^6

Summary of Fit

RSquare	0.991123
RSquare Adj	0.987025
Root Mean Square Error	0.016376
Mean of Response	0.05
Observations (or Sum Wgts)	20

Analysis of Variance

Source	DF	Sum of Squares	Mean Square	F Ratio
Model	6	0.38924017	0.064873	241.8977
Error	13	0.00348641	0.000268	**Prob > F**
C. Total	19	0.39272658		<.0001*

Parameter Estimates

Term	Estimate	Std Error	t Ratio	Prob>|t|
Intercept	0.071712	0.030941	2.32	0.0374*
Distance	-0.000367	0.000142	-2.58	0.0229*
(Distance-210)^2	4.9498e-6	2.553e-6	1.94	0.0746
(Distance-210)^3	6.4535e-8	1.434e-8	4.50	0.0006*
(Distance-210)^4	-5.27e-10	1.81e-10	-2.92	0.0120*
(Distance-210)^5	-2.72e-12	3.21e-13	-8.47	<.0001*
(Distance-210)^6	1.744e-14	3.35e-15	5.21	0.0002*

Figure 70 JMP Distribution Graph for the Transform Plate Boundary for Side A

Table 57
Table Showing the Percentage Values for the Number of Earthquakes at Segmented Distances from the Transform Plate Boundary With Respect to the Total Number of Earthquakes in that Particular Segment Side B

Distance from boundary	Average Percentile (%)	Difference (%)
20	70.64	
40	16.96	53.69
60	5.89	11.06
80	4.24	1.66
100	0.50	3.73
120	0.00	0.50
140	0.00	0.00
160	0.97	-0.97
180	0.79	0.18
200	0.00	0.79
220	0.00	0.00
240	0.00	0.00
260	0.00	0.00
280	0.00	0.00
300	0.00	0.00
320	0.00	0.00
340	0.00	0.00
360	0.00	0.00
380	0.00	0.00
400	0.00	0.00

Figure 71 and Figure 72 show the results for Table 57 plotted with the distance from the nominal centerline of the boundary as the independent variable.

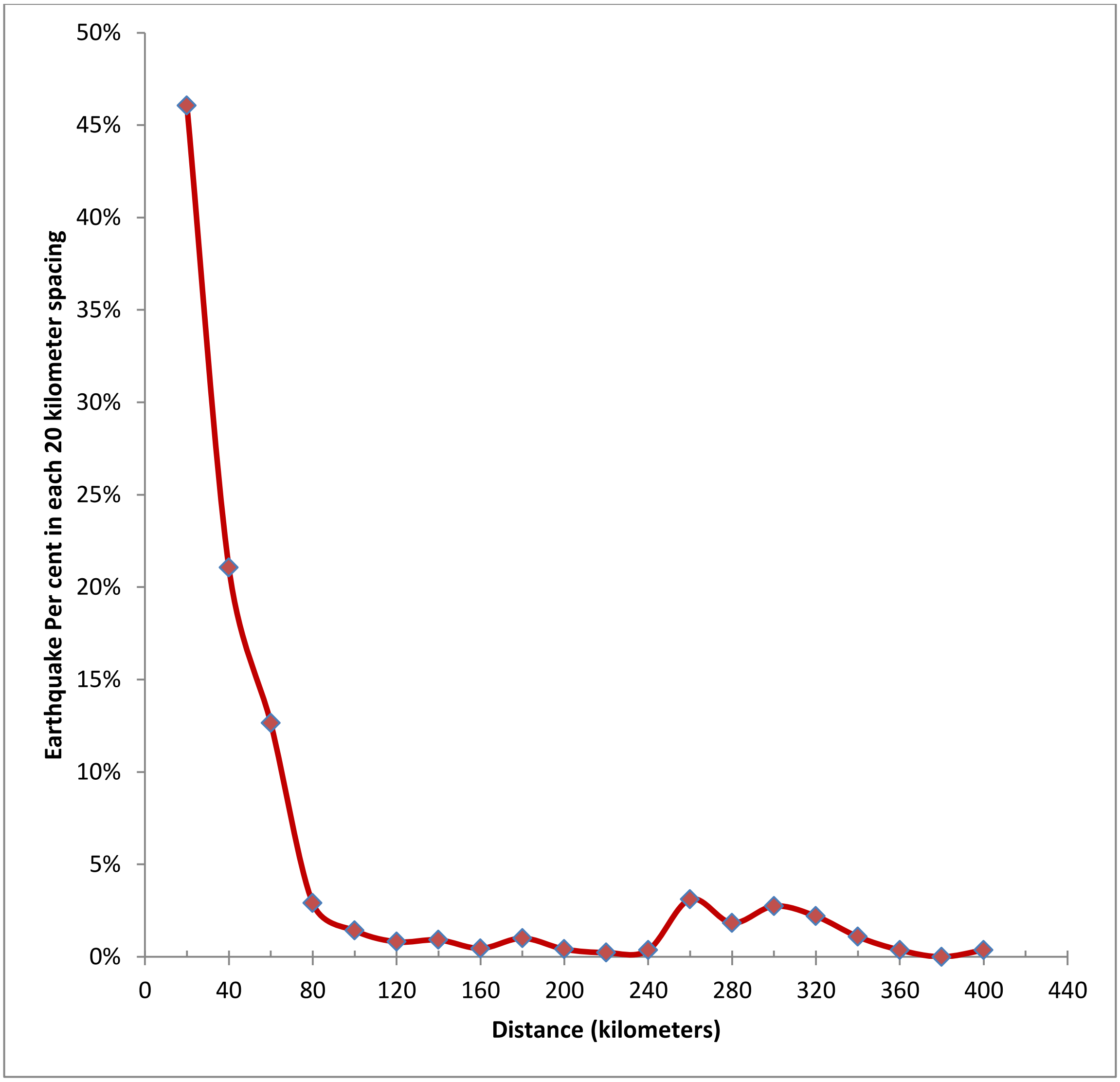

Figure 71 Graph Plotted for Linear Distance of the Earthquakes from the Plate Boundaries against the Percentage of the Number of Earthquakes Out of the Total Number of Earthquakes in for Transform Plate Boundary Side B

Bivariate Fit of Transform By Distance Set=B

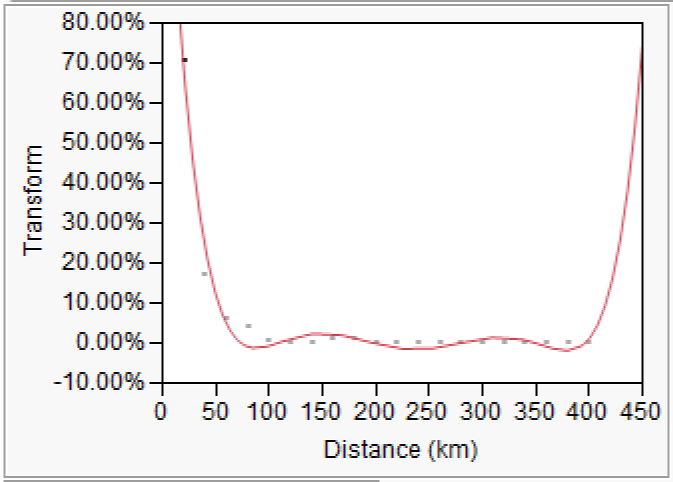

Polynomial Fit Degree=6

Polynomial Fit Degree=6

Transform = 0.1105352 - 0.0005613*Distance + 7.5268e-6*(Distance-210)^2 + 9.882e-8*(Distance-210)^3 - 8.483e-10*(Distance-210)^4 - 3.654e-12*(Distance-210)^5 + 2.521e-14*(Distance-210)^6

Summary of Fit

RSquare	0.977512
RSquare Adj	0.967133
Root Mean Square Error	0.028913
Mean of Response	0.05
Observations (or Sum Wgts)	20

Analysis of Variance

Source	DF	Sum of Squares	Mean Square	F Ratio
Model	6	0.47238651	0.078731	94.1826
Error	13	0.01086723	0.000836	**Prob > F**
C. Total	19	0.48325374		<.0001*

Parameter Estimates

Term	Estimate	Std Error	t Ratio	Prob>|t|
Intercept	0.1105352	0.054627	2.02	0.0641
Distance	-0.000561	0.000251	-2.24	0.0435*
(Distance-210)^2	7.5268e-6	4.508e-6	1.67	0.1189
(Distance-210)^3	9.882e-8	2.531e-8	3.90	0.0018*
(Distance-210)^4	-8.48e-10	3.19e-10	-2.66	0.0197*
(Distance-210)^5	-3.65e-12	5.66e-13	-6.45	<.0001*
(Distance-210)^6	2.521e-14	5.91e-15	4.26	0.0009*

Figure 72 JMP Distribution Graph for the Transform Plate Boundary Side B